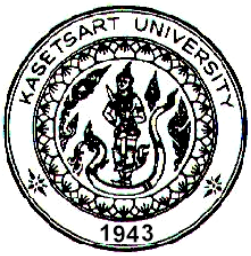

THESIS

QUANTUM CHEMICAL CALCULATIONS ON ELECTRONIC STRUCTURES AND ELECTRONIC PROPERTIES OF POLY(3,4-ETHYLENEDIOXYTHIOPHENE) (PEDOT) AND ITS DERIVATIVES

KANJANA ROTPRADIT

GRADUATE SCHOOL, KASETSART UNIVERSITY

2006

THESIS APPROVAL

GRADUATE SCHOOL, KASETSART UNIVERSITY

Master of Science (Chemistry)
DEGREE

Chemistry	Chemistry
FIELD	**DEPARTMENT**

TITLE: Quantum Chemical Calculations on Electronic Structures and Electronic Properties of Poly(3,4-ethylenedioxythiophene) (PEDOT) and Its Derivatives

NAME: Miss Kanjana Rotpradit

THIS THESIS HAS BEEN ACCEPTED BY

Supa Hannongbua **THESIS ADVISOR**
(Associate Professor Supa Hannongbua, Dr.rer.nat.)

Pensri Bunsawansong **COMMITTEE MEMBER**
(Miss Pensri Bunsawansong, Ph.D.)

Piboon Pantu **COMMITTEE MEMBER**
(Assistant Professor Piboon Pantu, Ph.D.)

Yerry Mahatumarattana **DEPARTMENT HEAD**
(Assistant Professor Yerry Mahatumarattana, B.Sc.)

APPROVED BY THE GRADUATE SCHOOL ON April 18, 2006

Vinai Artkongharn **DEAN**
(Associate Professor Vinai Artkongharn, M.A.)

THESIS

QUANTUM CHEMICAL CALCULATIONS ON ELECTRONIC STRUCTURES AND ELECTRONIC PROPERTIES OF POLY(3,4-ETHYLENEDIOXYTHIOPHENE) (PEDOT) AND ITS DERIVATIVES

KANJANA ROTPRADIT

A Thesis Submitted in Partial Fulfillment of
the Requirements for the Degree of
Master of Science (Chemistry)
Graduate School, Kasetsart University
2006

ISBN 974-16-1479-9

Kanjana Rotpradit 2006: Quantum Chemical Calculations on Electronic Structures and Electronic Properties of Poly(3,4-ethylenedioxythiophene) (PEDOT) and Its Derivatives. Master of Science (Chemistry), Major Field: Chemistry, Department of Chemistry. Thesis Advisor: Associate Professor Supa Hannongbua, Dr.rer.nat. 116 pages.
ISBN 974-16-1479-9

Structural geometries and energy gaps of poly(3,4-ethylenedioxythiophene) (PEDOT) and its derivatives were investigated, based on quantum chemical calculations. Potential energy curves of PEDOT and its derivatives were calculated by the semi-empirical AM1, *ab initio* (at HF/6-31G* and HF/6-31+G* levels) and density functional theory (at B3LYP/6-31G* and B3LYP/6-31+G* levels) methods. The results obtained indicate that *ab initio* and density functional theory show an anti conformation while AM1 method shows a distorted structure. For PEDOT derivatives, PEDOT-C_2H_5 shows an anti conformation while PEDOT-SO_2 and PDOT-CH_2OCH_3 show a distorted structure due to steric hindrance. The energy gaps of the corresponding polymers were obtained by extrapolating HOMO-LUMO energy differences and the lowest excitation energy of oligomers to infinite chain length. The energy gaps of PEDOT calculated at the TDDFT//B3LYP/6-31G** method is predicted to be 1.50 eV, which is consistent agreement with the experimental data (1.60 eV). In the case of PEDOT-C_2H_5 and PEDOT-CH_2OCH_3, the energy gaps calculated by TDDFT//B3LYP/6-31G** method are 1.48 eV and 1.50 eV respectively, which are underestimated with the experimental data. However, we found that the HOMO-LUMO energy differences can represent the energy gap of PEDOT-C_2H_5 and PEDOT-CH_2OCH_3 respectively. The extrapolated energy gap calculated by B3LYP/6-31G** level are 1.71 eV and 1.71 eV which are consistent with the experimental data, 1.75 eV and 1.78 eV, respectively. For PEDOT-SO_2, the energy gaps calculated by TDDFT//B3LYP/6-31G** method is 1.20 eV which shows a promising conducting polymer for further development.

Kanjana Rotpradit — Student's signature

Supa Hannongbua — Thesis Advisor's signature

07 / 04 / 06

ACKNOWLEDGEMENTS

Most of credits in this thesis should justifiably go to my advisor, Associate Professor Dr. Supa Hannongbua, for her valuable guidance, encouragement and kindness throughout the course of my graduate. Special thanks are due to my graduate committees, Dr. Pensri Bunswansong, Assistant Professor Dr. Piboon Pantu, and Assistant Professor Runbir Singh, representative of the Graduate School of Kasetsart University, for their extremely helpful comments and suggestions. This thesis would not have been completed without them.

The Postgraduate Education and Research Programs in Petroleum and Petrochemical Technology (ADB-MUA) are grateful for financial support, My colleagues at Laboratory for Computational and Applied Chemistry (LCAC), Kasetsart University are sincere thanked for their providing helpful assistance and sharing useful ideas and I would also like to thank all of staffs at Department of Chemistry, Faculty of Science, Kasetsart University for research facilities.

Finally, I would like to dedicate this thesis to my parents my brothers my sisters and also my friends for their encouragement and understanding me. They also support me with love and sincerity throughout the entire study.

Kanjana Rotpradit

March, 2006

TABLE OF CONTENTS

Page

LIST OF TABLES

LIST OF TABLES (cont'd)

LIST OF FIGURES

LIST OF FIGURES (cont'd)

LIST OF FIGURES (cont'd)

ABBREVIATIONS

AM1	=	Austin Model 1
AOs	=	Atomic Orbitals
BLYP	=	Beck-Lee-Yang-Parr functional
B3LYP	=	Becke's three parameter hybrid functional using the LYP correlation functional
DFT	=	Density Functional Theory
eV	=	Electron Volt
GTO	=	Gaussian-Type Orbital
HF	=	Hartree-Fock
HOMO	=	Highest Occupied Molecular Orbital
KS	=	Kohn-Sham
LCAO	=	Linear Combination of Atomic Orbitals
LCAO-MO	=	Linear Combination of Atomic Orbitals to Molecular Orbitals
LDA	=	Local Density Approximation
LEDs	=	Light Emitting Diodes
LUMO	=	Lowest Unoccupied Molecular Orbital
LYP	=	Lee-Yang-Parr functional
MNDO	=	Modified Neglect of Diatomic Overlap
MOs	=	Molecular Orbitals
PES	=	Potential Energy Surface
PEDOT	=	Poly(3,4-ethylenedioxythiophene)
PEDOT-C_2H_5	=	Poly(5-ethyldioxyno[2,3-c]thiophene)
PEDOT-SO_2	=	Poly(2,3-dihydro-thieno[3,4-*b*][1,4]dioxine-*b,b*-dioxide)
PEDOT-CH_2OCH_3	=	Poly(5-methoxy)(3,4-ethylenedioxythiophene) methanol
QM	=	Quantum Mechanics
SCF	=	Self-Consistent Field
STO	=	Slater Type orbital

ABBREVIATIONS (cont'd)

STO-3G	=	Slater Type Orbital approximated by 3 Gaussian Type Orbitals
TDDFT	=	Time-Dependent DFT
TDHF	=	Time-Dependent HF
UV-VIS	=	Ultraviolet-Visible Spectroscopy
ZINDO	=	Zerner's Intermediat Neglect of Differential Overlap

QUANTUM CHEMICAL CALCULATIONS ON ELECTRONIC STRUCTURES AND ELECTRONIC PROPERTIES OF POLY(3,4-ETHYLENEDIOXYTHIOPHENE) (PEDOT) AND ITS DERIVATIVES

INTRODUCTION

Conjugated polymers have attracted considerable attention as a novel class of organic semiconductors since discovery that the polyacetylene can be made conductive almost like a metal. Polyacetylene, known as a black powder, was prepared as a silvery film in 1974. In 1977, however, Heeger, MacDiarmid, Shirakawa and co-workers discovered that oxidation with chlorine, bromine or iodine vapour made polyacetylene films 109 times more conductive than they were originally (Chiang *el at*., 1977). Treatment with halogen was called "doping" by analogy with the doping of semiconductors. A key property of a conductive polymer is the presence of conjugated double bonds along the backbone of the polymer. In conjugation, the bonds between the carbon atoms are alternately single and double. Every bond contains a localized "sigma" (σ) bond which forms a strong chemical bond. In addition, every double bond also contains a less strongly localized "pi" (π) bond which is weaker.

Today conductive plastics are being developed for many uses, such as in corrosion inhibitors, compact capacitors, antistatic coatings and electromagnetic shieldings of computers. A second generation of electrical polymers has also appeared in film transistors (Meng *et al*., 2003 and Kudo 2005), light-emitting diodes (Zhang *et al*., 2000; Liu *et al*., 2002; Wu *et al*., 2004; Ortega *et al*., 2005) and solar cell (Yohannes *et al*., 2004).

Compared to inorganic materials, conjugated polymers have the advantages of easy control of the semi-conducting properties through chemical modification with great uniformity over large areas, leading to major potential cost savings in device manufacture. In the past decade great efforts have been devoted to the design and synthesis of light-emitting polymers (LEPs) for applications in light-emitting diodes

(LEDs) in which three primary colors (blue, red and green) are essential for full color displays. However, white light emission is recently emerging to be a major area of research activity (Gong *et al*., 2004; Moiorano *el at*., 2005; Tsou *et al*., 2005; Vardeny *et al*., 2005; Wei, *et al*., 2005). The organic materials will be the main target for developing white light emission because of a difficult problem to generate white light using inorganic semiconductors. LEDs and transistors based on conjugated materials are now being actively developed for commercial applications in emissive devices by a number of companies. A number of conjugated backbone structures, as shown in Fig. 1, have been shown to be of importance in realizing various emissive colors.

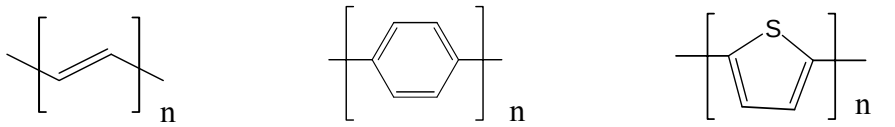

Polyacetylene (PA) Poly (para-phenylene) (PPP) Polythiophene (PT)

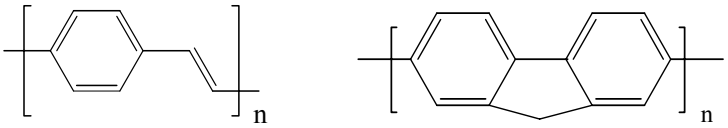

Poly(para-phenylenevinylene) (PPV) Polyfluorene (PF)

Figure 1 Conjugated backbone structures of conducting polymers.

Conjugated polymers are extensively investigated for the development of a variety of organic-based electronic applications (Friend *et al*., 1999). Among the numerous polymers that have been developed and studied over the past decades, poly(3,4-ethylenedioxythiophene) (PEDOT) is one of the most important conductive polymers studied worldwide because of the ease of processing and tuning of electronic and optical properties. PEDOT is a low energy gap polymer with high conductivity and good thermal and chemical stability (Groenendaal *et al*., 2000). For this study, PEDOT is chosen because it is the most widely used for industrially

important conducting polymer. The major advantage is high stability in the doped state, with conducting properties that remain almost unaltered with aging in environmental conditions. However, their main drawback was the instability of the conductive form. The poly(3,4-ethylenedioxythiophene) shows a remarkable stability as compared to other members of the polythiophene family (Jonas *et al*., 1991; Dietrich *et al*., 1994; Groenendaal *et al*., 2000). However it is still insoluble and its applications are thus limited to that of commercial dispersion in aqueous poly(styrenesulfonic acid) (Jonas *et al*., 1995; Jonas *et al*., 1997; Lerch *et al*., 1998). To overcome this problem, substitution with a long flexible alkyl chain would lead to soluble polymers as already reported in the polythiophene series (Jen *et al*., 1985; Sato *et al*., 1986; Hotta *et al*., 1987).

So, the insolubility of PEDOT can be easily removed by substitution of hydrogen atom in the dioxyethylene ring by a long alkyl group. Soluble alkyl-substituted poly(ethylenedioxythiophene)s first synthesised by Kumar and Reynolds (Kumar *et al*., 1996) are soluble in common organic solvents. They also retain their electroactivity after many redox cycles and can be made conductive via oxidative doping in solution.

In the decade, derivatives of PEDOT have been synthesized by attaching alkyl pendant groups containing 8 and 14 carbon atoms (Sankaran *et al*., 1997) onto the dioxane ring (Fig. 2.), leading to an increase of both their solubility and stability. Moreover, the alkyl dioxy substituent in the 3 and 4 positions prevents the occurrence of αβ coupling. Thus, the unique structures of the PEDOT derivatives yield an attractive combination of electronic and mechanical properties that represent promising materials from an engineering viewpoint. The electronic structure of poly(3,4-ethylenedioxythiophene) (PEDOT) and its derivatives are shown in Fig. 2.

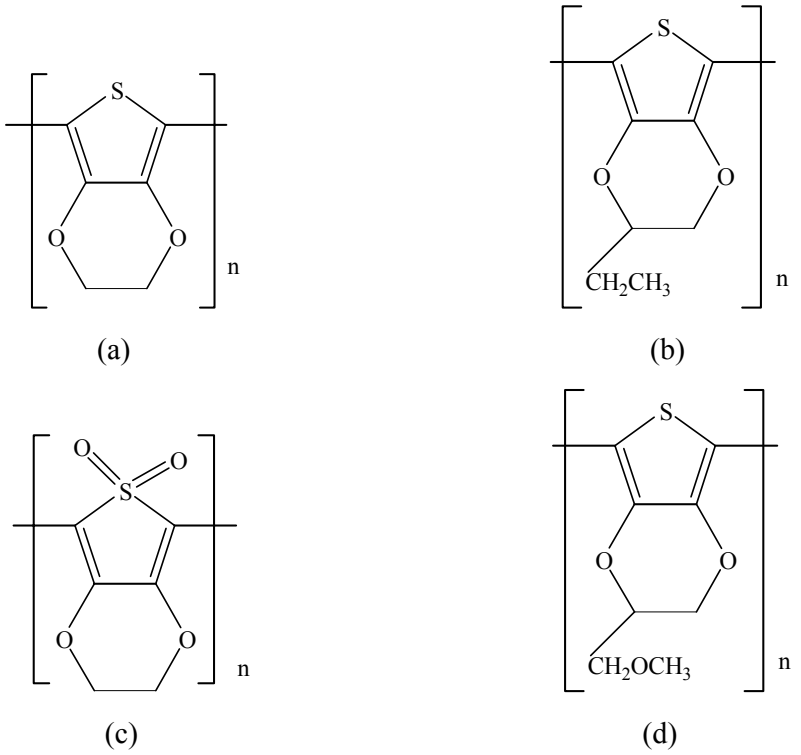

Figure 2 Structures of poly(3,4-ethylenedioxythiophene) (PEDOT) (a) and its derivatives (b, c and d).

Today PEDOT has been investigated in many research fields both in experimental and theoretical approaches. In experimental, PEDOT can be studied from basic polymer science (Pron *et al*., 2002) through material science (Groenendaal *et al*., 2002) such as electrochemistry (Ghosh *et al*., 2000), electronics (Ghosh *et al*., 1999), optoelectronics (Bayer *et al*., 1988; Carlberg *et al*., 1996; Bharathan *et al*., 1998), photovoltaics (Yohannes *et al*., 1998; Arias *et al*., 1999; Zhang *et al*., 2002) corrosion protection (Khan *et al*., 1999), novel cell systems (Philips company 1998) down to biosensors (Yamato *et al*., 1995) as future prospects. The reasons for such widespread interest are its much sought for properties like high conductivity, interesting electrical and spectrochemical properties associated with its low band gap, electrochromic and antistatic properties and good stability all of which pave the way into numerous important applications (Jonas *et al*., 1991; Heywang *et al*., 1992).

There are several theoretical studies (Dkhissi *et al*., 2002; Hong 2003; Osikowicz *et al*., 2003; Aleman *et al*., 2004; Aleman *et al*., 2005; Agaya *et al*., 2005; Yang *et al*., 2005) that investigate physical and chemical properties of PEDOT and its derivatives. For electronic and optical properties, the transition (or excitation) energy from the ground state to the first dipole-allowed excited state can be calculated theoretically and used to compare directly with the experimental results. The implicit assumption underlying the theoretical approximation is that the lowest singlet excited state can be described by only one singly excited configuration in which an electron is promoted from the highest occupied molecular orbital (HOMO) to the lowest unoccupied molecular orbital (LUMO). In fact, the orbital energy difference between HOMO and LUMO is a crude estimation of the transition energy and an accurate description of the lowest singlet excited state requires a linear combination of a number of excited configurations. Despite such deficiency, the calculated HOMO-LUMO gap agrees qualitatively with the experimental energy gap in many cases (Beljonne *et al*., 1995; Bredas *et al*., 1995; Hirata *et al*., 1999; Negri *et al*., 2000). There exist a variety of theoretical approaches for evaluating this quantity for oligomers as well as infinite polymers. The crudest estimate is the orbital energy difference between the HOMO and LUMO, obtained from Hartree-Fock or density functional theory calculations. Among those theories, Hartree-Fock-based methods such as configuration interaction singles (CIS) (Foresman *et al*., 1992) and the random phase approximation (RPA), which is equivalent to the time-dependent HF (TDHF) (Wiberg *et al*., 2002), usually provide only the qualitative or semiquantitative descriptions for the low-lying excited states. Fortunately, time-dependent density functional theory (TDDFT) (Gross *et al*., 1990; Bauernschmitt *et al*., 1996; Jamorski *et al*., 1996; Casida *et al*., 1998) was a success to some extent. The fusion of a significant quantitative improvement with moderate computational cost has attracted the increasing favor of chemists in the TDDFT method. Over the past few years, it has advanced to one of the most popular theoretical approaches to calculate excited-state properties of medium-sized and large molecules up to about 200 second-row atoms. Moreover, the TDDFT method was also successfully employed to extrapolate energy gaps of the polymers from the calculated excitation energies of the oligomers (Wiberg *et al*., 1998; Kwon *et al*., 2000; Gao *et al*., 2002;

Zhang *et al*., 2002; Zhang *et al*., 2003). However, these have also pointed out that TDDFT systematically underestimates the excitation energies by 0.4-0.7 eV compared to the experimental results (Kwon *et al*., 2000; Gao *et al*., 2002; Zhang *et al*., 2002; Yu *et al*., 2003). The reason for this is due to the limitation of the current approximate exchange-correlation functionals in correctly describing the exchange-correlation potential in the asymptotic region (Ma *et al*., 2002). However, reasonable results can still be expected here, because HF/DFT hybrid functionals such as B3LYP can partially overcome the asymptotic problem (Diaz *et al*., 1981; Gao *et al*., 2002). For linear oligoenes, recent studies on the excited state energies of the first dipole-allowed ^{1}Bu states also showed that TDDFT calculations with the B3LYP functional correctly reproduce the general trend of decreasing excitation energy with increasing chain length, with a systematic underestimation of only approximately 0.3-0.5 eV (Zhang *et al*., 2002; Zhang *et al*., 2003; Yu *et al*., 2003). Therefore, TDDFT with the B3LYP functional is expected to be a relatively reliable tool for evaluating the excitation energies of the low-lying excited states for small- and medium-sized molecules.

In addition, the effects of substituent size and molecular symmetry on the geometry and excitation energy of alkyl derivatives of conducting polymer were investigated by quantum-chemical calculations. The so-called “oligomer approach” (Cornil *et al*., 1995) can be used to model the single chain properties of the full polymer. For examples, HOMO-LUMO energy gaps of the polymers are estimated by extrapolating the excitation energies of the oligomers to infinite chain length. Although the model system is far simpler than the real polymer, it has successfully provided understanding of the experimental results.

Ab initio density functional theory, methods that can be used to estimate the HOMO-LUMO energy gap, sometimes agrees fairly well with the experimental band gap in many cases (Oliveira *et al*., 2000) perhaps this due to the error cancellations. Time-dependent density functional theory is a recently developed tool for calculating excitation energies. Ma *et al.* (2002) employed TDDFT to calculate band gaps and effective conjugation lengths of conjugated polymer. They obtained band gaps of the

polymer by extrapolating vertical excitation energies of the trimers through pentamers to infinite chain length. TDDFT was also applied to calculate vertical excitation energies of linear polyene oligomers; butadiene to decapentaene (Hsu *et al*., 2001). In addition, this method is also used to study electroluminescent polymer (Yu *et al*., 2003; Suramitr *et al*., 2005).

Many experimental and theoretical works have been devoted to the structures and electronic properties of conjugated polymers in the ground state. In addition, optimization ground-state geometries can be utilized for the absorption energies (Belletete *et al*., 2000; Briere *et al*., 2004). On the other hand, theoretical investigation on the excited states is limited by complications associated with the changes in molecular structure upon excitation. In the case of conjugated polymer for light-emitting diode applications, optimization of the excited state is essential for the computation of emission energies. Theoretical methods which are performed for investigating absorption and emission processes are time-dependent density functional theory (TDDFT), configuration interaction (CIS) and semi-empirical ZINDO (Poolmee *et al*., 2005).

In this study, we employed semi-empirical, *ab initio*, and density functional theory with the B3LYP functional to investigate the structures and electronic properties of poly(3,4-ethylenedioxythiophene) (PEDOT) and its derivatives. Moreover, TDDFT with the B3LYP functional and semi-empirical ZINDO are used to determine the vertical excitation energies of studies polymers. Furthermore, the effect of repeating unit length of PEDOT on its band-gap energy will also be investigated.

LITERATURE REVIEWS

Significance of PEDOT

Since the development of poly(3,4-ethylenedioxythiophene) (PEDOT) in the late 1980s by scientists at Bayer A.G. (Bayer *et al*., 1988), this polymer to date received an ever-accelerating scientific interest throughout the world. The reasons for such widespread interest are its much sought for properties like high conductivity, interesting electrical and spectrochemical properties associated with its low band gap, electrochromic and antistatic properties and good stability, all of which paved this polymers way into numerous important applications (Jonas *et al*., 1991; Heywang *et al*., 1992). These properties originate from the high regularity of the polymer backbone bonds, which are purely α–α' coupled, thanks to the blocking of unfavourable β positions by the cyclic 3,4-dioxy substituent (dioxane group). The two oxygen atoms that bonde directly to the thiophene backbone enrich the conjugated π-bond with electrons, lowering the oxidation potential of the polymer, while the cyclic character of the ethylenedioxy substituent curbs the disorder that otherwise linear side groups could introduce into the polymer structure. A review of the state of development of PEDOT's chemistry and contemporary applications together with a rich list of references has been given by Groenendaal *et al*. (2002). The electronic properties of a conductive polymer can be altered through doping.

Nowadays it is widely accepted that depending upon the doping level two different charge carrying species can prevail i.e., polarons and bipolarons both of which can propagate the electrical current along the polymer chain (Chen *et al*., 1986; Van Haare *et al*., 1998). Polarons carry a magnetic moment and can therefore be observed and distinguished from diamagnetic bipolarons by means of ESR spectroscopy. Their spectroscopic response is sensitive however to the chemical environment they reside in and since bipolarons constitute a part of that environment, the spectroscopic response of polarons will be influenced by the presence of bipolarons as well as any other paramagnetic species in the polymer material. This influence will be evident not only at high doping levels where polarons become

oxidised to bipolarons but also at intermediate doping levels where both species coexist together (Harima *et al*., 2000). The influence of the doping level on such properties of PEDOT as conductivity and carrier mobility has already been studied (Zotti *et al*., 2000). Recently Zykwinska *et al*. (2003) have published results on the ESR spectro-electrochemical studies of PEDOT during doping and subsequent dedoping. These results revealed some interesting information about the behaviour of paramagnetic species during these processes like the hysteresis of the potential dependence of concentration of spins, strong interactions between polarons at intermediate doping levels and the presence of an ESR signal in the dedoped polymer. Some of these features of PEDOT have been already observed by Kvarnstrsom *et al*. (1999) by means of in situ IR and EQCM. One of the features of PEDOT is its extraordinary stability towards different aging factors both physical and chemical. One of the first stability studies of PEDOT concerned its thermal stability with respect to such properties as conductivity (Heywang *et al*., 1992; Pei *et al*., 1994; Huang *et al*., 2003). It was found that PEDOT could with stand temperatures just above 100 °C for considerable lengths of time, without notable loss of conductivity. Rannou *et al*. (1999) have studied the kinetics of conductivity decay at higher temperatures, while Winter *et al*. have studied the structural changes taking place in PEDOT upon its thermal treatment. When the electrochemical approach towards synthesis of PEDOT has been applied, investigations of electrochemical stability of this polymer have also been initiated. Studies of PEDOT and other thiophene polymers in such 'extended' potential windows past the potential of electrochemical stability of the polymer have been reported in several papers throughout the last years. Heinze *et al*. (2002) reported that overoxidation of PEDOT up to 3.0 V leads to evolution of a strong double and irreversible oxidation peak. Such treatment led to inactivation of electrochemical properties of the material. Kvarnstrom *et al.* (1999) have evaluated the onset of degradation potential at 1.9 V. Comparing this value with a boundary at ca. 1.4 V for other polythiophenes (Bobacka *et al*., 1991), it can be seen that PEDOT is indeed an electrochemically stable material. The effect of high oxidation potentials on other properties of PEDOT has also been investigated. Lapkowski *et al*. (2000) have demonstrated a finite potential window of conductivity of PEDOT, while Du *et al*. (2003) have reported in

a recent study the effect of polymerisation potential on PEDOT's conductivity and ESR response. Also recently, a detailed study of electrochemical dissolution of polythiophene has been presented by Aoki and co-workers.

Synthesis of PEDOT

Poly(3,4-ethylenedioxythiophene) was synthesized with a varity of methods. Li *et al*. (2004) synthesized the poly(3,4-ethylenedioxythiophene) films in an aqueous sodium dodecyl sulfate and lithium tetrafluoroborate electrolyte solution. They found that PEDOT films prepared in this medium exhibit novel electrochemical and optical properties. Cyclic voltammetric results indicate that the dodecyl sulfate (DS^-) anions are trapped in the polymer matrix when PEDOT is deposited onto gold substrate. The larger DS anions are immobile and stay in the polymer during a redox process, whereas cation movement dominates the charge compensation, moving in and out of the polymer matrix, when the PEDOT film is redox-cycled. The infared and X-ray photoelectron spectroscopic results further confirmed the incorporation of DS into the PEDOT film. Surface plasmon resonance was used to investigate the film growth and the optical properties of PEDOT films upon doping and dedoping at two laser wavelengths. With growing film thickness, an increase in doping level as well as an increase in refractive index was detected. The resonance curves change dramatically when the PEDOT film is switched to different doping states, suggesting important change of the film dielectric constant and electrochromic property. Cho Ko *et al*. (2004) studied and synthesized the two single–and a dual-type electrochromic devices (ECDs) based on poly(3,-tatradecylthiophene) (PTDT) and poly(3,4-ethylenedioxythiophene) with litium salt in PMMA gel-media. They found that in the single-type ECDs, red PTDT (λ_{max}:494 nm) and blue PEDOT (: 596 nm) in the reduced states could be switched to their bleached oxidized forms. In the dual-type ECD, the color changed between dark red (:502 nm) and dark blue (:602 nm) by switching the applied voltage (E(PTDT) versus E(PEDOT)) between -2.2 and 2.2 V. Its electronic absorption was a combination of those of PTDT and PEDOT. Its optical switching rate was much faster than the single-type ECDs. It is presumably because the capacitive charging of each bare ITO electrode in the single-type ECDs partially

compensates the applied voltage while in the dual-type ECD, both the electrodes participate in the faradaic reactions. In this dual-type ECD, when one of the electrodes takes part in coloring electrode, the other takes part in complementary electrode coloring leading to fast switching.

Synthesizes of PEDOT derivatives have been reported in several papers. Sankaran *et al*. (1997) synthesized two new derivatives of 3,4-ethylenedioxy-thiophene (EDOT), specifically 5-octyldioxeno[2,3-c]thiophene (EDOT-C_8) and 5-tetradecyldioxeno[2,3-c]thiophene (EDOT-C_{14}). They found that the cyclic voltam-metry of PEDOT-C_8 and EDOT-C_{14} in 0.1 M TBAP/CH_3CN show irreversible monomer oxidation peaks (Ep,m) at 0.89 and 0.93 V respectively. Multiple scans yield electroactive and conducting polymer films on electrode surfaces. The PEDOT-C_8 and PEDOT-C_{14} forms oxidize with relatively low peak potentials at -0.22 and -0.19 V respectively, indicating the doped form of the polymer to be quite stable. Both PEDOT-C_8 and PEDOT-C_{14} show two reduction processes with peaks at -0.18 and -0.16 V (Ec2, p) and -0.55 and -0.36 V (Ec1, p) respectively. Optoelectrochemical studies reveal an energy gap of 1.75 eV for both polymers. The polymers are electrochromic, relatively transmissive and light gray in the oxidized form, while being opaque and deep purple in the reduced form exhibiting high electrochromic contrasts. Long term switching studies carried out in 0.1 M $LiClO_4$/PC with Li/Li+ as a reversible counter electrode shows that PEDOT, PEDOT-C_8, and PEDOT-C_{14} retained 65%, 50%, and 62% of their electroactivity after 6000, 9000, and 16000 double switches respectively. Moreover, two sulfonated polythiophene derivatives poly[(3-thienyl)-ethoxybutane-sulfonate] [poly(I)] and poly[2-(3-sulfinopropyl)-2,3-dihydrothieno[3,4-b][1,4]dioxin] [poly(II)] have been synthesized by chemical poly-merization with $FeCl_3$ (Tran-Van *et al*., 2004). Due to its lower oxidation potential, poly(II) is easily polymerized in water in contrast to poly(I). Both conducting polymers are water soluble and can be spray coated due to the immobilization of sulfonated group covalently links. These polymers can be self-doped with acidic vapors. Sulfonated poly(3,4-ethylenedioxythiophene) thin films were shown to be highly stable in air in their doped state contrary to the thiophene derivatives. Finally

they have compared in preliminary results ion exchange properties of these two polymers to make possible the preparation of radioactive sources.

Poly(3,4-ethylenedioxythiophene) nanoparticles were synthesized with enhanced conductivity and processbility by oxidative polymerization in dodecylbenzene sulfonic acid (DBSA) micellar solutions (Choi *et al*., 2004). DBSA was used to act simultaneously as a surfactant to form micelles and as a doping agent. Monomers of EDOT, which have extremely low solubility to water, were easily solubilized in aqueous DBSA micellar solution. The effects of DBSA on the resulting PEDOT structure morphology and electrical properties were investigated when DBSA was used in combination with two different oxidants, i.e., iron(III)chloride and ammonium persulfate. The electrical conductivity varied with the polymerization conditions, and was relatively high up to 50 S/cm. The morphology of the particles, determined by Field Emission Scanning Electron Microscopy (FE-SEM), appeared to be quite spherical and their sizes ranged from 35 to 100 nm in diameter. The colloidal properties of the PEDOT nanoparticles were also investigated. Conducting poly ~3,4-ethylenedioxythiophene nanowires were synthesized by using an electrochemical polymerization method with a nanoporous template (Kim *et al*., 2003). Scanning and transmission electron microscopy confirmed the formation of conducting polymer nanowires (~CPNWs) with an open end. The formation and the electrical properties of the CPNWs formed were dependent on synthetic conditions, such as the doping level, the polymerization time, and the applied current. The measured electrical conductivity of a single strand of CPNW was 3.431023 S/cm at room temperature. From the ultraviolet and visible absorbance spectra, they observed a π–π * transition at 2.1 eV for the de-doped systems. A field emission cell of CPNW nanotips was fabricated. The turn-on field of the CPNWs was 3.54 V/mm at 10 mA/cm^2, and the current density increased up to 100 mA/cm^2 at 4.5 V/mm. The field enhancement factor of CPNW nanotips was 1200, which is comparable to those of carbon nanotubes. Moreover, Nanofibers of poly(3,4-ethylenedioxythiophene) (PEDOT) have been electrochemically synthesized by the template method and their morphology determined using electron microscopy (Choi *et al*., 2001). A comparative resonant Raman scattering study has been performed on films, bundles

of fibers and individual fibers of different diameters. Their temperature dependent transport properties have also been investigated and compared with the case of a PEDOT thin film. The PEDOT is found to be in an insulating state close to the metal–insulator transition. The temperature dependence of the fibers' conductance is larger than for the films, and this variation increases for a smaller fiber diameter. These results suggest that a confining effect on the PEDOT structure occurs during the electrochemical synthesis in the template.

Electronic properties of PEDOT

The relaxation kinetics of poly(3,4-ethylenedioxythiophene) (PEDOT) electro-deposited on platinum electrode surface were studied in a room temperature ionic liquid, 1-ethyl-3-methylimidazolium bis((trifluoromethyl) sulfonyl)amide (EMITFSI), by means of large amplitude potential step experiments (Randriamahazaka *et al*., 2005). The influence of the applied potential and the film thickness were analyzed. They have developed a kinetic model allowing the determination of the kinetic features. Accordingly, two time or kinetic constants, for both oxidation and reduction that were in relation to PEDOT film morphology were determined. These kinetic constants seemed independent to the applied potential. They showed that the kinetic constants for the fast process depended upon the thickness of the polymer film. However, the time constant for the slow process was virtually independent of the film thickness. They have also introduced dimensionless variables that can be used to analyze the global process. Accordingly, the kinetics for the oxidation were faster than that of reduction. These results were in agreement with the ion transfer mechanisms during the redox switching of PEDOT in EMITFSI in which a departure of cation occurred during the oxidation.

Copolymerization is often used to prepare a new polymer with properties different from the constituent homopolymers. Generally speaking, the physical and chemical properties of a copolymer are in between those of the respective homo polymers but significantly distinct from those of a composite and a blend. Jin *et al*. performed electropolymerization (EP) of styrene and pyrrole monomers and found

that the product polymer was a copolymer of pyrrole and styrene instead of composite or blend of polypyrrole and polystyrene (Jin *et al*., 2000). Regarding the unique properties of PEDOT, copolymerizations of EDOT and other monomers such as 3-methylthiophene (Yohannes *et al*., 1997), *N*-ethylcarbazole (Sadki *et al*., 2003), pyrrole and *N*-substituted carbazole (Giebler *at al*., 1993) have been reported. The electrocopolymerizations of the above cases are difficult due to the differences on the oxidative potentials of the two monomers applied, i.e. monomer with the lower oxidative potential was preferentially polymerized on the electrode. The quality of the monolayer deposited on the electrode has been demonstrated to be strongly dependent on the experimental conditions, i.e. solvent, dipping time, electrode surface state (Mekhalif *et al*., 1995), the monomer structures (Davidson *et al*., 1988) and concentrations. All have profound influences on the structure and the electrochemical properties of the resulting polymers.

Electropolymerizations (EPs) of thiophene (Th), 3,4-ethylenedioxythiophene (EDOT) and the mixed monomers of Th and EDOT in 0.05 M Et4NClO4/propylene carbonate (PC) solution were performed to prepare polymer films as potential cathode materials in lithium ion batteries (Chang *et al*., 2005). The incorporation of EDOT units into the pure polythiophene (PTh) chain leads to large alternations on the experimental conditions of EPs and the properties of the resulting polymer films. Onset potential of the EPs was reduced with the participation of EDOT component. The resulting polymers, PTh, poly(3,4-ethylenedioxythiophene) and poly(thiophene-co-3,4-ethylenedioxythiophene) (PTh–EDOT) were then served as cathode materials to test their capabilities to transport lithium ion in 1.0 M LiPF6/ethylene carbonate/dimethyl carbonate solution. With the inherent EDOT unit, PEDOT and PTh–EDOT have better charge capacity, stability and response rate than pure PTh. Among the copolymers, PTh–EDOT (1/1) even shows better stability than pure PEDOT homopolymer. The advantage of using EDOT as copolymer component is thus confirmed.

Phenyl-capped 3,4-ethylenedioxythiophene oligomers (Ph-~EDOT)*n*-Ph) were recently synthesized (Apperloo *et al*., 2002) (Fig. 3.). These oligomers are

stable in air because the phenyl groups block the α positions in the thiophene rings. The oligomers are expected to form crystalline condensed films, as is the case for oligothiophenes, (Horowitz *et al*., 1996; Horowitz *et al*., 2000) which may result in high charge-carrier mobilities. Furthermore, EDOT-based oligomers have a more rigid planar π-electron system compared to oligothiophenes due to *intrachain* interactions mediated by sulfur and oxygen atoms (Apperloo *et al*., 2002), and therefore may stack more efficiently. In addition, the phenyl-capped EDOT oligomers are solution processable.

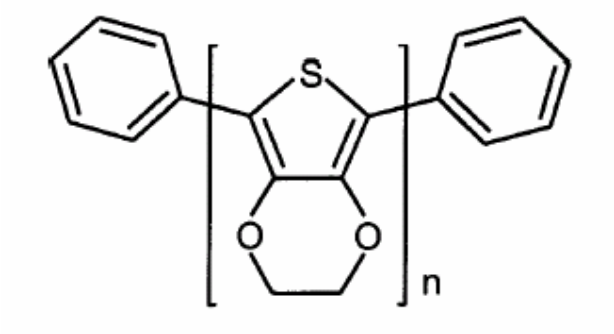

Figure 3 Chemical structure of phenyl-capped oligo~3,4-ethylenedioxy-thiophene (Apperloo *et al*., 2002).

The electronic structure of a series of phenyl-capped 3,4-ethylenedioxy-thiophene oligomers has been studied using ultraviolet photoelectron spectroscopy (UPS) in combination with theoretical calculations (Osikowicz *et al*., 2003). The calculations were performed for isolated oligomers within the framework of density-functional theory, using the Becke1Lee–Yang–Parr exchange-correlation functional. Excellent agreement between the UPS spectra and the quantum-chemical calculations allowed for unambiguous interpretation of the results. They use the asymptotic extension of electronic properties of oligomers to discuss the electronic structure of neutral poly(3,4-ethylenedioxythiophene). In addition, experimentally determined ionization potentials for thin films prepared by vapor deposition and spin coating are reported, and are found to depend on the preparation method. The discrepancy is assigned to differences in the molecular packing. The results show that theory based on RHF calculations is not adequate, when used to simulate the UPS spectra. Calculations were then performed for isolated oligomers within the DFT framework,

using the B3LYP functional. Excellent agreement between the experimental data and UPS spectra simulated on the basis of DFT results was obtained. This points to the role of electron correlation effects and allows for an unambiguous interpretation of the experimental data. Moreover, they have reported a monotonical decrease of the IP's with respect to the increased number of double bonds in the oligomers. This allows for an estimation of the IP of even larger oligomers, according to: IP[eV]=9.8/NDB+4.2. Differences in the IP for spin coated versus vapor deposited films were observed. A systematic decrease of the IP's for vapor deposited films was observed upon heating, with resulting values similar to those measured in spin coated films at high temperature. The temperature induced modifications of the IP were related to changes in the molecular packing. Based on the data for the oligomers, they estimated the bulk IP of the neutral PEDOT polymer to be 4.2 eV. The frontier band structure can be predicted from the evolution of the spectral features in the investigated series of oligomers. Similarly to polythiophene, the highest occupied and dispersed band arises from the overlap of EDOT orbitals that have a strong contribution on the C_α carbon atoms, but none on the sulfur atom, whereas the formation of a localized band involves overlap of orbitals with negligible amplitude on the carbon atoms in C_α position.

Theoretical investigation on PEDOT

There are several theoretical studies that investigate physical and chemical properties of poly(3,4-ethylenedioxythiophene) and its derivatives. Geometric and electronic structures were studied by quantum-chemical calculations (Dkhissi *et al*., 2002). The relative stability of the two possible structures for PEDOT (aromatic-like and quinoid-like) has been evaluated on oligomers of increasing size. The results obtained on PEDOT are compared to those collected on polythiophene and polyisothianapthalene, i.e., two parent conjugated polymers that are known to possess an aromatic and quinoid ground state respectively. The calculations indicate that the ground state of neutral PEDOT is aromatic-like. Moreover, the geometric and electronic structure of 3,4-ethylenedioxythiophene oligomers have been calculated with and *Ab initio* Hartree–Fock (HF/6-31G) method (Dkhissi *et al*., 2002). In order

to understand the influence of oxidized sulfon units on the electronic structure and optical properties of PEDOT, different octamers, differing by the amount and position of the rings bearing a SO_2 group were studied. The calculations indicate that the optical transitions are shifted with respect to the pure PEDOT. These shifts are due to the charge transfer or the large twisting angles between the repeating units in the polymers. Hong (2003) compared the conformation and electronic structures of poly(3,4-ethylenedioxythiophene) and poly(3,4-ethylenedothiathiophene) (PEDTT) in the neutral and doped states through AM1 band calculations and modified extened Hückel band calculations. The calculations indicate that in the neutral states, PEDOT possess a quite flat potential curve ranging from helical angles of 60°-120°. PEDTT has a deep potential curve at the twisting angle of 90°. In the doped states, both polymers become planar and possess zero band gaps.

Aleman *et al*. (2004) studied the molecular geometry, torsional potential, and selected electronic properties (ionization potential and band gap) of the 3,4-ethylenedioxythiophene dimer in both neutral and doped (radical cation) states by using quantum mechanical methods. Calculations were performed using the HF, B3LYP, B3PW91, MPW1PW91, and MP2 methods and the 6-31G*, 6-31+G**, and 6-311++G** basis sets. In all cases, calculations on the neutral and radical states were carried out considering the restricted and unrestricted formalisms, respectively. Results have been compared with experimental data when available. Furthermore, five derivatives of the 3,4-ethylenedioxythiophene dimer were built by changing the heteroatoms at both the five- and six-membered rings. Their conformational and electronic properties were studied using B3PW91/6-31+G** calculations. Results indicated that the material generated by interchanging the positions of the oxygen and sulfur atoms with respect to the parent compound presents very promising properties. Moreover, *ab initio* and DFT quantum mechanical calculations on the structure and the electronic spectral of 2,3-ethylenedioxythiophene-, thiophene- and 2,3-ethylenedithiafurane-containing oligomers have been studied (Aleman *et al*., 2005). Calculations were performed on oligomers formed by *n* repeating units, where *n* ranges from 1 to 8. The bond-length alternation patterns in the -system, the importance of long-range interactions in the stabilization of oligomer chains, the

energies of the HOMO and LUMO orbitals and the values of the lowest transition energy have been examined allowing a systematic comparison among the three families of conducting polymers. Results indicate that the planar *anti* conformation is not stable for *n*-EDTF due to the strong repulsive interactions between the sulfur atoms of rings *i* and *i* + 2, while *n*-EDOT tends to adopt this conformation. The preference of *n*-EDTF by the *anti–gauche* conformation produces a favorable stabilization energy when *n* increases, which was not detected in the oligomers with a planar conformation. These stabilizing effects are due to the interactions between the dipoles of the EDTF units. On the other hand, comparison of the bond length alternation patterns revealed that the contribution of the quinoid form to the aromatic-like electronic structure of the investigated oligomers is lager for *n*-EDTF than for *n*-EDOT and *n*-THP. However, calculation of the electronic properties reveals that the lowest IP and Eg correspond to the *n*-EDOT oligomers. Comparison between results obtained for *n*-EDOT and *n*-THP indicates an excellent agreement with experimental data. Regarding *n*-EDTF oligomers, it should be noted that the inter-change of the heteroatoms with respect to *n*-EDOT does not improve the IP or Eg.

Poly(3,4-ethylenedioxythiophene) doped with poly(4-styrene-sulphonate) (PSS) has been widely used in light emitting devices as the hole transport layer and in photovoltaic devices as the hole-collecting layer. Various quantum chemical calculations were carried out for the investigation of low-lying excited states of ethylenedioxythiophene, and styrenesulphonic acid (Agalya *et al*., 2004). The lowest adiabatic transition energies were calculated using the configuration interaction singles method. The time-dependent density functional theory was also applied for the calculation of the vertical excitation energies. Differential self-consistent-field-based density functional theory is well known to show good performance for the geometry of the excited state and hence it was also applied to study the first singlet excited state. In addition to the calculation of the monomer, the electronic properties of PEDOT were calculated by the periodic density functional theory method. Results indicated that the first excited state is mainly due to the orbital contribution from HOMO to LUMO level for ethylenedioxythiophene. The high oscillator strength values show the most intense transition during the excitation process. The bandgap

energy for PEDOT is evaluated by periodic DFT method and it decreases with increments in the number of repeating unit in the periodic unit cell. The calculated energy gap for PEDOT with tetramer repeating units agrees reasonably well with the experimental value.

Yang *et al*. (2005) studied three fluorene-based copolymers, copoly(2,5-ethylenedioxythiophene-*alt*-9,9¢-dimethylfluorene) (PEF), copoly(2,5-pyridine-*alt*-9,9¢-dimethylfluorene) (PPyF), and poly [(fluorene-2,7-diyl)-*alt*-(1,3,4-oxadiazole-2,5-diyl)] (PFO), in which ¢H-L [the energy difference between the highest occupied molecular orbital (HOMO) and the lowest unoccupied molecular orbital (LUMO), when $n = \infty$], the lowest excitation energies (Eg), ionization potentials (IP), electron affinities (EA), and λ_{abs} and λ_{em} are fine-tuned by the regular insertion of electron-donating unit 3,4-ethylenedioxythiophene or electron-withdrawing units pyridine and 1,3,4-oxadiazole. The results show that the alternate incorporation of electron-donating moiety EDOT increases the HOMO energy and thus reduces the IPs, and consequently the hole injection was greatly improved. On the other hand, even though both kinds of charge carriers improve the electron-accepting ability, the results show that electron-withdrawing moieties greatly facilitate electron transport. Especially in PFO, the highly planar structural character results from the strong push-pull effect between the fluorene ring and the 1,3,4-oxadiazole ring and a weak interaction between the nitrogen and oxygen atoms in the 1,3,4-oxadiazole ring and the hydrogen atom of the fluorene ring, significantly lowering the LUMO energy levels and thus improving the electron-accepting and transporting properties by the low LUMO energy levels.

METHODS OF CALCULATIONS

1. Models Setup

In this study, PEDOT oligomers and its derivatives were studied. The molecular structure models are shown in Fig. 4. The geometries of PEDOT and its derivatives oligomers were generated by HyperChem 7.0 program. Then, all calculations were carried out by the GAUSSIAN 03 program running on a Linux PC 2.5 GHz.

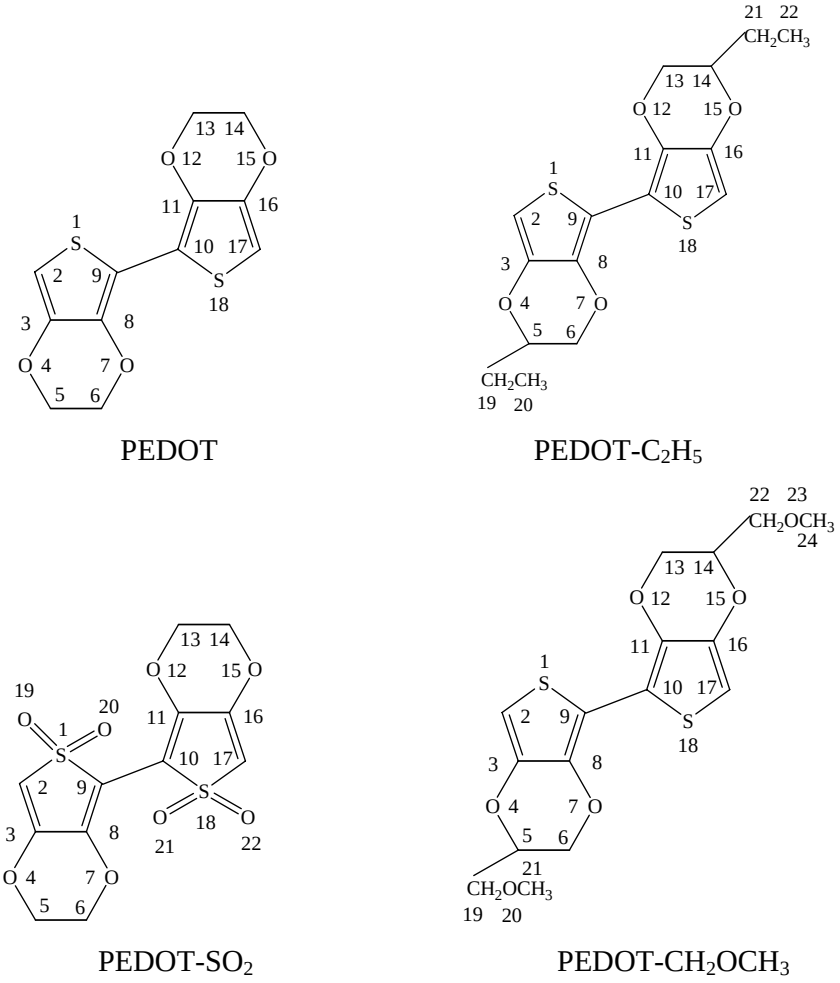

Figure. 4 Molecular structures of PEDOT and its derivatives, used in this studied.

The alkyl groups at the 5 and 14 positions of the EDOT unit of PEDOT-$C_{14}H_{29}$ and PEDOT-$CH_2OC_{14}H_{29}$ were replaced by ethyl and methyl groups to reduce calculating time. It was found that the presence of alkyl groups at the 5 and 14 positions does not significantly effect on the equilibrium geometry of PEDOT derivatives. Moreover, the length of the long side chains located at EDOT unit does not significantly effect the electronic properties of the polymer. Therefore, it was found that HOMO-LUMO energy difference does not change significantly when the alkyl group increases as illustrated in Table 1. Furthermore, the excitation energies are also shown in Table 2. Calculated results were not only found for PEDOT-$C_{14}H_{29}$ but also in the same way for the case of PEDOT-$CH_2OC_{14}H_{29}$. Consequently, the models used in this study are shown in Fig. 5.

Table 1 HOMO-LUMO energy difference of EDOT monomer and dimer when the alkyl group at EDOT unit increases. B3LYP/6-31G* method was used for calculations.

R	Monomer			Dimer		
	E(HOMO) (eV)	E(LUMO) (eV)	ΔE (eV)	E(HOMO) (eV)	E(LUMO) (eV)	ΔE (eV)
H	-8.51	3.86	12.37	-4.86	-0.81	5.67
CH_3	-8.51	3.86	12.37	-4.80	0.75	5.50
C_2H_5	-8.51	3.86	12.37	-7.20	2.80	10.00
C_3H_7	-8.52	3.85	12.37	-7.20	2.80	10.00
C_4H_9	-8.50	3.87	12.37	-7.20	2.80	10.00
C_5H_{11}	-8.51	3.86	12.37	-7.20	2.80	10.00
C_6H_{13}	-8.47	3.89	12.36	-7.22	2.78	10.00
C_7H_{15}	-8.47	3.89	12.36	-7.22	2.78	10.00
C_8H_{17}	-8.47	3.89	12.36	-7.20	2.80	10.00
C_9H_{19}	-8.47	3.90	12.37	-7.20	2.80	10.00
$C_{10}H_{21}$	-8.48	3.89	12.37	-7.21	2.79	10.00

Table 2 Excitation energy of EDOT monomer and dimer when the alkyl group at EDOT unit increases. TDB3LYP/6-31G**//B3LYP/6-31G* method was used for calculations. (The longer side chain was not calculated due to the constant value of the excitation energy starting from propyl group).

R	Monomer		Dimer	
	Excitation energy (eV)	Oscillator strength	Excitation energy (eV)	Oscillator strength
H	5.31	0.1596	3.89	0.4784
CH_3	5.42	0.1557	3.89	0.5024
C_2H_5	5.42	0.1598	4.13	0.5086
C_3H_7	5.42	0.1579	4.12	0.5247
C_4H_9	5.42	0.1596	4.12	0.5433
C_5H_{11}	5.42	0.1664	4.12	0.5453

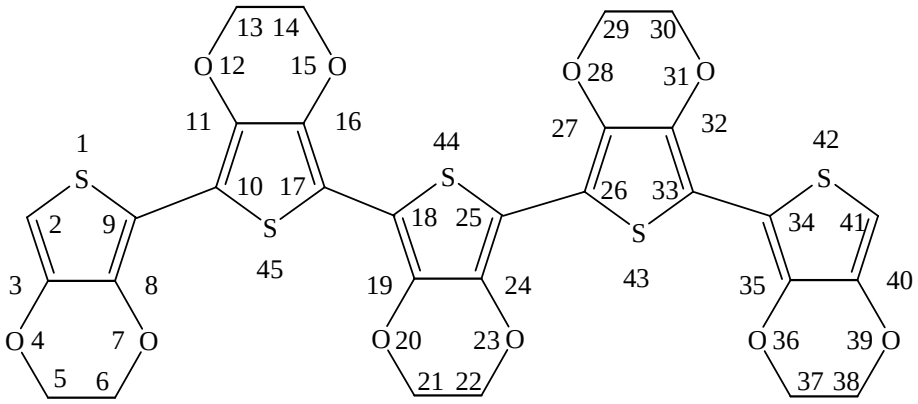

PEDOT

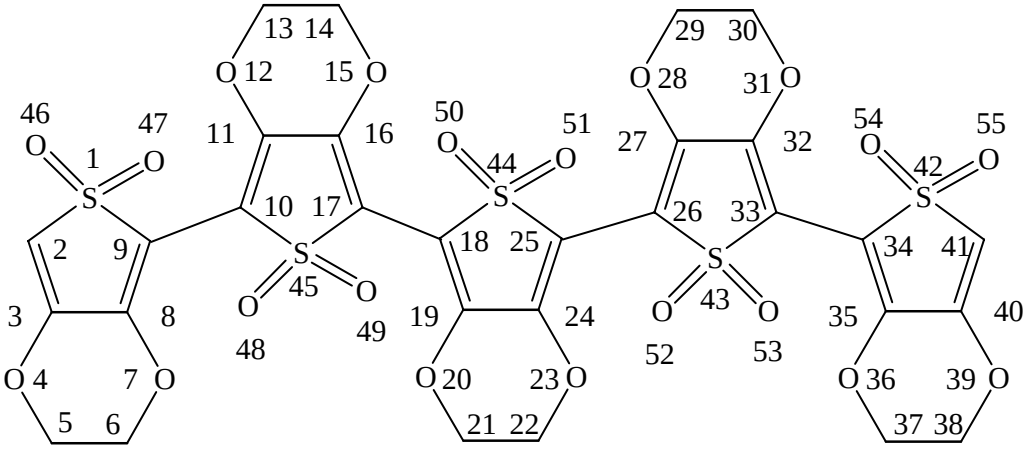

PFDOT-SO_2

Figure 5 Models and atomic numbering of PEDOT and its derivatives used in this study.

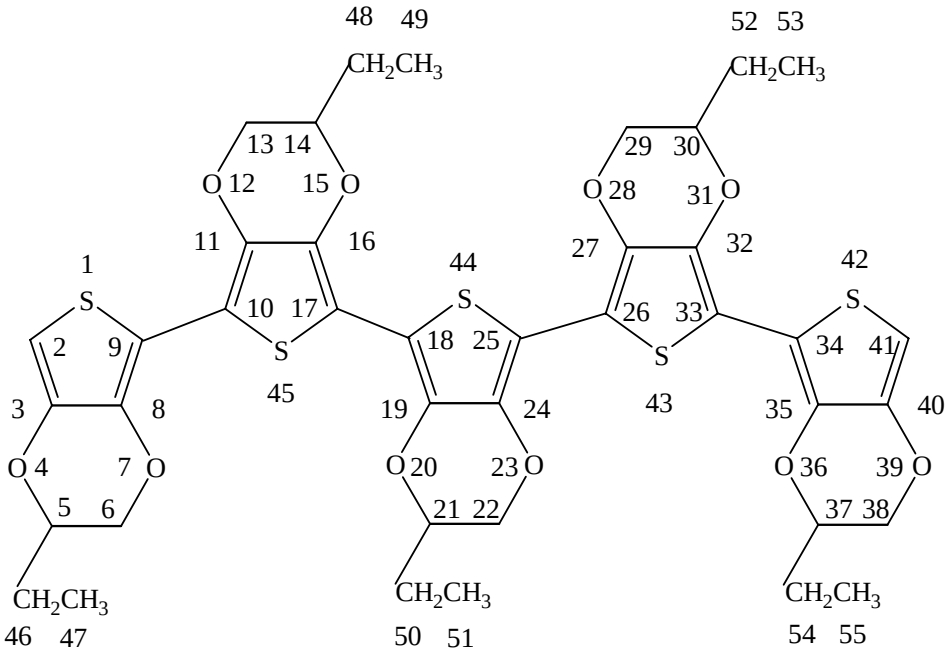

PEDOT-C_2H_5

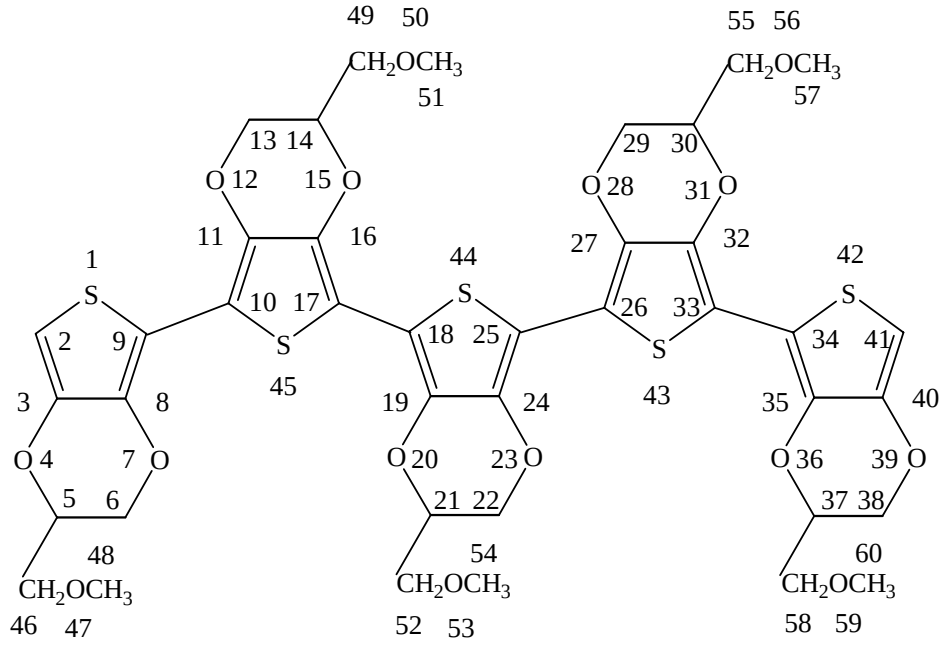

PEDOT-CH_2OCH_3

Figure 5 (cont'd)

2. Conformational Analysis and Geometrical Optimization

Potential energy curves of EDOT dimer were investigated at the semi-empirical AM1, *ab initio* (at HF/6-31G* and HF/6-31+G* levels), and density functional theory (at B3LYP/6-31G* and B3LYP/6-31+G* levels) methods. Conformational analysis was done by changing the torsional angle (θ = C8-C9-C10-C11) by 12 steps between θ = 0° and θ = 360°. To obtain the final torsional angles of the conformers in each minima, calculations of these geometries were performed without constraint on the dihedral angle.

In case of PEDOT-C_2H_5, PEDOT-SO_2 and PEDOT-CH_2OCH_3 dimer, the ground-state potential energy curves along the torsional angle (θ = C8-C9-C10-C11) were calculated by using the B3LYP/6-31G* level. In the calculations, the torsional angle was changed by 12 steps between θ = 0° and θ = 360°, whereas all the other geometrical parameters were fixed.

3. Electronic property of poly(3,4-ethylenedioxythiophene) (PEDOT) and Its Derivatives

Energy gap

Estimated energy gaps of the polymer were obtained by plotting the HOMO-LUMO energy differences calculated by using the semi-empirical (AM1), *ab initio* (at HF/6-31G* and HF/6-31+G* levels), and density functional theory (at B3LYP/6-31G* and B3LYP/6-31+G* levels) methods and the inverse of the number of monomer units (1/N) and extrapolating the number of units to infinity. In the case of excitation energies, we calculated by using the semi-empirical (ZINDO) and time-dependent density functional theory (TDDFT) methods at the optimized geometries of the ground state using the different methods (semi-empirical(AM1), *ab initio* and density functional theory methods). Energy gap estimated from excitation energies was also performed in the similar manner for all polymers studies.

RESULTS AND DISCUSSION

1. Conformational and Structural Analysis

At the beginning, the conformational analysis was carried out. The partial optimized torsional angle (θ) for the electronic ground state between EDOT part were performed by semi-empirical (AM1), *ab initio* (at HF/6-31G* and HF/6-31+G* levels) and density functional theory (at B3LYP/6-31G* and B3LYP/6-31+G* levels) methods. The relative potential curves of the obtained results for EDOT dimer are shown in Fig. 6.

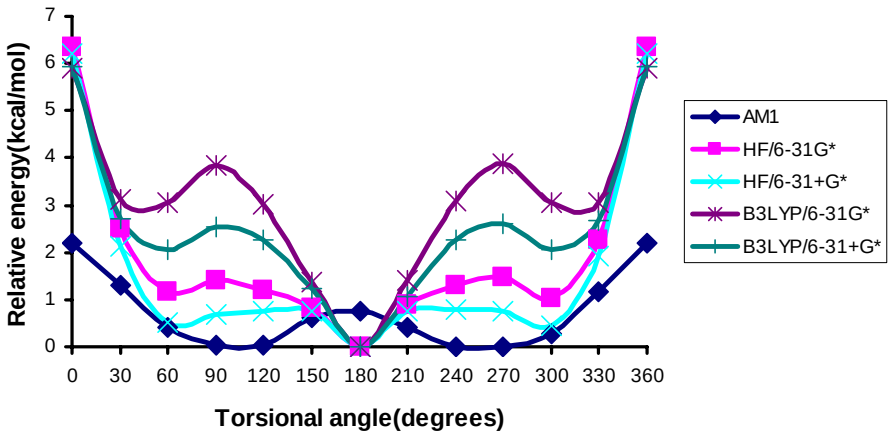

Figure 6 Comparison of potential energy curves as a function of torsional angle (θ = C8-C9-C10-C11) obtained for EDOT dimer. The curves were calculated by the AM1, HF/6-31G*, HF/6-31+G*, B3LYP/6-31G* and B3LYP/6-31+G* methods.

As shown in Fig. 6, it was found that the EDOT dimer is symmetric molecule. The potential energy curves of EDOT dimer calculated from *ab initio* and DFT methods are quite different from the AM1 results. It was found that the potential energy curves calculated from those methods showed two local minima. *Ab initio* (at HF/6-31G* and HF/6-31+G* levels) and DFT (at B3LYP/6-31G* and B3LYP/6-

31+G* levels) methods provided two minima corresponding to θ around 30° – 60° and 180°. In the case of AM1 method, the potential energy curve also showed two local minima corresponding to θ around 90° – 120° and 180°. Moreover, the global minimum predicted by *ab initio* and DFT methods appear at θ = 180° (anti conformation), rather than at θ = 150°. (anti-gauche conformation) as occurs for the thiophene dimer (Aleman *et al*., 1996). Furthermore, the anti-gauche conformation was also characterized as the global minimum for isothianaphthene dimer, in which each unit is formed by the fusion of a benzene ring upon thiophene. Thus, values of θ = 132.9°, θ = 129.9°, and θ = 126.5°. were calculated at the HF/6-31G*, B3PW91/6-31G*, and MP2/6-31G* levels (Viruela *et al*., 1997) respectively, indicating that the reduction of the angle θ alleviates the steric interactions induced by the benzene rings. Similarly, the anti-gauche conformation was predicted as the most stable for polypentafulvalenes, a family of polycyclic compounds in which the two fused rings of each unit are coplanar (Hong 2000). However, the repulsive contacts of EDOT between each sulfur atom and the dioxane fused onto the neighboring thiophene are eliminated by the twist conformation of the six-membered rings. This conformation reduces the C-O-C bond angle increasing the distance between the sulfur and oxygen atoms. Fig 7. shows the anti minimum of EDOT dimer detected at the B3PW91/6-31G* level, in which the twist conformation is specifically displayed. Furthermore, the double bond character of the inter-ring bond of EDOT is larger than those of the thiophene dimer, enhancing the stability of the planar conformation in the former. Therefore, PEDOT with dioxane rings fused onto thiophene rings presents less steric hindrances than those encountered with disubstituted polythiophene. The oxygen atoms, which are directly attached at the 3- and 4-positions, exert an electron donating effect that reduce the band gap. The conformations of EDOT dimer at the different torsional angles calculated at B3LYP/6-31G* level are shown in the Fig. 8.

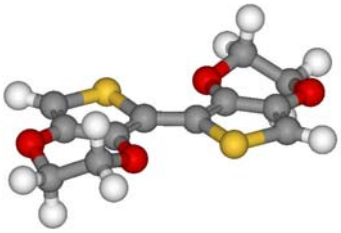

Figure 7 Molecular structure of the anti minimum obtained for EDOT dimer at the B3PW91/6-31G* level. The twist conformation of the fused dioxane rings is illustrated. (Aleman *et al*., 2004)

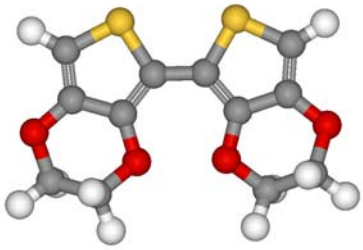

(a)

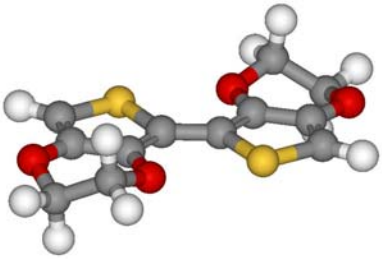

(b)

Figure 8 Conformations of EDOT dimer calculated by the B3LYP/6-31G* level.
a) syn conformation (θ = 90°) b) syn-gauche conformation (θ = 50°)
c) gauche-gauche conformation (θ = 90°)
d) anti conformation (θ = 180°)
e) anti-gauche conformation (θ = 150°)

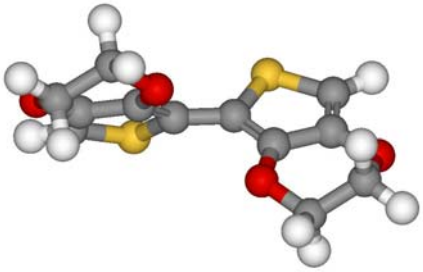

(c)

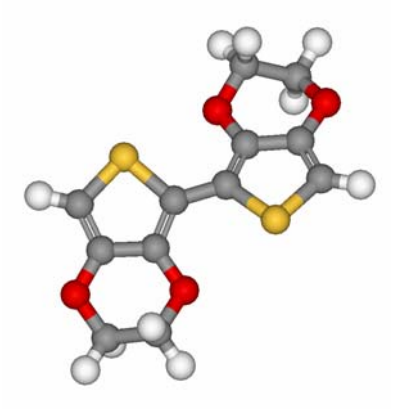

(d)

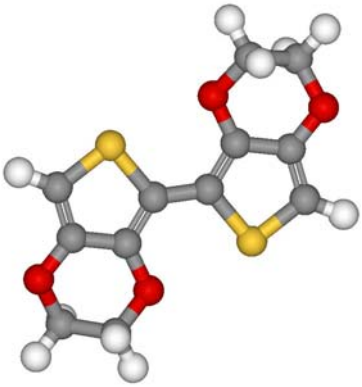

(e)

Figure 8 (cont'd)

A local minimum appears for EDOT dimer at θ ~ 50° (syn-gauche conformation), which is about 1.0-3.0 kcal/mol less stable than the global minimum. Both minima are separated by the gauche-gauche barrier at θ = 90°. This is unfavored by about 1.50-3.80 and 0.80-2.68 kcal/mol with respect to the anti and syn-gauche minima. All calculations were done by the HF and DFT methods in conjunction with the 6-31G* basis set.

The electronic density contours of the frontier orbitals for EDOT dimer at the different torsional angles calculated at B3LYP/6-31G* level are shown in Fig. 9. Accordingly, it was found that the electronic density contours of the frontier orbitals for EDOT dimer at syn-gauche and gauche-gauche conformations are quite different as compared with the others. Whereas, the electronic density contours of the frontier orbitals at syn conformation shows electronic density contours of the frontier orbitals similar with anti conformation. However, the conformer at syn conformation give a higher relative energy (Fig. 6) than anti conformation due to the steric hindrance. Considering the LUMO at syn-gauche and gauche-gauche conformations, it was found that the LUMO for these conformations are less delocalized compared with the others. This brings us to the fact that syn-gauche and gauche-gauche conformations give a high rotational potential energy due to the steric hindrance. This means that syn conformation, syn-gauche conformation and gauche-gauche conformation are not stable for EDOT dimer.

HOMO LUMO

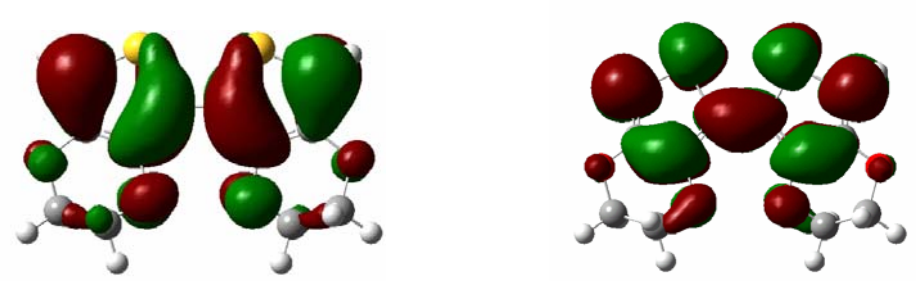

(a)

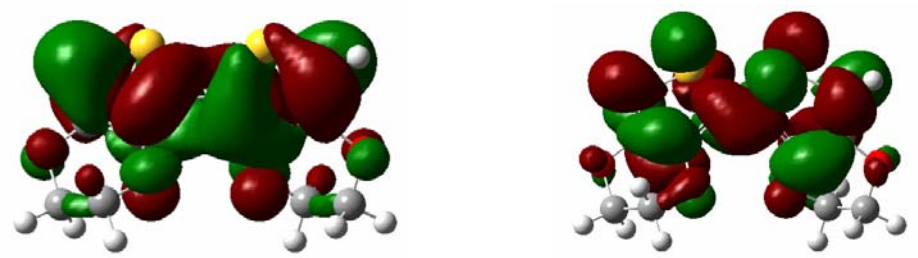

(b)

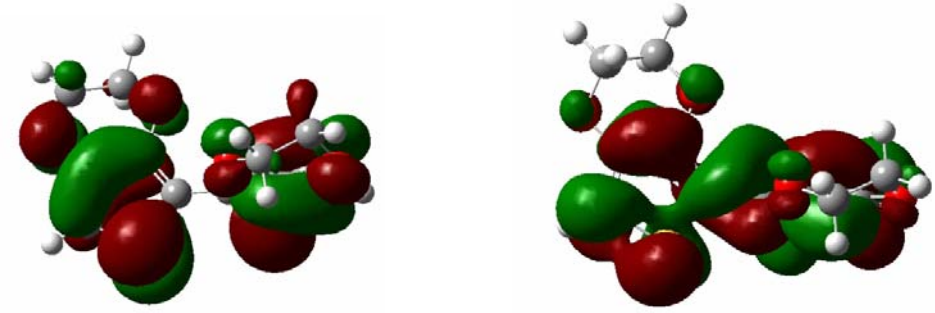

(c)

Figure 9 Electronic density contours of the frontier orbitals for EDOT dimer calculated by the B3LYP/6-31G* level.

a) syn conformation b) syn-gauche conformation

c) gauche-gauche conformation d) anti conformation

e) anti-gauche conformation

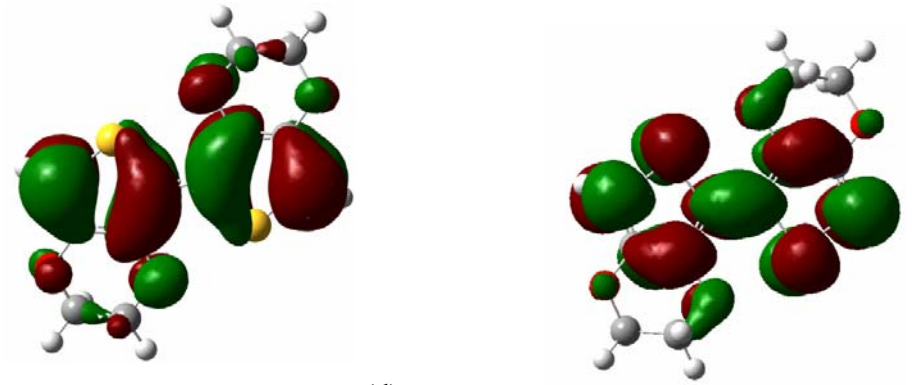

(d)

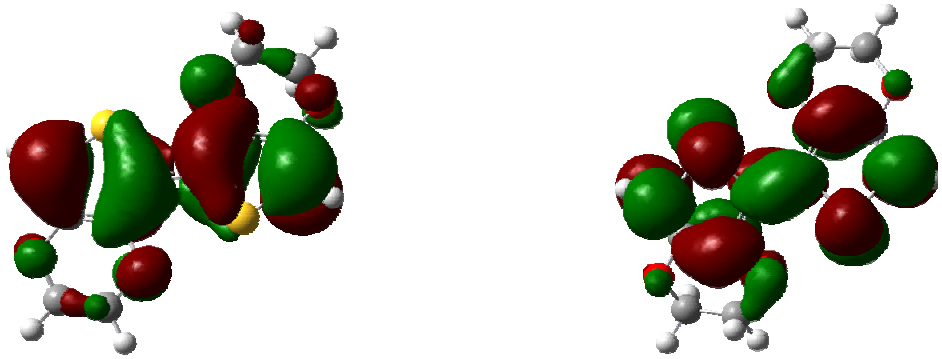

(e)

Figure 9 (cont'd)

Comparison between the AM1 and HF curves and those obtained with the DFT methods. It indicates that the former does not provide a precise representation of the torsional potential energy of EDOT dimer, which is due to the neglection of electron correlation effects. Thus, the energies of the syn-gauche and gauche-gauche conformations are underestimated about 1.89 and 2.62 kcal/mol respectively, by the noncorrelated methods in the conjunction with the 6-31G* basis set. Furthermore, the AM1 and HF methods provide the syn-gauche minimum at $\theta = 107°$ and 56° respectively, this value being at least 57° and 6° higher than that predicted by the B3LYP method in conjuction with the 6-31G* basis set. The influence of the basis set in the rotational barrier of EDOT dimer was compared. As can be seen, the relative energies of EDOT dimer are overestimated when diffuse functions are not considered. Thus, the 6-31G* basis set gives relative energy higher than 6-31+G* by about 10-50%.

The ground state geometry parameters of PEDOT pentamer as obtained from AM1, a*b initio* and density functional theory are shown in Table 5. The numbering of the atoms is assigned in Fig. 5. Accordingly, it was found that the geometries obtained from *ab initio* are not significantly different as compared with those obtained from DFT methods. They showed an anti coplanar structure at ground state. However, C-C and C-S bond distances calculated from *ab initio* method are shorter than those from DFT method by about 0.2 Å. In addition, C-C and C-S bond distances calculated from AM1 method are shorter than those from *ab initio* and DFT methods. Moreover, the C=C and C-O bond distances calculated from AM1 methods are quite similar to those from DFT method, while *ab initio* shows shorter C=C and C-O bond distances as compared with those methods. Kwon *et al*. (2000) used DFT and AM1 method calculations for thiophene oligomer geometries. They found that optimized geometries of DFT method are in excellent agreement with the solid state structures. In their work, calculated C-C inter-ring bond distances (~1.45 Å) and C-S bond distances (~1.75 Å) at the B3LYP/6-31G* level are almost equal to experiment (C-C, 1.45 Å; C-S, 1.75 Å), while bond distances calculated from AM1 (C-C, 1.42 Å; C-S, 1.58 Å) are shorter than experiment due to the nature of the AM1 parametrization. In this work, C-C inter-ring bond distances calculated at the B3LYP/6-31G* level (1.44 Å) are found to be shorter as compared with the C-C inter-ring bond distances of the thiophene units obtained from the solid state structures. Nevertheless, the C-S bond distances calculated at the B3LYP/6-31G* level are quite different than the C-S bond distances of the thiophene unit obtained from the solid state. It was found that the C-S bond distances obtained from those methods at the outside (C-S = 1.73 Å) are shorter than at the center of the polymer backbone (C-S = 1.77 Å), while the C-S bond distances of the thiophene units are quite similar along the main chain of the structure (Table 4). This brings us to the fact that the dioxane group which is attached at thiophene units have effect on the thiophene geometries.

Table 3 Comparison of the C-C bond distances of PEDOT obtained from the B3LYP/6-31G* level with polythiophene x-ray structure[(a)].

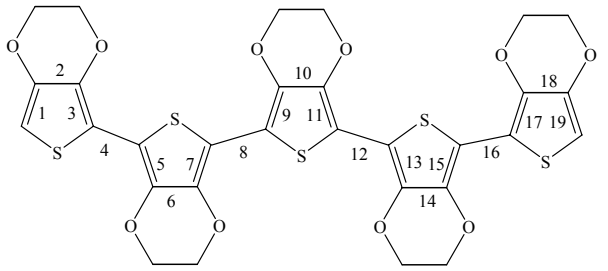

Bond number	Bond distance (angstrom)	
	Polythiophene[(a)]	PEDOT
1	1.342	1.365
2	1.408	1.429
3	1.388	1.381
4	1.439	1.439
5	1.355	1.381
6	1.405	1.418
7	1.364	1.382
8	1.444	1.435
9	1.370	1.382
10	1.400	1.417
11	1.380	1.382
12	1.444	1.436
13	1.367	1.382
14	1.403	1.418
15	1.376	1.381
16	1.441	1.439
17	1.370	1.381
18	1.405	1.429
19	1.378	1.365

[(a)] Horowitz *et al*. (1995)

Table 4 Comparison of the C-S bond distances of PEDOT obtained from the B3LYP/6-31G* level with polythiophene x-ray structure [(a)].

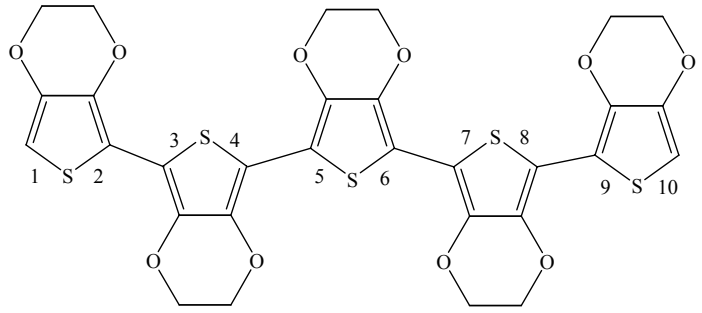

Bond number	Bond distance (angstrom)	
	Polythiophene[(a)]	PEDOT
1	1.709	1.739
2	1.730	1.767
3	1.736	1.766
4	1.738	1.768
5	1.731	1.767
6	1.739	1.767
7	1.732	1.767
8	1.734	1.768
9	1.732	1.766
10	1.734	1.739

[(a)] Horowitz *et al*. (1995)

Table 5 Ground state geometrical parameters of the PEDOT pentamer, obtained from AM1, HF/6-31G*, HF/6-31+G*, B3LYP/6-31G* and B3LYP/6-31+G* methods. (bond distance in angstrom and bond angle in degrees)

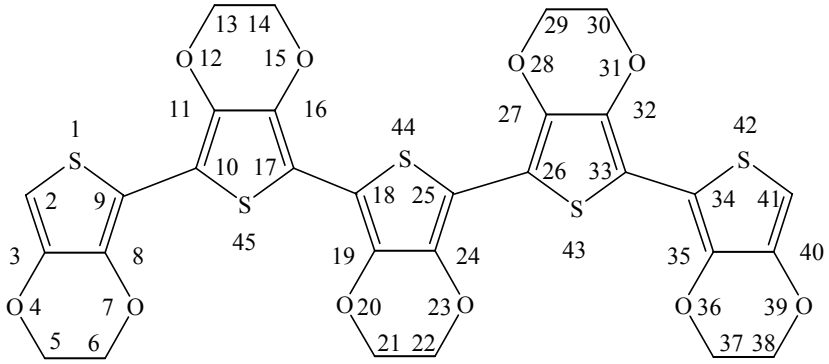

Geometrical parameter	Method				
	AM1	HF/ 6-31G*	HF/ 6-31+G*	B3LYP/ 6-31G*	B3LYP/ 6-31+G*
Bond distance					
S1-C2	1.667	1.727	1.727	1.739	1.739
C2-C3	1.377	1.339	1.341	1.365	1.366
C3-O4	1.376	1.352	1.351	1.371	1.372
O4-C5	1.437	1.409	1.410	1.431	1.434
C5-C6	1.521	1.515	1.515	1.522	1.523
C6-O7	1.437	1.410	1.411	1.432	1.434
O7-C8	1.375	1.351	1.351	1.371	1.371
C8-C9	1.385	1.352	1.354	1.381	1.383
C9-C10	1.425	1.459	1.459	1.439	1.441
C1-C11	1.386	1.350	1.351	1.381	1.382
C11-O12	1.376	1.351	1.351	1.371	1.371
O12-C13	1.437	1.410	1.411	1.432	1.435
C13-C14	1.521	1.515	1.515	1.522	1.523
C14-O15	1.437	1.409	1.410	1.432	1.434
O15-C16	1.376	1.351	1.351	1.371	1.371
C16-C17	1.386	1.351	1.352	1.382	1.384

Table 5 (cont'd)

Geometrical parameter	Method				
	AM1	HF/6-31G*	HF/6-31+G*	B3LYP/6-31G*	B3LYP/6-31+G*
C17-C18	1.426	1.457	1.458	1.435	1.437
C18-C19	1.386	1.351	1.352	1.382	1.384
C19-O20	1.376	1.351	1.351	1.371	1.371
O20-C21	1.437	1.409	1.410	1.431	1.434
C21-C22	1.521	1.515	1.515	1.522	1.522
C22-O23	1.437	1.409	1.410	1.431	1.434
O23-C24	1.376	1.351	1.351	1.371	1.372
C24-C25	1.386	1.351	1.352	1.382	1.384
C25-C26	1.426	1.457	1.458	1.436	1.437
C26-C27	1.386	1.351	1.352	1.382	1.384
C27-O28	1.376	1.351	1.351	1.371	1.371
O28-C29	1.437	1.409	1.410	1.432	1.434
C29-C30	1.521	1.515	1.515	1.522	1.522
C30-O31	1.437	1.410	1.411	1.432	1.435
O31-C32	1.376	1.351	1.351	1.371	1.371
C32-C33	1.386	1.350	1.351	1.381	1.382
C33-C34	1.425	1.459	1.459	1.439	1.440
C34-C35	1.385	1.352	1.354	1.381	1.383
C35-O36	1.375	1.351	1.351	1.371	1.371
O36-C37	1.437	1.410	1.411	1.432	1.435
C37-C38	1.521	1.515	1.515	1.522	1.522
C38-O39	1.437	1.409	1.410	1.431	1.434
O39-C40	1.376	1.352	1.351	1.371	1.372
C40-C41	1.377	1.339	1.410	1.365	1.366
C41-S42	1.667	1.727	1.727	1.739	1.739
S42-C34	1.693	1.751	1.749	1.767	1.766

Table 5 (cont'd)

Geometrical parameter	Method				
	AM1	HF/ 6-31G*	HF/ 6-31+G*	B3LYP/ 6-31G*	B3LYP/ 6-31+G*
C33-S43	1.684	1.748	1.748	1.766	1.765
S43-C26	1.684	1.749	1.748	1.768	1.767
C25-S44	1.683	1.749	1.748	1.767	1.766
S44-C18	1.683	1.749	1.748	1.767	1.766
C17-S45	1.684	1.749	1.748	1.768	1.767
S45-C10	1.684	1.748	1.748	1.766	1.765
C9-S1	1.693	1.751	1.749	1.768	1.766
C3-C8	1.440	1.435	1.435	1.429	1.429
C11-C16	1.438	1.428	1.428	1.418	1.418
C19-C24	1.437	1.428	1.428	1.417	1.417
C27-C32	1.438	1.428	1.428	1.418	1.418
C35-C40	1.440	1.435	1.435	1.429	1.428
Torsional angle					
C8-C9-C10-C11	107.2	179.9	179.9	179.7	179.9
C16-C17-C18-C19	106.9	179.5	179.4	179.6	179.9
C24-C25-C26-C27	106.9	179.5	179.4	179.7	179.8
C32-C33-C34-C35	107.1	179.4	179.6	179.6	179.5

Moreover, C-C bond distances in the thiophene unit of the EDOT pentamer are also different with the thiophene oligomers. This revealed that the dioxane group which is attached at thiophene unit affects on the thiophene geometries. Thus**,** using AM1 and HF methods, π-electrons are more localized, this is due to the neglect of electron correlation. Comparing PEDOT with the polythiophene, the addition of a dioxane group at positions 3 and 4 of the thiophene unit does significantly affect the bond length of the thiophene rings including the inter-ring bond distance. This is obvious because the steric hindrance was caused by the dioxane group. Furthermore, PEDOT provides planar structures having the torsional angle about of 180°. Aleman

et al. (2004) have studied structure and electronic properties of PEDOT. They found that the C-C and C-S bond distances calculated by *ab initio*, DFT and MP2 methods are quite different with the thiophene units. Comparing *ab initio* and DFT methods, Dkhissi *et al*. (2002) found that the structures obtained from *ab initio* are consistent with a localized character of the charge, whereas the DFT method tends to delocalize the geometric modifications. A possible explanation presented by Siebbeles *et al*. (2002, 2004, 2005) for the higher degree of delocalization in DFT is the presence of electron correlation. They pointed out that the two methods are developed from different monoelectronic operators with different theoretical frameworks. DFT includes the electron correlation, whereas in *ab initio* calculations, the dynamic correlation is not taken into consideration. The extent to which electron correlation is taken into consideration has a large effect on the delocalization of excess charge. Moreover, the DFT results suggest that the existence of localized charges in solids should be attributed to impurities or defects in the films or crystals. These defects were caused by chemical natures, such as polymerization mistakes causing cross-links or broken conjugation. Moreover, the localization of charges can be induced by conformational defects caused by interchain interactions. However, it has also been suggested that the delocalization in DFT is an artifact due to the approximate description of the exchange interaction. To gain insight into the effects of the exchange part of the functional on the charge delocalization, Fratiloiu *et al*. (2005) employed BLYP and B3LYP to calculate charge distributions. The results show that the effect of improving the description of the exchange interaction does not lead to a significant localization of the charge. The presence of electron correlation is responsible for increasing the charges delocalization.

Considering the geometries obtained from the DFT method (at B3LYP/6-31G* and B3LYP/6-31+G* levels), it was found that the geometries are planar. Moreover, the inter-ring bond distances are shorter than those obtained from the HF/6-31G* and HF/6-31+G* calculations. However, comparison between 6-31G* and 6-31+G* basis sets shows that the different basis sets quite similar geometric structure. The optimized geometries of the pentamer as obtained from different methods are shown in Fig. 10. The inter-ring bond distances of the oligomer as

obtained from different methods are also analyzed and plotted against the bond number as shown in Fig. 11.

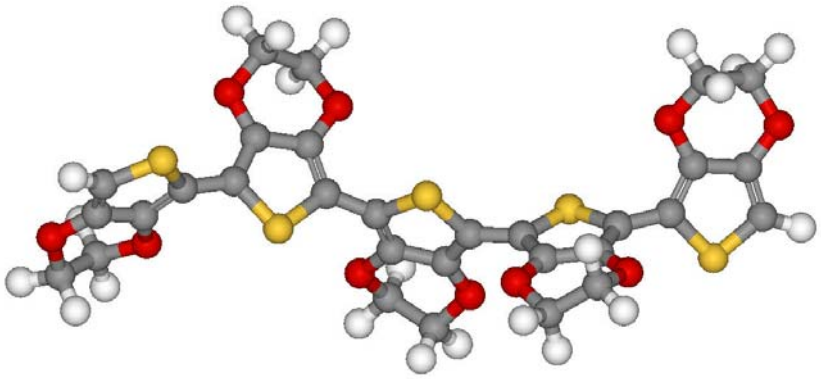

AM1

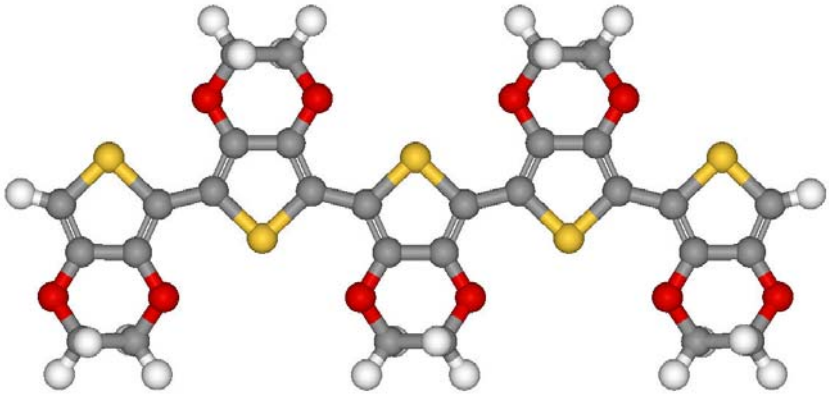

HF/6-31G*

Figure 10 Optimized geometries of PEDOT pentamer obtained from AM1, *ab initio* and DFT methods.

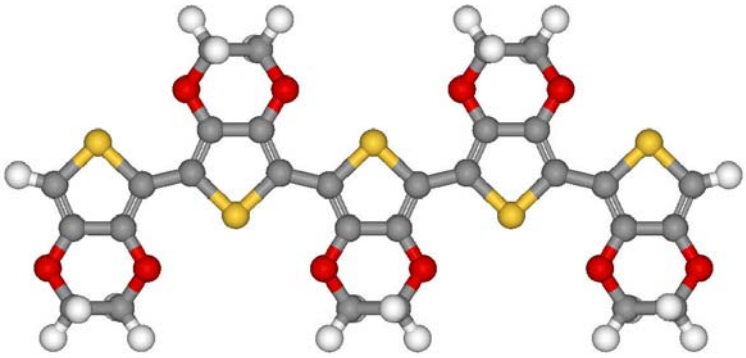

HF/6-31+G*

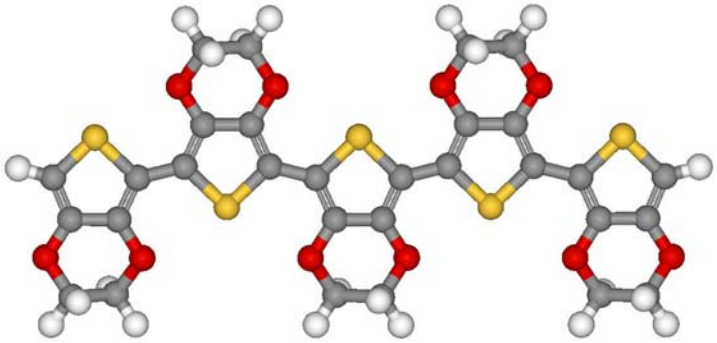

B3LYP/6-31G*

Figure 10 (cont'd)

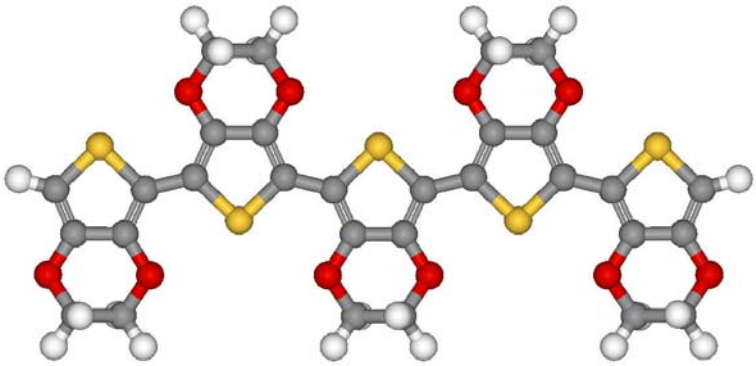

B3LYP/6-31+G*

Figure 10 (cont'd)

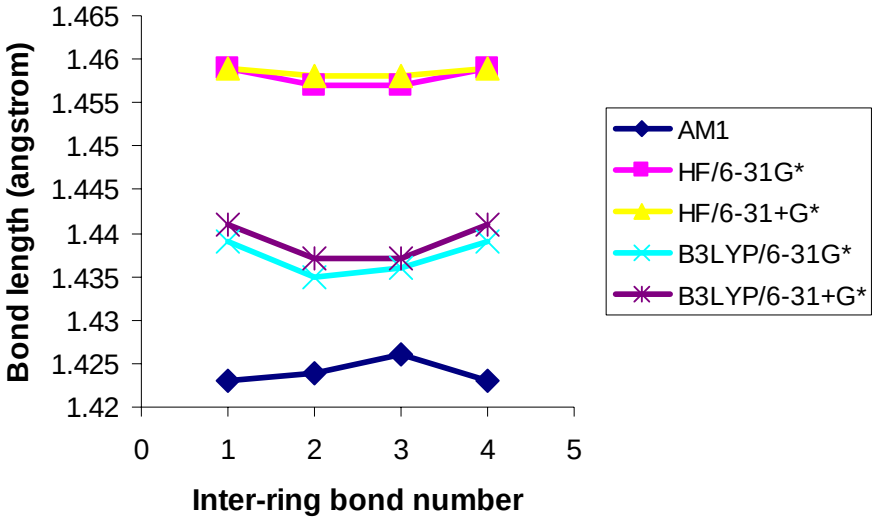

Figure 11 Inter-ring bond distances of PEDOT pentamer obtained from different methods.

Based on the optimized geometries, it is found that the inter-ring bond distances obtained from AM1 method are shorter than those obtained from HF and DFT methods (Fig. 11). Moreover, this shorter inter-ring bond distance does effect the conjugation along the main chain of the structure as obtained from the energy gap calculated by the same method (Table 10.). The planarity of the oligomer significantly increases the conjugation along the main chain. In addition, the inter-ring bond distances obtained from those methods remain constant along the main chain of the structures. As shown in Table 6 the inter-ring torsional angles obtained from the AM1 optimized geometry are smaller than those obtained from HF and DFT methods. Therefore, the geometry of the oligomers obtained from AM1 and *ab initio* methods are not optimal as compared to the results obtained from the DFT method which are well in agreement with experimental data in terms of both structural parameters and energetic results. Also, the inter-ring torsional angle obtained from those methods remain constant along the main chain of the structure.

Table 6 Inter-ring torsional angles of the PEDOT optimized geometries (starting from the left hand side of the optimized geometries as shown in Fig. 5.), obtained from the different methods.

Method	Inter-ring torsional angle (degrees)
AM1	107.2, 106.9, 106.9, 107.1
HF/6-31G*	179.9, 179.5, 179.5, 179.4
HF/6-31+G*	179.9, 179.4, 179.4, 179.3
B3LYP/6-31G*	179.7, 179.6, 179.7, 179.6
B3LYP/6-31+G*	179.9, 179.9, 179.8, 179.5

Potential energy curve calculations of PEDOT-C_2H_5, PEDOT-SO_2 and PEDOT-CH_2OCH_3 were performed by density functional theory (B3LYP/6-31G* level) and provide a reliable geometry in case of PEDOT. They are illustrated in Fig. 12 and 13. Moreover, the optimized geometrical parameters of PEDOT-C_2H_5, PEDOT-SO_2 and PEDOT-CH_2OCH_3 pentamer calculated at B3LYP/6-31G* level

are presented in Table 7. From Fig. 12, this bring us to the fact that PEDOT-C_2H_5 and PEDOT-CH_2OCH_3 dimer molecules posses anti-conformation. Moreover, rotational potential energy curve of PEDOT-C_2H_5 is quite similar to PEDOT-CH_2OCH_3. A comparison of the geometry of PEDOT, PEDOT-C_2H_5, PEDOT-SO_2 and PEDOT-CH_2OCH_3 dimer shows that the torsional angles of PEDOT-C_2H_5, and PEDOT-CH_2OCH_3 dimer molecules are quite similar to EDOT dimer ($\theta = 180°$). This indicates that the side chain is not effective for the dimer of those molecules. However, PEDOT-SO_2 shows a distorted structure with $\theta = 176°$ (Fig. 13). This means that thienyl-S,S-dioxide which is functionalized at the EDOT unit provide a steric effect. Besides that, a very low rotational energy barrier of PEDOT-C_2H_5, PEDOT-SO_2 and PEDOT-CH_2OCH_3 at $\theta \sim 45°$ was observed to allow a wide range of non-planar conformation. In addition, the potential energy curves of PEDOT-C_2H_5, PEDOT-SO_2 and PEDOT-CH_2OCH_3 showed two local minima which are located at $\theta \sim 45°$ and $\theta = 180°$. Interestingly, the conformer with the torsional angle of 45° showed steric hindrance generated from ethyl, methoxy and thienyl-S,S-dioxide groups attached on EDOT unit. Therefore, the energy of this conformer is slightly higher than that located at $\theta = 180°$. This revealed that the molecule posses anti-conformation in the ground state. In addition, a very low rotational energy barrier at $\theta = 180°$ was observed which allows a wide range of anti-conformations. This result is quite similar to the case of EDOT dimer.

Surprisingly, a local minima of PEDOT-C_2H_5, PEDOT-SO_2 and PEDOT-CH_2OCH_3 appeared quite similar with the torsional angle of EDOT dimer molecule ($\theta = 45°$, $\theta = 50°$ respectively). This indicates that the side chain does not effect the dimer of those molecules. Comparison of the potential energy curves of PEDOT-C_2H_5, PEDOT-SO_2 and PEDOT-CH_2OCH_3 revealed that PEDOT-SO_2 shows potential energy higher than those molecules.

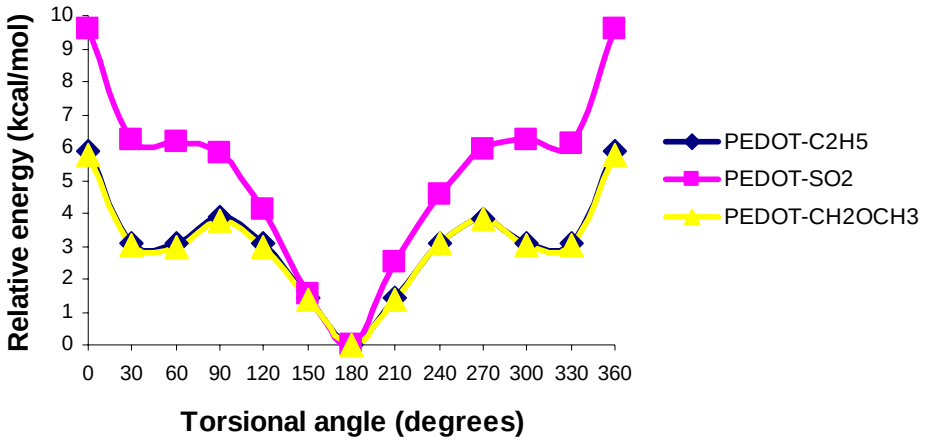

Figure 12 Potential energy curves of PEDOT-C_2H_5, PEDOT-SO_2 and PEDOT-CH_2OCH_3 dimer calculated at B3LYP/6-31G* level. The torsional angle is changed by 30° between θ = 0° and θ = 360°.

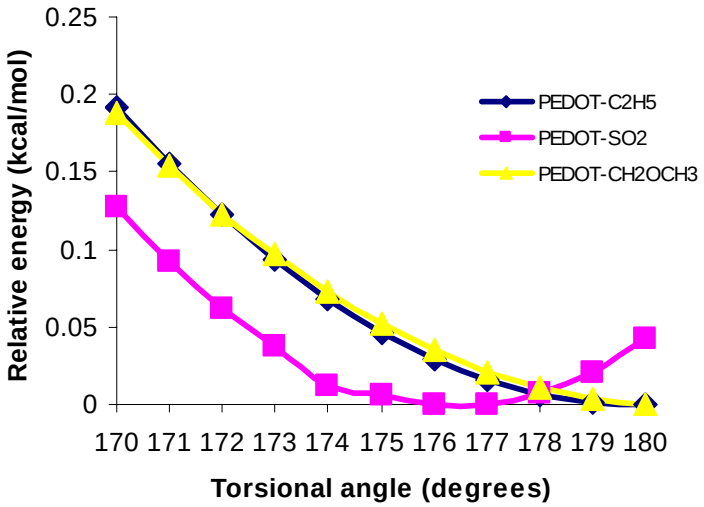

Figure 13 Potential energy curves of PEDOT-C_2H_5, PEDOT-SO_2 and PEDOT-CH_2OCH_3 dimer calculated at B3LYP/6-31G* level. The torsional angle is changed by 1° between θ = 170° and θ = 180°.

Table 7 Optimized structural parameters of PEDOT-C_2H_5, PEDOT-SO_2 and PEDOT-CH_2OCH_3 pentamer calculated at B3LYP/6-31G* level. (Bond length in angstrom, and torsional angle in degrees)

Geometrical parameter	Bond distance (angstrom)		
	PEDOT-C_2H_5	PEDOT-SO_2	PEDOT-CH_2OCH_3
Bond length			
S1-C2	1.740	1.778	1.739
C2-C3	1.365	1.344	1.365
C3-O4	1.369	1.350	1.370
O4-C5	1.441	1.440	1.441
C5-C6	1.527	1.515	1.529
C6-O7	1.433	1.438	1.432
O7-C8	1.370	1.347	1.371
C8-C9	1.381	1.360	1.381
C9-C10	1.439	1.423	1.439
C1-C11	1.381	1.364	1.381
C11-O12	1.370	1.344	1.369
O12-C13	1.433	1.440	1.431
C13-C14	1.528	1.515	1.528
C14-O15	1.442	1.440	1.444
O15-C16	1.369	1.344	1.370
C16-C17	1.383	1.365	1.383
C17-C18	1.435	1.421	1.436
C18-C19	1.383	1.365	1.383
C19-O20	1.369	1.345	1.371
O20-C21	1.441	1.439	1.443
C21-C22	1.528	1.516	1.528
C22-O23	1.432	1.439	1.432
O23-C24	1.370	1.345	1.370
C24-C25	1.382	1.365	1.383
C25-C26	1.435	1.421	1.435

Table 7 (cont'd)

Geometrical parameter	Bond distance (angstrom)		
	PEDOT-C_2H_5	PEDOT-SO_2	PEDOT-CH_2OCH_3
C26-C27	1.382	1.365	1.382
C27-O28	1.370	1.344	1.370
O28-C29	1.432	1.440	1.431
C29-C30	1.527	1.515	1.528
C30-O31	1.442	1.440	1.444
O31-C32	1.369	1.344	1.371
C32-C33	1.381	1.364	1.382
C33-C34	1.439	1.423	1.44
C34-C35	1.381	1.360	1.382
C35-O36	1.369	1.347	1.370
O36--C37	1.442	1.438	1.444
C37-C38	1.528	1.515	1.528
C38-O39	1.432	1.441	1.431
O39-C40	1.369	1.350	1.368
C40-C41	1.365	1.344	1.365
C41-S42	1.740	1.778	1.738
S42-C34	1.766	1.837	1.766
C33-S43	1.765	1.825	1.765
S43-C26	1.766	1.829	1.764
C25-S44	1.766	1.828	1.765
S44-C18	1.767	1.828	1.766
C17-S45	1.767	1.829	1.766
S45-C10	1.765	1.825	1.763
C9-S1	1.767	1.837	1.766
C3-C8	1.428	1.479	1.427
C11-C16	1.417	1.459	1.417
C19-C24	1.417	1.458	1.417

Table 7 (cont'd)

Geometrical parameter	Bond distance (angstrom)		
	PEDOT-C_2H_5	PEDOT-SO_2	PEDOT-CH_2OCH_3
C27-C32	1.419	1.459	1.418
C35-C40	1.428	1.479	1.428
C14-C46	1.525	-	-
C46-C47	1.532	-	-
C30-C48	1.525	-	-
C48-C49	1.532	-	-
C5-C50	1.525	-	-
C50-C51	1.532	-	-
C21-C52	1.525	-	-
C52-C53	1.532	-	-
C37-C54	1.525	-	-
C54-C55	1.532	-	-
C14-C46	-	-	1.534
C46-O47	-	-	1.409
O47-C48	-	-	1.421
C30-C49	-	-	1.532
C49-O50	-	-	1.409
O50-C51	-	-	1.421
C5-C52	-	-	1.529
C52-O53	-	-	1.410
O53-C54	-	-	1.421
C21-C55	-	-	1.533
C55-O56	-	-	1.409
O56-C57	-	-	1.421
C37-C58	-	-	1.533
C58-O59	-	-	1.409
O59-C60	-	-	1.421

Table 7 (cont'd)

Geometrical parameter	Bond distance (angstrom)		
	PEDOT-C_2H_5	PEDOT-SO_2	PEDOT-CH_2OCH_3
S1-O46	-	1.470	-
S1-C4O	-	1.469	-
S45-O49	-	1.468	-
S45-O48	-	1.468	-
S44-O51	-	1.468	-
S44-O50	-	1.468	-
S43-O52	-	1.468	-
S43-O53	-	1.468	-
S42-O55	-	1.469	-
S42-O54	-	1.470	-
Torsional angle			
θ =C8-C9-C10-C11	179.5	176	178
θ =C16-C17-C18-C19	179.6	176	172
θ =C24-C25-C26-C27	179.7	176	178
θ =C32-C33-C34-C35	179.6	176	173

According to Fig. 13, comparing with the anti conformation energy barrier of PEDOT-C_2H_5, PEDOT-SO_2 and PEDOT-CH_2OCH_3, it was found that the anti conformation energy barrier of PEDOT-SO_2 is higher than those molecules. This means that thienyl-S,S-dioxide group which is functionalized at the EDOT unit provide more steric effect of the polymer backbone. Moreover, the energy difference between two minima is higher as compared with other two molecules. These results indicate that the functionalization of the thienyl sulfur to the corresponding S,S-dioxide leads to the rigidification of the molecular skeleton. Considering the ground state geometry of PEDOT-SO_2 it was found that the oxygen atoms of the SO_2 moiety lie roughly at the same distance of 1.47 Å above and below the pentaatomic ring. In addition, with respect to the thiophene molecule, the loss of the aromatic conjugation by the S atom implies C-S, C-C and C=C bond lengthening as compared with

PEDOT, PEDOT-C_2H_5 and PEDOT-CH_2OCH_3. The optimized geometrical structures of PEDOT, PEDOT-C_2H_5, PEDOT-SO_2 and PEDOT-CH_2OCH_3 pentamer obtained from the B3LYP/6-31G* level are shown in Fig. 14. The inter-ring bond distance and the inter-ring torsional angle of those molecules are also analyzed and plotted against the bond number as shown in Fig. 15 and Fig. 16.

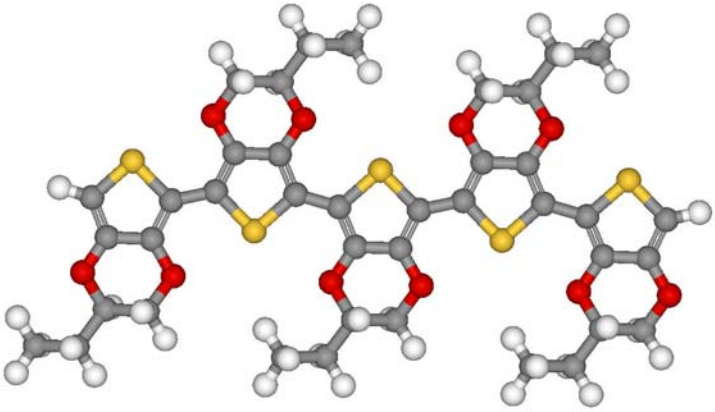

PEDOT-C_2H_5

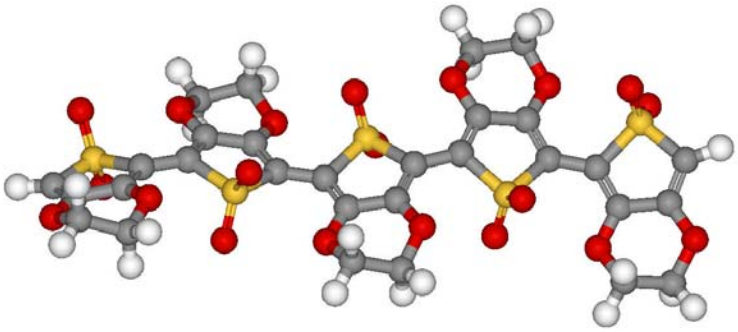

PEDOT-SO_2

Figure 14 PEDOT-C_2H_5, PEDOT-SO_2, PEDOT-CH_2OCH_3 pentamer obtained from the B3LYP/6-31G* level.

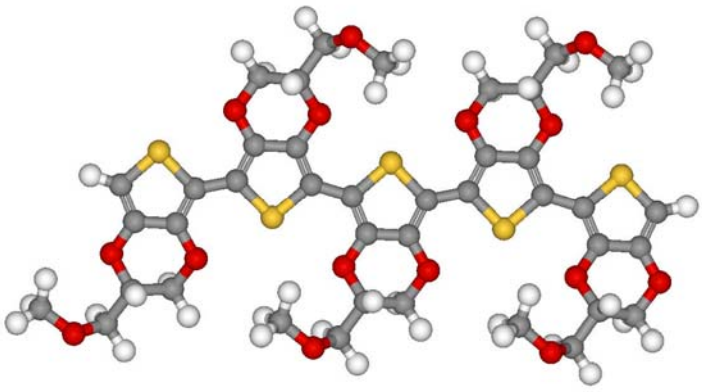

PEDOT-CH_2OCH_3

Figure 14 (cont'd)

According to Table 7, comparison of the C-C, C-O and C-S bond distances, it was found that PEDOT-C_2H_5 and PEDOT-CH_2OCH_3 show C-C, C-O and C-S bond distances similar to the PEDOT structure. In the case of PEDOT-SO_2, the C-S bond distances are higher than PEDOT and those molecules, while the C-O bond distances are shorter as compared with those molecules. However, the C-C inter-ring bond distances from those molecules remain constant along the main chain of the structure. In the case of PEDOT-SO_2, the C-C inter-ring bond distances are shorter than those molecules as shown in the Table 8.

Table 8 Inter-ring bond distances of the optimized geometries of PEDOT-C_2H_5, PEDOT-SO_2 and PEDOT-CH_2OCH_3 obtained from the B3LYP/6-31G* calculations.

Molecule	Inter-ring bond distance (angstrom)
PEDOT	1.439, 1.435, 1.436, 1.439
PEDOT-C_2H_5	1.437, 1.438, 1.435, 1.439
PEDOT-SO_2	1.423, 1.421, 1.421, 1.423
PEDOT-CH_2OCH_3	1.439, 1.436, 1.435, 1.440

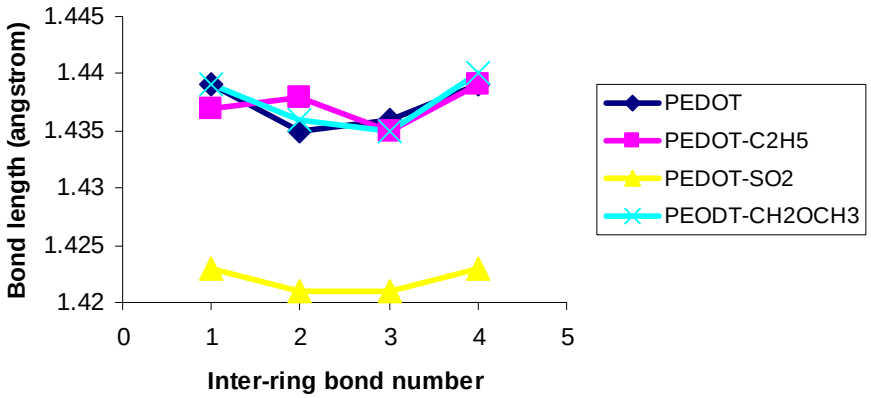

Figure 15 Inter-ring bond distances of PEDOT, PEDOT-C_2H_5, PEDOT-SO_2 and PEDOT-CH_2OCH_3 obtained from the B3LYP/6-31G* calculations.

Considering the inter-ring torsional angles, it was found that PEDOT-C_2H_5 shows the inter-ring torsional angle quite similar with PEDOT structure, while PEDOT-SO_2 and PEDOT-CH_2OCH_3 show distorted inter-ring torsional angles. Dikhissi *et al*. (2004) performed HF/6-31G* calculations of PEDOT-SO_2 finding a torsional angle of 154°. However, PEDOT-C_2H_5 and PEDOT-SO_2 show inter-ring torsional angle quite constant along the main chain of the structure (θ = 179°, θ = 176° respectively). In the case of PEDOT-CH_2OCH_3, it was found that the inter-ring torsional angles do not constant along the main chain of the structure due to the long side chain of the methoxy groups. The inter-ring torsional angles of the optimized geometries of PEDOT-C_2H_5, PEDOT-SO_2 and PEDOT-CH_2OCH_3 obtained from the B3LYP/6-31G* calculations are shown in the Table 9.

Table 9 Inter-ring torsional angles of the optimized geometries of PEDOT-C_2H_5, PEDOT-SO_2 and PEDOT-CH_2OCH_3 obtained from the B3LYP/6-31G* calculations.

Molecule	Inter-ring torsional angle (degrees)
PEDOT	179.7, 179.6, 179.7, 179.6
PEDOT-C_2H_5	179.5, 179.5, 179.9, 179.9
PEDOT-SO_2	176.3, 176.9, 176.9, 176.3
PEDOT-CH_2OCH_3	178.3, 172.8, 178.9, 173.1

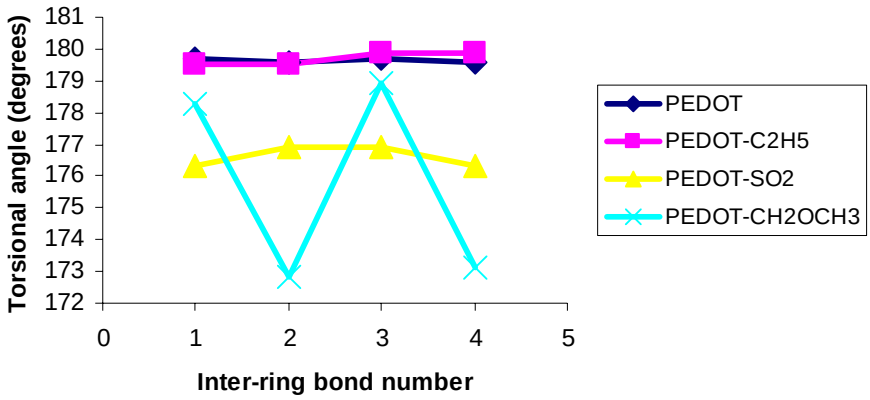

Figure 16 Inter-ring torsional angles of of PEDOT, PEDOT-C_2H_5, PEDOT-SO_2 and PEDOT-CH_2OCH_3 obtained from the B3LYP/6-31G* calculations.

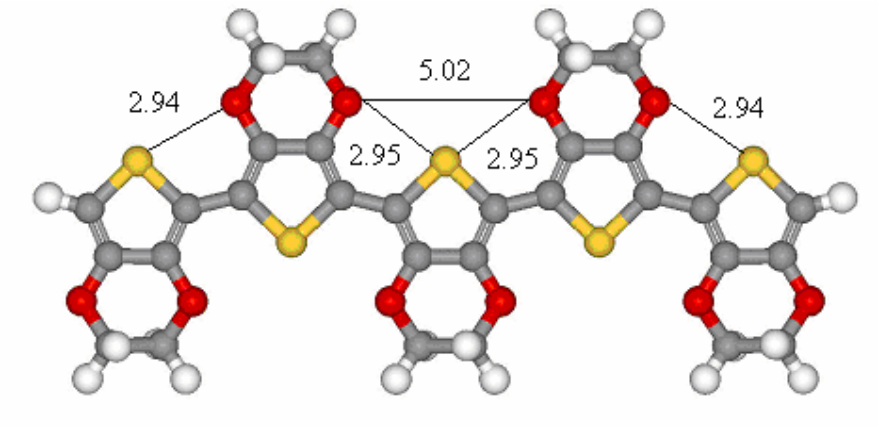

PEDOT

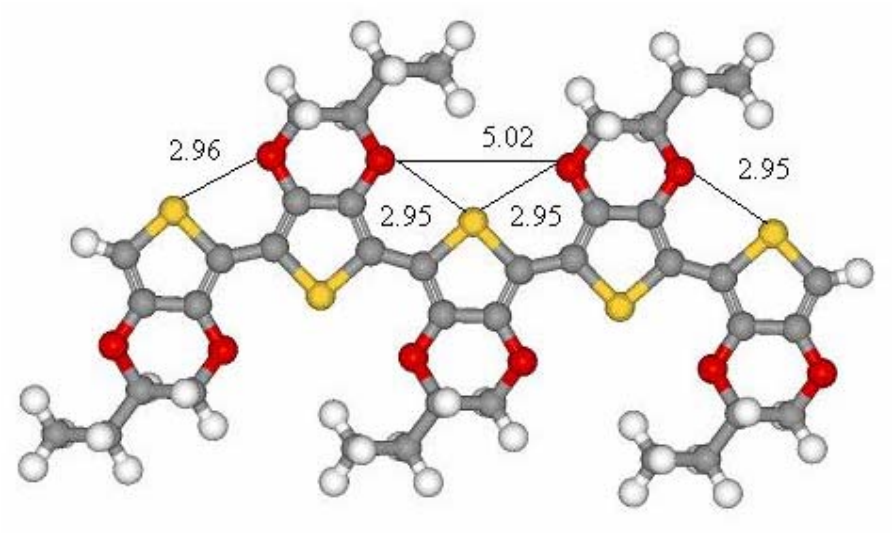

PEDOT-C_2H_5

Figure 17 Comparison of the S-O and O-O bond distances between PEDOT and PEDOT-C_2H_5 obtained from the B3LYP/6-31G* calculations.

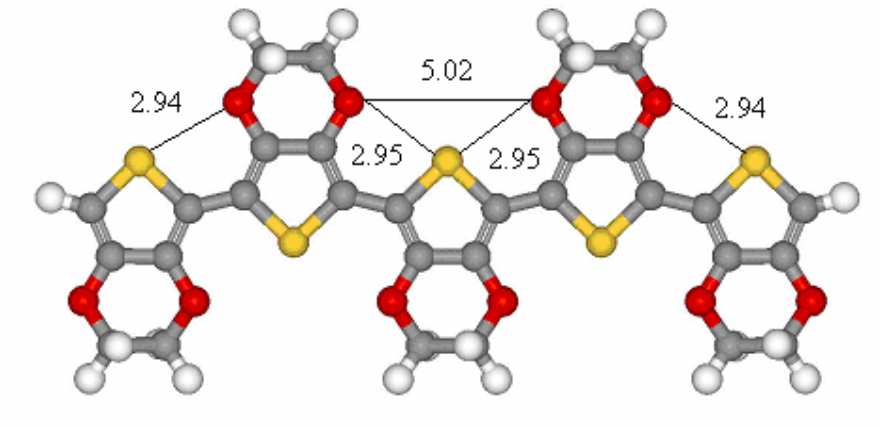

PEDOT

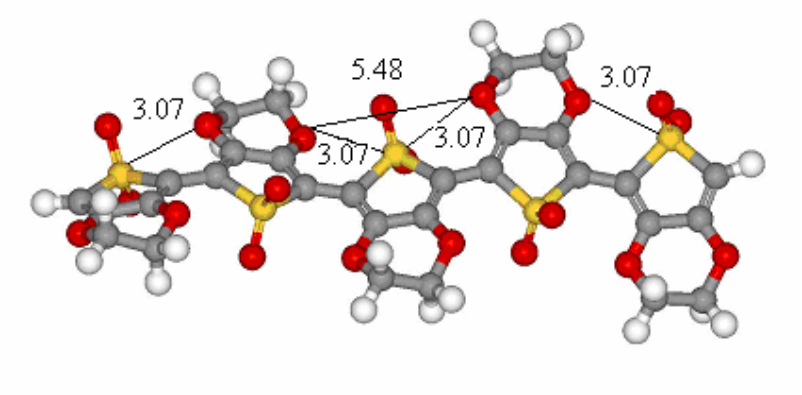

PEDOT-SO_2

Figure 18 Comparison of the S-O and O-O bond distances between PEDOT and PEDOT-SO_2 obtained from the B3LYP/6-31G* calculations.

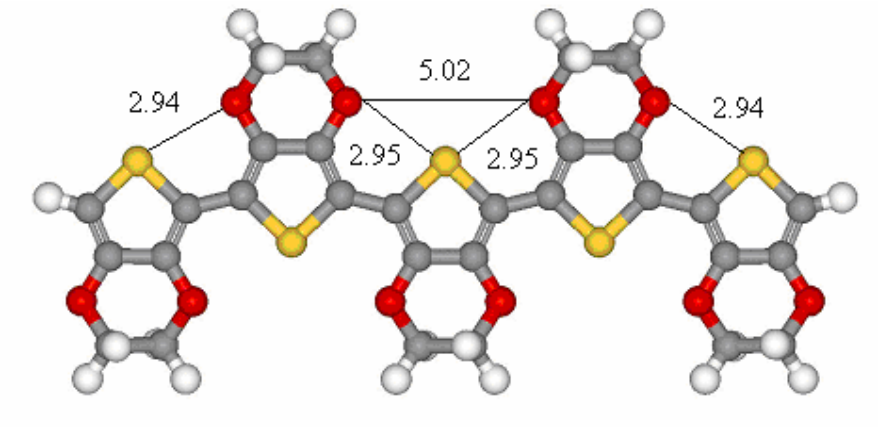

PEDOT

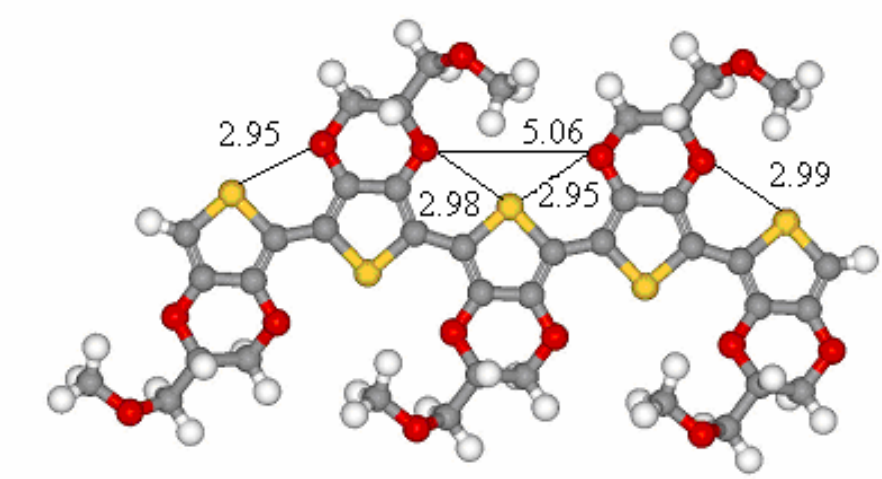

PEDOT-CH_2OCH_3

Figure 19 Comparison of the S-O and O-O bond distances between PEDOT and PEDOT-CH_2OCH_3 obtained from the B3LYP/6-31G* calculations.

Comparison of the O-O and S-O interaction distances of PEDOT-C_2H_5, PEDOT-SO_2 and PEDOT-CH_2OCH_3 with PEDOT structure as shown in the Fig. 17-19 shows that PEDOT-C_2H_5 O-O and S-O interaction distances are quite similar with PEDOT, while PEDOT-CH_2OCH_3 and PEDOT-SO_2 show more repulsive interactions between oxygen atoms and between oxygen and sulfur atoms of the repeating units as compared with those molecules. Thus, the distances between such two oxygen atoms increases from 5.02-5.48 Å and between oxygen and sulfur atoms increases from 2.94-3.07 Å when the anti conformation becomes distorted.

Considering the Frontier Molecular Orbitals, it is useful to examine the highest occupied orbitals and the lowest virtual orbitals for PEDOT and its derivatives. This is because the relative ordering of the occupied and virtual orbitals provides reasonable qualitative indication of the excitation properties and of the ability of electron or hole transport. The first dipole-allowed electron transitions, as well as the strongest electron transitions with largest oscillator strength, correspond almost exclusively to the promotion of an electron from HOMO to LUMO. The electronic density contours of PEDOT, PEDOT-C_2H_5, PEDOT-SO_2 and PEDOT-CH_2OCH_3 obtained from the B3LYP/6-31G* calculations are shown in Fig. 20.

As shown in Fig. 20, all the frontier orbitals spread over the whole π-conjugated backbone, although the largest contributions come from different parts of the monomer units. There is interring antibonding between the bridge atoms, and there is intraring bonding between the bridge carbon atom and its conjoined atoms in the HOMO. On the contrary, there is interring bonding in the bridge single bond and intraring antibonding between the bridge atom and its neighbor in the LUMO. In general, the HOMO possesses antibonding character between the subunits. This may explain the nonplanarity observed for these oligomers in their ground states. On the other hand, the LUMO of all oligomers generally shows bonding character between the two adjacent subunits. This implies that the singlet excited state involving mainly the promotion of an electron from the HOMO to the LUMO should be more planar.

Comparison between those molecules, it indicated that the electronic density contours of PEDOT-C_2H_5 and PEDOT-CH_2OCH_3 are quite similar with PEDOT contours. This demonstrates that the side chain does not effect the structure including the energy gap of these polymers (1.60 eV, 1.75 eV and 1.78 eV respectively). In the case of PEDOT-SO_2, the electronic contours are different from those molecules due to the effect of the thienyl-S,S-dioxide groups. Moreover, the LUMO remains more delocalized on the center parts of the conjugated backbone. This brings us to the fact that PEDOT-SO_2 gives the lowest energy gap as compared with those molecules.

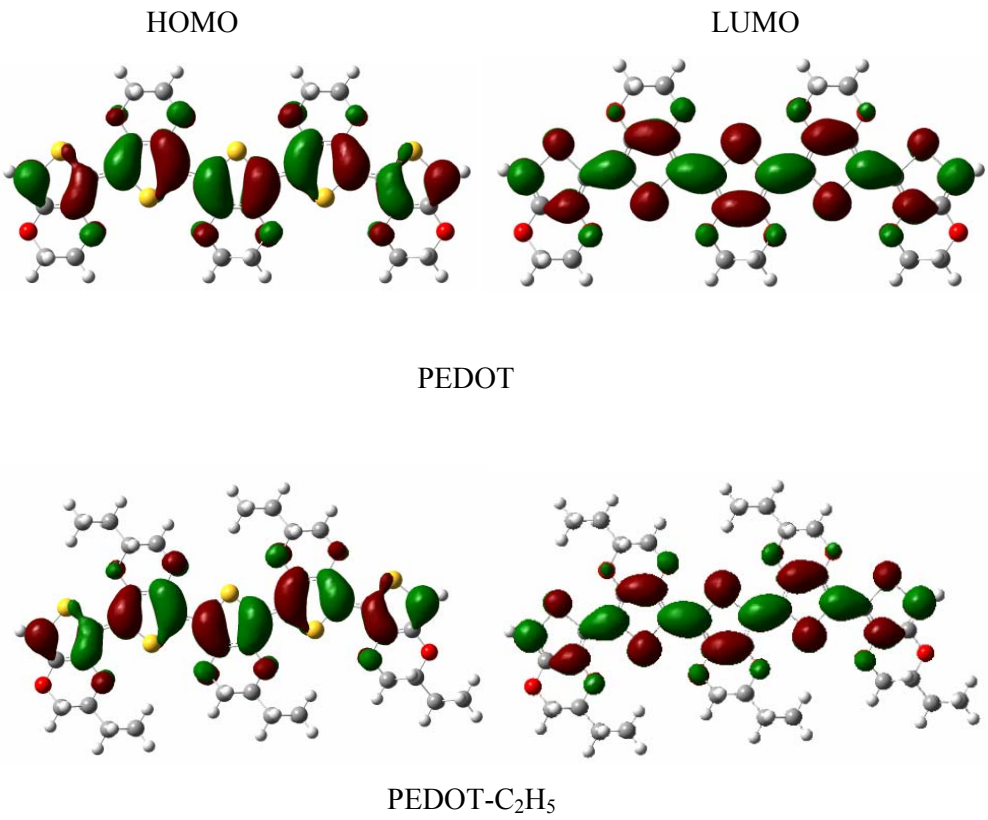

Figure 20 Electronic density contours of PEDOT, PEDOT-C_2H_5, PEDOT-SO_2 and PEDOT-CH_2OCH_3 obtained from the B3LYP/6-31G* calculations.

HOMO LUMO

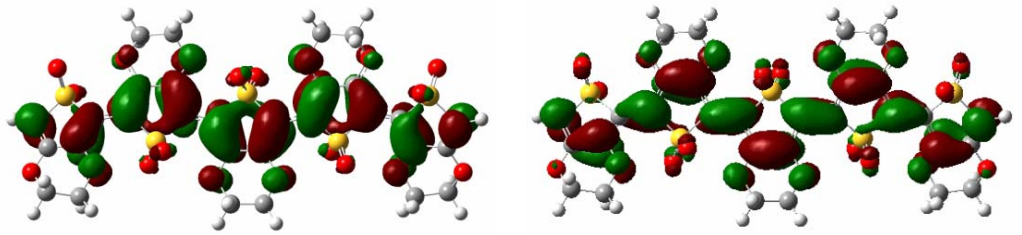

PEDOT-SO_2

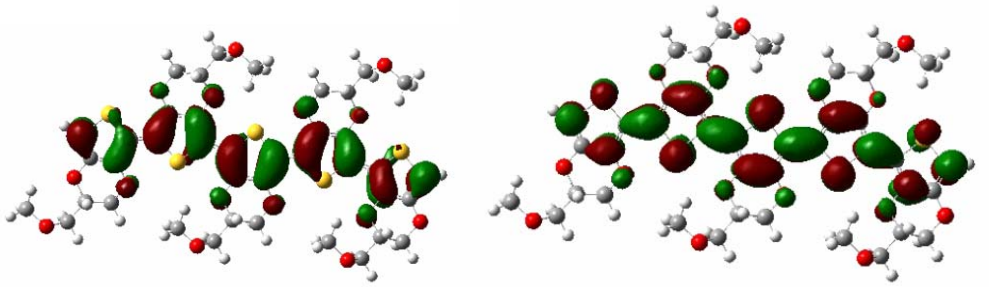

PEDOT-CH_2OCH_3

Figure 20 (cont'd)

2. HOMO-LUMO Energy differences

In experiment, the HOMO and LUMO energies were calculated from one empirical formula proposed by Bre´das *et al*. (1983) based on the onset of the oxidation and reduction peaks measured by cyclic voltammetry, assuming the absolute energy level of ferrocene/ferrocenium to be 4.8 eV below vacuum. The HOMO and LUMO energies can be calculated by density functional theory (DFT) in this study. However, it is noticeable that solid-state packing effects are not included in the DFT calculations, which tends to significantly reduce the torsion angles between adjacent units and consequently affects the HOMO and LUMO energy levels in a thin film compared to an isolated molecule as considered in the calculations. Even if these calculated HOMO and LUMO energy levels are not accurate, it is possible to use them to get information by comparing similar polymers and oligomers.

In theory, the energy gap of polymer $(M)_n$ can be extrapolated by the orbital energy difference between HOMO and LUMO (Hay, 2002; Hong *et al*., 2001). B3LYP functional has improved the XC functional that included part of the exact exchange energy from the adiabatic connection method. Properties of organic molecules are well predicted by such hybrid method. It is worth reminding that Salzner *et al*. (1997) in their study of the low band gaps polymers using density functional theory hybrid functionals concluded that DFT hybrid methods provide energy gaps in good agreement with vertical excitation energies from UV-absorption spectra. Therefore, the calculated HOMO-LUMO energy differences are shown in Table 10. Moreover, the HOMO-LUMO energy differences were extrapolated to the infinite chain length of the polymer and the results are depicted in Fig. 21.

Table 10 HOMO-LUMO energy differences of the PEDOT oligomers, calculated by the B3LYP/6-31G**//AM1, B3LYP/6-31G**//HF/6-31G*, B3LYP/6-31G** //HF/6-31+G* and B3LYP/6-31G**//B3LYP/6-31G* and B3LYP/6-31G**//B3LYP/6-31+G* methods.

oligomer	HOMO-LUMO Energy gap(eV)				
	B3LYP/6-31G** //AM1	B3LYP/6-31G**// HF/6-31G*	B3LYP/6-31G**// HF/6-31+G*	B3LYP/6-31G**// B3LYP/6-31G*	B3LYP/6-31G**// B3LYP/6-31+G*
n=2	5.15	4.36	4.05	4.05	4.03
n=3	4.89	3.67	3.66	3.30	3.29
n=4	4.82	3.29	3.29	2.89	2.88
n=5	4.80	3.07	3.07	2.63	2.62
n=∞	4.53	2.22	2.23	1.70	1.71
Exp.					1.60[(a)]

[(a)] Dietrich *et al*. (1994)

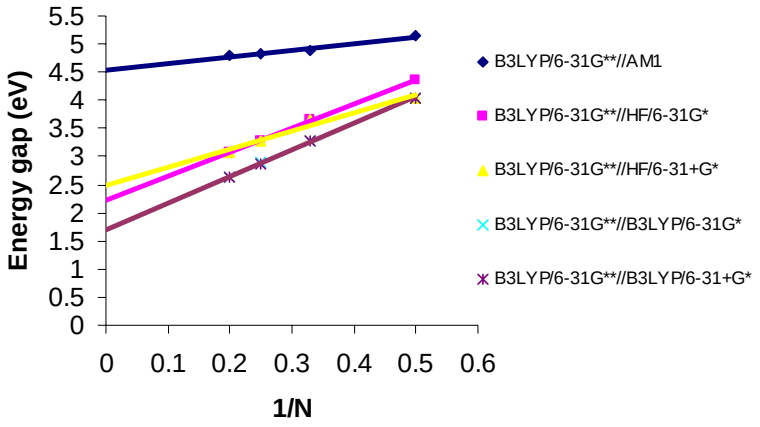

Figure 21 Energy gaps of PEDOT oligomers extrapolated from the plot of HOMO-LUMO energy differences of the oligomers versus the inverse number of monomer units.

According to Fig. 21, it was found that the obtained HOMO-LUMO energy differences by the B3LYP/6-31G**//AM1, B3LYP/6-31G**//HF/6-31G* and B3LYP/6-31G**//HF/6-31+G* levels are far from the experimental data (1.60 eV; Dietrich *et al*. (1994). This means that semi-empirical and *ab initio* methods give geometry structure not optimal to represent that energy gap of this polymer studied. However, HOMO-LUMO energy differences performed by the B3LYP/6-31G** with DFT optimized geometries give good results as compared with the experimental data. As a result, the orbital energy gap between HOMO and LUMO is an approximation to the transition energy since the transition energy also contains significant contribution from some two-electron integrals. It is know that HOMO-LUMO energy differences obtained from *Ab initio* and DFT calculations are the crudest estimate. However, Alguno *et al*. (2000) have studied the energy gaps of the polythiophene using HF and DFT methods employing various combinations of exchange and correlation function with electron core potential (ECP) split valence basis sets. They pointed out that DFT calculations with hybrid functions (B3LYP and B3P86) gave excellent results (4.06 eV and 4.11 eV) which are in good agreement with the experiment energy gap (4.05 eV). Aleman *et al*. (2005) performed *ab initio* (at HF/6-31G* level) and density functional theory (at B3LYP/6-31G* level) for structural calculation and employed single point calculations at the B3LYP/6-31G*

level for HOMO-LUMO energy differences of PEDOT. The results show that the HOMO-LUMO energy differences are 7.62 eV and 2.75 eV respectively. Comparing different basis set (6-31G* and 6-31+G*), it was found that they show a similar HOMO-LUMO energy differences.

3. The Lowest Excitation Energies

In order to obtain more accurate energy gaps, the spectrum methods (ZINDO and TD-DFT/B3LYP/6-31G**) were applied in this study to calculate the excitation energy. In calculating the excitation energies by both methods, the first excited state with significant oscillator strength ($\pi \rightarrow \pi^*$ transition) was used and it was also the lowest excited state for all oligomers. All extrapolated energy gaps as obtained from various methods are summarized in Table 11. Moreover, extrapolated energy gaps for oligomers by the ZINDO and TDDFT methods, based on semi-empirical, *ab initio* and density functional theory optimized geometries are shown in Fig. 22.

Table 11 The extrapolated energy gaps of PEDOT oligomers calculated at various methods

Method	Energy gap (eV)
ZINDO//AM1	3.06
ZINDO//HF/6-31G*	1.92
ZINDO//HF/6-31+G*	1.91
ZINDO//B3LYP/6-31G*	1.48
ZINDO//B3LYP/6-31+G*	1.48
TDDFT//AM1	3.89
TDDFT//HF/6-31G*	1.93
TDDFT//HF/6-31+G*	1.91
TDDFT//B3LYP/6-31G*	1.52
TDDFT//B3LYP/6-31+G*	1.52
Experimental data	1.60[(a)]

[(a)] Dietrich *et al*. (1994)

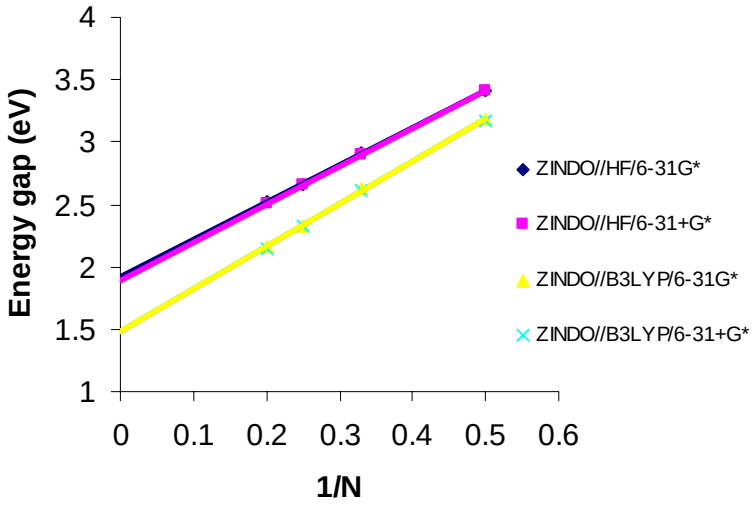

(a)

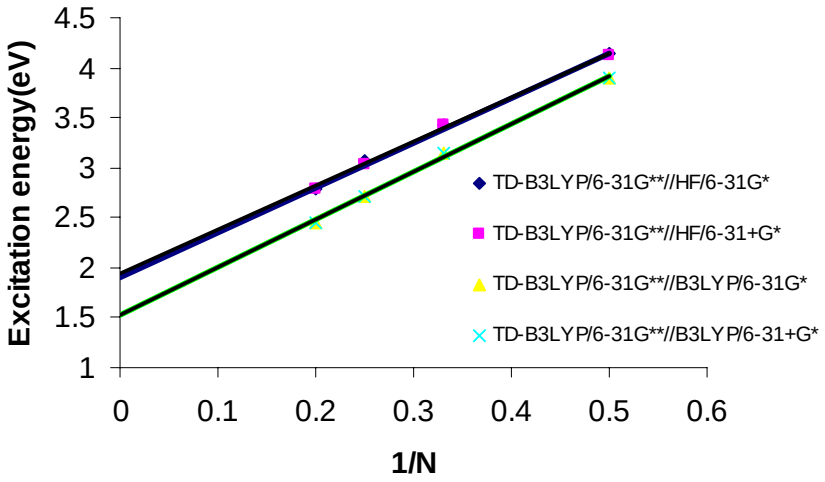

(b)

Figure 22 Energy gap of PEDOT oligomers extrapolated from the plot of excitation energy versus the inverse number of monomer units; (a) ZINDO method (b) TDDFT method.

According to Table 11, the extrapolated energy gap from semi-empirical ZINDO and TD-B3LYP/6-31G** excitation energies based on AM1- and HF-optimized geometries are overestimated as compared with the experimental data. Whereas, the extrapolated energy gap from TD-B3LYP/6-31G** excitation energies based on DFT-optimized geometries are in excellent agreement with the experimental data. However, semi-empirical ZINDO and TDDFT methods based on DFT-optimized geometries showed underestimated energy gaps. This caution should be taken with these experimental measures because the optical band gap, which is approximated by the longest wavelength absorption or emission band, should be larger than the electrochemical band gap that is estimated from the difference between the first oxidation and reduction potentials. The underestimation of the theoretical values must be partially attributed to the small number of EDOT monomers considered in the present calculations. The reduction of the gap with increasing chain length is a well-known behavior that has been shown in numerous theoretical studies of π-conjugated polymers, (Salzner *et al*., 1997; Nobotoki *et al*., 1996; Ehrendorfer *et al*., 1994; Ehrendorfer *et al*., 1995; Conil *et al*., 2003) including PEDOT (Salzner *et al*., 2002). Thus, this effect was shown by previous calculations employing the B3PW91 functional with the Stevens-Bach-Krauss pseudopotentials (Stevens *et al*., 1994) and split valence plus polarization basis sets predicted an energy gap of 2.06 eV for PEDOT, whereas values of 6.43 eV and 4.68 eV were provided for EDOT and the dimer respectively (Salzner *et al*., 2002). Thus, a reduction of about 50% was detected when going from the dimer to the polymer. They have also checked the influence of the number of EDOT units on the energy gap. For this purpose, additional calculations were performed at the B3PW91/6-31+G** level on compounds containing one and three EDOT units. The energy gaps of the optimized structures were 5.65 eV and 3.30 eV respectively, confirming that the gap decreases when the amount of EDOT units increases. Dkhissi *et al*. (2004) performed *ab initio* (at HF/6-31G level) structure and electronic property calculations of PEDOT pentamer. The results show that the energy gap of PEDOT is 2.45 eV. Aleman *et al*. (2004) performed B3PW91 level prediction of the energy gap of PEDOT. It was found that the 4.0 eV of energy gap is considerably overestimated with respect to the experimental data. Moreover, the same authors performed HF/6-

31G* level structure calculation and employed the B3LYP/6-31G* calculated energy gap of PEDOT. The results show that the energy gap is 2.75 eV.

It was found that the spectrum method can be used to predict energy gap of PEDOT. In addition, geometry from the DFT method (at B3LYP/6-31G* and B3LYP/6-31+G* levels) provides more optimal structure for the polymers studied. However, B3LYP/6-31G* level was chosen to study electronic structure and electronic property of PEDOT derivatives due to reduce calculation time.

Calculated excitation energies for PEDOT-C_2H_5, PEDOT-SO_2 and PEDOT-CH_2OCH_3 oligomers are plotted against the inverse number of monomer units and extrapolated to an infinite number of units as shown in Fig. 23-25. Extrapolated band gaps are summarized in Table 12.

Table 12 The extrapolated energy gaps of PEDOT, PEDOT-C_2H_5, PEDOT-SO_2 and PEDOT-CH_2OCH_3 calculated by the TD/B3LYP/6-31G** level.

Molecule	Energy gap (eV)		
	TD-B3LYP/6-31G**	Exp.	Calculation
PEDOT	1.52	1.60[(a)]	-
PEDOT-C_2H_5	1.48	1.75[(b)]	-
PEDOT-SO_2	1.02	-	2.71[(c)]
PEDOT-CH_2OCH_3	1.50	1.78[(d)]	-

[(a)] Dietrich *et al*. (1994) [(b)] Sankaran *et al*. (1997) [(c)]Dkhissi *et al*. (2004) [(d)] Kumar *et al*. (1996)

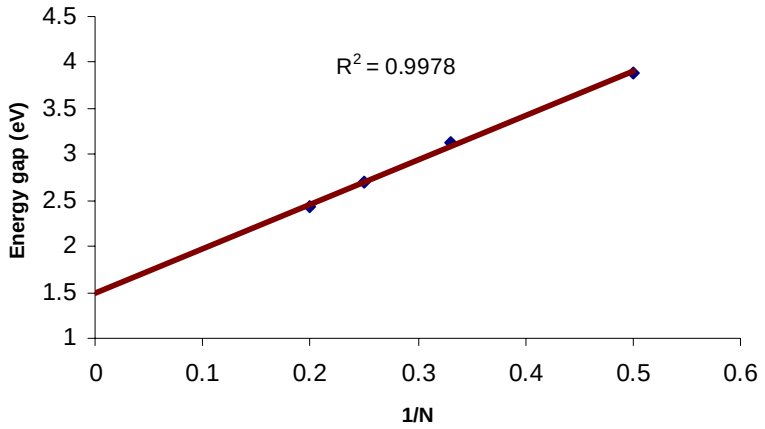

Figure 23 Extrapolated energy gap of PEDOT-C_2H_5 oligomers obtained from the TDDFT//B3LYP/6-31G** calculations.

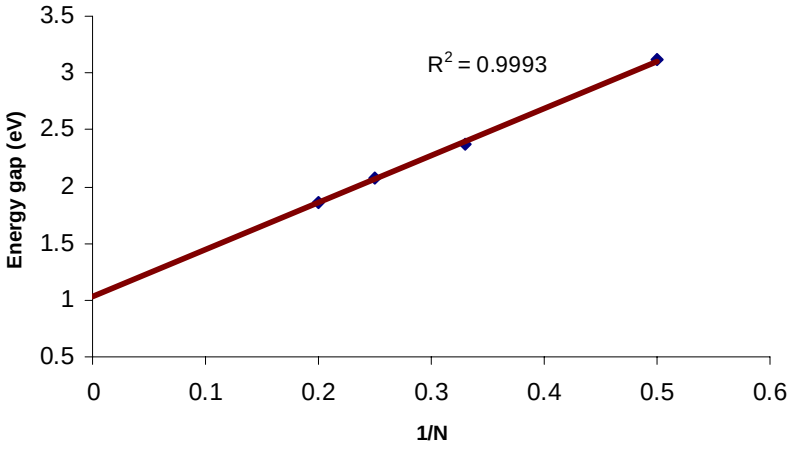

Figure 24 Extrapolated energy gap of PEDOT-SO_2 oligomers obtained from the TDDFT//B3LYP/6-31G* calculations.

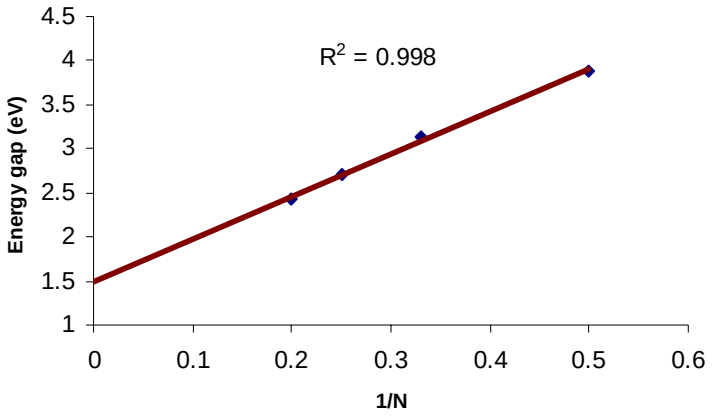

Figure 25 Extrapolated energy gap of PEDOT-CH_2OCH_3 oligomers obtained from the TDDFT//B3LYP/6-31G* calculations.

In the case of PEDOT-C_2H_5 and PEDOT-CH_2OCH_3, TDDFT(B3LYP/6-31G**)//B3LYP/6-31G* calculations were utilized for obtaining the extrapolated energy gap. It was found that the extrapolated energy gaps are 1.48 eV and 1.50 eV respectively, as shown in Table 12 and illustrated in Fig. 23 and 25, and are underestimated as compared with the experimental value (1.75 eV (Sankaran *et al*. 1997) and 1.78 eV (Kumar *et al*. 1996) respectively)**.** This is due to the approximation of exchange potentials from the theory of this method. In practice, the accuracy of TDDFT employing the most widely available exchange-correlation functions, are approximations to the true functional. Therefore, a disadvantage of this method is the fact that performance can hardly be improved without introduction of better functionals, which are, however, not available in any straightforward way. The deviation between TDDFT-calculated and experimental excitation energies were reported to be between 0.0 and 1.0 eV (Bauernschmitt *el at*., 1996). The average accuracy for polycyclic hydrocarbons is about 0.3 eV (Heinze *et al*., 2000). Salzner, *et al*. (1998) performed DFT calculations on a series of oligomers to estimate band gaps for polyacetylene, polythiophene, polypyrrole, polythiazole, and a thiophene-thiazole copolymer. Using a slightly modified hybrid function, they obtained band gaps within 0.1 eV of experimental solid-state values.

Moreover, we found that the HOMO-LUMO energy differences can represent the energy gap of PEDOT-C_2H_5 and PEDOT-CH_2OCH_3 as depicted in Fig. 26 and 27 respectively. The extrapolated energy gaps are 1.71 eV and 1.71 eV respectively, which are consistent with the experimental data (1.75 eV and 1.78 eV respectively).

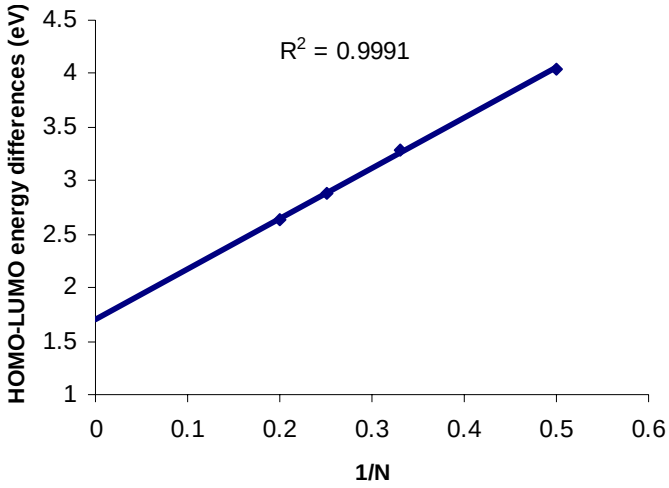

Figure 26 Extrapolated energy gap of PEDOT-C_2H_2 obtained from the B3LYP/6-31G** calculations.

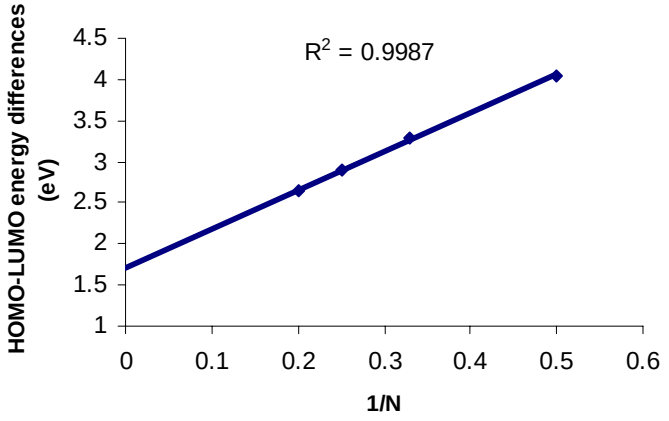

Figure 27 Extrapolated energy gap of PEDOT-CH_2OCH_3 obtained from the B3LYP/6-31G** calculations.

According to Fig. 24, it was found that the obtained energy gap of PEDOT-SO_2 performed by TDDFT method is 1.02 eV. Dkhissi *et al*. (2004) performed HF/6-31G* calculations on a series of oligomers and used INDO method to estimate band gaps for PEDOT-SO_2. They found that energy gap is 2.71 eV.

The energy gaps of PEDOT, PEDOT-C_2H_5, PEDOT-SO_2 and PEDOT-CH_2OCH_3 relative to polythiophene (PT) were discussed. The calculated energy gas obtained by TDDFT is 4.06 eV for PT (Alguno *et al*., 2000), which is higher than those of PEDOT, PEDOT-C_2H_5, PEDOT-SO_2 and PEDOT- CH_2OCH_3 with the same corresponding methods. This indicates that the energy gap of polythiophene can be improved by introducing the dioxane unit into the backbone of PT. These is obviously because the dioxane unit increases the torsional angle between thiophene units so as to enhance the effective conjugated length along the main chain. Aleman *et al*. (1995) found that the torsional angle of PT obtained from the optimized ground state geometry is about 150°. Moreover, the calculated energy gaps of PEDOT-C_2H_5, PEDOT-SO_2 and PEDOT-CH_2OCH_3 are less than those of PT. However, PEDOT-SO_2 provided the narrowest energy gap as compared to those molecules.

CONCLUSIONS

Quantum chemical calculations have been performed on the structure and electronic property of poly(3,4-ethylenedioxythiophene)(PEDOT) and its derivatives. Potential energy curves of PEDOT was calculated by the semi-empirical AM1, *ab initio* (at HF/6-31G* and HF/6-31+G* levels) and density functional theory (at B3LYP/6-31G* and B3LYP/6-31+G* levels) methods. The results obtained indicate that *ab initio* and density functional theory show an anti conformation while AM1 method shows a distorted structure. For PEDOT derivatives, potential energy curves calculated by the B3LYP/6-31G* level. The results show that PEDOT-C_2H_5 shows an anti conformation while PEDOT-SO_2 and PDOT-CH_2OCH_3 show a distorted structure due to steric hindrance.

Band gap in PEDOT and its derivatives have been extrapolated from calculated excitation energies of oligomers with the extrapolation being linear in reciprocal oligomer length. The HOMO-LUMO energy differences for PEDOT performed by the B3LYP/6-31G**//AM1, B3LYP/6-31G**//HF/6-31G*, B3LYP/6-31G**//HF/6-31+G* levels are far from the experimental data. However, HOMO-LUMO energy differences performed by the B3LYP/6-31G** level with DFT optimized geometries show good results as compared with the experimental data. Moreover, the semi-empirical ZINDO and TDDFT/B3LYP/6-31G** were applied to calculate the excitation energy. The extrapolated energy gap from TDDFT/B3LYP/6-31G** excitations energies using DFT-optimized geometries are in excellent agreement with the experimental data.

In the case of PEDOT-C_2H_5 and PEDOT-CH_2OCH_3, the extrapolated energy gap from TDDFT/B3LYP/6-31G** excitation energy using B3LYP/6-31G* level optimized geometries are underestimated relative to the experimental data. However, the HOMO-LUMO energy differences can represent the energy gap of PEDOT-C_2H_5 and PEDOT-CH_2OCH_3. The extrapolated energy gap of both oligomers are found to be similar (1.71 eV), which is consistent with the experimental data (1.75 eV and 1.78 eV respectively). Moreover, the obtained energy gap of PEDOT-SO_2 performed

by TDDFT/B3LYP/6-31G** method is 1.02 eV. These results are intriguing when compared against more common conducting polymers. Given the promising theoretical data on PEDOT and its derivatives, further such studies should be conducted using DFT, ZINDO and TDDFT methods to find new compounds that may improve on properties of conducting polymer.

LITERATURE CITED

Agaya, G., C. Lv, X. Wang, M. Koyama, M. Kobo and A. Miyamoto. 2005. Theoretical study on the electronic and molecular properties of ground and excited states of ethylenedioxythiophene and styrenesulphonic acid. **Appl. Sur. Science**. 244: 195-198.

Aleman, C., E. Armelin, J. I. Iribarren, F. Liesa, M. Laso and J. Casanovas. 2005. Strutural and electronic properties of 3,4-ethylenedioxythiphene, 3,4-ethylenedisulfanylfurane and thiophene oligomers: A theoretical investigation. **Synth. Met**. 149: 151-156.

_____, and J. Casanovas. 2004. Theoretical investigation of the 3,4-ethylenedioxy-thiophene dimer and unsubstituted heterocyclic derivatives. **J. Phys. Chem A.** 108: 1440-1447.

Bauernschmitt, R. and R. Ahlrichs. 1996. Treatment of electronic excitations within the adiabatic approximation of time independent density functional theory. **Chem. Phys. Lett**. 256: 454-464.

Beljionne, D., Z. Shuai, R. H. Friend and J. L. Bredas. 1995. Theoretical investigation of the lowest singlet and triplet states in poly(p-phenylene-vinylene) oligomers. **J. Chem. Phys**. 102: 2042-2049.

Belletete, M., S. Beaupre, J. Bouchard, P. Blondin, M. Leclerc and G. Durocher. 2000. Theoretical and experimental investigations of the spectroscopic and photophysical properties of fluorine-phenylene and fluorine-thiophene derivatives; Precursors of light-emitting polymers. **J. Phys. Chem**. **B**. 104: 9118-9125.

Bredas, J. L., R. Silbey, D. S. Boudreaux, and R. R. Chance. 1983. Chain-length dependence of electronic and electrochemical properties of conjugated systems: polyacetylene, polyphenylene, polythiophene, and polypyrrole. **J. Am. Chem. Soc.** 105(22): 6555-6559.

Briere, J. –F. and M. Cote. 2004. Elctronic, structural, and optical properties of conjugated polymers based on carbazole, fluorine, and borafluorene. **J. Phys. Chem. B**. 108: 3123-3129.

Chang, C. C., L. J. Her and J. L. Hong. 2005. Copolymer from electropolymerization of thiophene and 3,4-ethylenedioxythiophene and its use as cathode for litium ion battery. **Electrochimita Acta**. 50: 4461-4468.

Cho Ko, H., S. Park and H. Lee. 2004. Characteristics of dual-type electrochromic device based on poly(3-tetradecylthiophen) and poly(3,4-ethylenedioxy-thiophene). **Synth. Met**. 143: 31-35.

Choi, J. W., M. G. Han, S. Y. Kim, S. G. Oh and S. S. Im. 2004. Poly(3,4-ethylene-dioxythiophene) nanoparticles prepared in aqueous DBSA solutions. **Synth. Met**. 141; 293-299.

Chiang, C. K., C. R. Fincher, Jr. Y. W. Park, A. J. Heeger, H. Shirakawa, E. J. Louis, S. C. Gau and A. G. MacDiarmid. 1997. Electrical conductivity in doped polyacethylene. **J. Phys. Rev. Lett**. 39: 1098-1101.

Conil, J., B. Beljonne and J. L. Bredas. 1995. Poly(p-phenylene vinylene) in light emitting diodes: Nature of lowest singlet and triplet excited states and effect of derivatization. **J. Chem. Phys**. 103: 834-841.

_____, I. Gueli, A. Dkhissi, J. C. Sancho-Garcia, E. Hennebicq, J. P. Calbert, V. Lemaur, D. Beljonne, and J. L. Bredas. 2003. Electronic and optical properties of polyfluorene and fluorine-based copolymers: A quantum-chemical characterization. **J. Chem. Phys.** 118(14): 6615-6623.

Dkhissi, A., D. Beljonne, R. Lazzaroni, F. Louwet, L. Groenendaal and J. L. Bredas. 2003. Density functional theory and Hartree-Fock studies of the geometric and electronic structure of neutral and doped ethylenedioxythiophene (EDOT) oligomers. **J. of Quantum Chemistry**. 91; 517-523.

Du, X. and Z. Wang. 2003. Effects of polymerization potential on the properties of electrosynthesized PEDOT films. **Electrochimita Acta**. 48: 1713-1717.

Fichet, O., f Tran-Van, D. Teyssie and C. Chevrot. 2002. Interfacial polymerization of a 3,4-ethylenedioxythiophene derivative using Langmuir-Blodgett technique. Spectroscopic and electrochemical characterizations. **Thin Solid Film**. 411: 280-288.

Foresman, J., M. Head-Gordon, J. A. Pople and M. J. Frisch. 1992. Toward a systematic molecular orbital theory for Excited States. **J. Phys. Chem**. 96: 135-149.

Friend, R. H., R. W. Gymer, A. B. Holmes, J. H. Burroughes, R. N. Marks, C. Taliani, D. D. C. Bradley, D. A. Dos Santos, J. L. Bredas, M. Logdlund and W. R. Salaneck. 1999. Electroluminescence in conjugated polymers. **Nature**. 397: 121-128.

Frisch, M. J., G. W. Trucks, H. B. Schlegel, G. E. Scuseria, M. A. Robb, J. R. Cheeseman, J. A. Montgomery Jr., T. Vreven, K. N. Kudin, J. C. Burant, J. M. Millam, S. S. Iyengar, J. Tomasi, V. Barone, B. Mennucci, M. Cossi, G. Scalmani, N. Rega, G. A. Petersson, H. Nakatsuji, M. Hada, M. Ehara, K. Toyota, R. Fukuda, J. Hasegawa, M. Ishida, T. Nakajima, Y. Honda, O. Kitao, H. Nakai, M. Klene, X. Li, J. E. Knox, H. P. Hratchian, J. B. Cross, C. Adamo, J. Jaramillo, R. Gomperts, R. E. Stratmann, O. Yazyev, A. J. Austin, R. Cammi, C. Pomelli, J. W. Ochterski, P. Y. Ayala, K. Morukuma, G. A. Voth, P. Salvador, J. J. Dannenberg, V. G. Zakrzewski, S. Dapprich, A. D. Daniels, M. C. Strain, O. Farkas, D. K. Malick, A. D. Radbuck, K. Raghavachari, J. B. Foresman, J. V. Ortiz, Q. Cui, A. G. Baboul, S. Clifford, J. Cioslowski, B. B. Stefanov, G. Liu, J. Liashenko, P. Piskorz, I. Komaromi, R. L. Martin, D. J. Fox, T. Keith, M. A. Al-Laham, C. Y. Peng, A. Nanayakkara, M. Challacombe, P. M. W. Gill, B. Johnson, W. Chen, M. W. Wong, C. Gonzalez, J. A. Pople. 2003. **Gaussian 03**, Revision B.03, Gaussian Inc., Pittsburgh, PA.

Gao, Y., C. G. Liu and Y. S. Jiang. 2002. Electronic structure of thiophene oligomer dications: An alternative interpretation from the spin-unrestricted DFT study. **J. Phys. Chem**. 106: 5380-5384.

Garreau, S., G. Froyer and G. Louarn. 2001. Comparison between poly(3,4-ethylene-dioxythiophene) and alkyl derivatives. **Synth. Met**. 119: 323-324.

_____, G. Louarn, G. Froyer, M. Lapkowski and O. Chauvet. 2001. Spectroelectro-chemical studies of the C14-alkyl derivative of poly(3,4-ethylenedioxy-thiophene) (PEDOT). **Electrochimita Acta**. 46: 1207-1214.

Gong, X., D. Moses, A. J. Heeger and S. Xiao. 2004. White light electrophospho-rescence from polyfluorene-based light-emitting diode. Utilization of fluorine defects. **J. Phys. Chem B**. 108: 8601-8605.

Harima, Y., T. Eguchi, K. Yamashita, K. Kojima and M. WShiotani. 1999. An in situ ESR study on poly(3-methylthiophene) : charge transport due to polarons and bipolarons before the evolution of metallic conduction. **Synth. Met**. 105: 121-128.

_____ , Y., Y. Konugi, H. Tang, K. Yamashita, M. Shiotani, J. Ohshita and A. Kunai. 2000. Transport and in situ ESR studies on polymer films composed of quinquethiophenes bridged by monosilanylene units. **Synth. Met**. 113: 173-183.

Heinze, P., J. Xuezhong, M. S. Liu and A. K. –Y. Jen. 2002. Highly efficient fluorene- and benzothiadiazole-baased conjugated copolymers for polymer light-emitting diodes. **Macromolecules**. 35: 6094-6100.

Hirata, S. and M. H. Gordon. 1999. Time-dependent density functional theory within the Tamm-Dankoff approximation. **Chem. Phys. Lett**. 314: 291-299.

Horowitz, G., B. Bachet, A. Yassar and P. Lang, F. Demanze, J. Fave and F. Garnier. 1995. Growth and characterization of sexithiophene single crystals. **Chem. Mater**. 7: 1337-1341.

Hong, S. Y. 2003. Comparison of conformations and electronic structures of poly(3,4-ethylenedioxythiophene) and poly(3,4-ethylenedthiathiophene) in the neutral and doped states. **Synth. Met**. 135-136: 439-441.

_____, S. Y., S. J. Kwon and S. C. Kim. 1996. Theoretical study of geometrical and electronic structures of new p-conjugated thiophene copolymer. **J. Chem. Phys**. 104: 1140-1146.

Hotta, S., S. D. D. V. Rughooputh, A. J. Heeger, F. Wudl. 1987. Spectroscopic studies of soluble poly(3-alkylthienylenes). **Macromolecules**. 20: 212-215.

Hsu, C-P., S. Harata and M. Head-Gordon. 2001. Excitation energies from Time-Dependent Density Fuctional Theory for linear polyene oligomer; butadiene to decapentaene. **J. Chem. A**. 105: 451-458.

Huang, J., P. F. Miller, J. C. Mello, A. J. Mello and D. D. C. Bradley. 2003. Influence of thermal treatment on the conductivity and morphology of PEDOT/PSS films. **Synth. Met**. 139: 569-572.

Jong, M. P., A. W. Denier, X. Crispin, W. Osikowicz, W. R. Salaneck and L. Gronenedaal. 2003. The electronic structure of n- and p-doped phenyl-capped 3,4-ethylenedioxythiophene trimer. **Chem. Physics**. 118: 6495-6502.

Jonas, F., L. Scharader. 1991. Conductive modifications of polymers with polypyrroles and polythiophenes. **Synth. Met**. 41-43: 831-836.

Khan, M. A. and S. P. Armes. 1999. Synthesis and characterization of micrometer-sized poly(3,4-ethylenedioxythiophene)-coated polystyrene latexes. **Langmuir**. 15: 3469-3475.

Ko, H. C., S. Park and H. Lee. 2004. Characteristics of dual-type electrochormic device based on poly(3-tretradecylthiophene) and poly(3,4-ethylenedioxy-thiophene). **Syn. Met**. 143: 31-35.

Kudo. K. 2005. Organic light emitting transistors. **Current Applied Physics**. 5: 337-340.

Kumar, A. and J. R. Reynolds. 1996. Soluble alkyl-substituted poly(ethylenedioxy-thiophenes) as electrocromic materials. **Macromolecules**. 29: 7629-7635.

Kvarnstrom, C., H. Neugebauer, S. Blomquist, H. J. Alonen, J. Kankare and A. Evaska. 1999. In situ spectroelectrochemical characterization of poly(3,4-ethylenedioxythiophene). **Electrochimica Acta**. 44: 2739-2750.

Kwon, O. and M. L. Mckee. 2000. Theoretical calculation of band gaps in the aromatic structures of polythieno[3,4-b]benzene and polythieno[3,4-b]pyrazine. **J. Phys. Chem A.** 104: 7106-7112.

Lapkowski, M. and A. Pron. 2000. Electrochemical oxidation of poly(3,4-ethylene-dioxythiophene) "in situ" conductivity and spectroscopic investigations. **Syn. Met**. 110: 79-83.

Li, C. and T. Imae. 2004. Electrochemical and optical properties of the poly(3,4-ethylenedioxythiophene) film electropolymerized in an aqueous sodium dodecyl sulfate and litium tetrafluoroborate medium. **Macromolecules**. 37: 2411-2416.

Liu, B., W. L. Yu, H. Y. Lai and W. Huang. 2000. Synthesis, characterization, and structure-property relationship of novel-fluorene-thiophene based conjugated copolymers. **Macromolecules**. 33: 8945-8952.

Ma, J., S. Li, and Y. Jiang. 2002. Time dependent DFT study on band gaps and effective conjugation lengths of polyacetylene, polyphenylene, polypentafulvene, polycyclopentadiene, polypyrrole, polyfuran, polysilole, polyphosphole, and polythiophene. **Macromolecules.** 35: 1109-1115.

Meng, H., J. Zheng, A. J. Loinger, B. –C. Wang, P. G. V. Patten and Z. Bao. 2003. Oligofluorene derivatives as high-performance semiconductors for organic thin film transistors. **Chem Matters**. 15: 1778-1787.

Moiorano, V., E. Perrrone, S. Carallo, A. Biasco, P. Pompa, R. Cingolani, A. Croce, R. I. R. Blyth and J. Thompon. 2005. White, phoporescence, wet-processed, organic light emitting diode on a window-glass substrate. **Synth. Met**. 151: 147-151.

Negri, F. and G. Orlandi. 2000. Quantum chemical simulation of the resonance Raman spectra of stilbene radical ions: a test case for the study of charge carriers in doped PPV. **J. Mol. Struct**. 521:197-209.

Oliveira, M. A. D., H. A. Duarte, J-. M. Pernaut and W. B. D. Almeida. 2000. Energy gaps of α,α-substituted oligothiophenes from semiempirical, *ab initio*, and density functional methods. **J. Phys. Chem. A**. 104; 8256-8262.

Oretega, A. V. and I. N. D. Silva. 2005. Application to intelligent systems for specification of automotive equipments using LED. **Applied Soft Computing**. 6: 18-25.

Osikowicz, W., A. W. Denier van der Gon, L. Groenendaal, M. Fahlman, D. Beljonne, R. Lazzaroni and W. R. Salaneck. 2003. A Joint theoretical and experimental study on the electronic properties of phenyl-capped 3,4-ethylenedioxythiophene oligomers. **Chem. Phys**. 119: 10415-10416.

Poolmee, P., M. Ehara, S. Hannongbua and H. Nakatsuji. 2005. SAC-CI theoretical investigation on electronic structure of fluorine-thiophene oligomers. **Polymer**. 46: 6474-6481.

Randriamahazaka, H., C. Plesse, D. Teyssie and C. Chevrot. 2005. Relaxation kinetics of poly(3,4-ethylenedioxythiophene) in 1-ethyl-3-methylimidazolium bis((trifluoromethyl)sulfonyl)amide ionic liquid during potential step experiments. **Electrochimica Acta**. 50: 1515-1522.

Rannou, P. and M. Nechtschein. 1999. Ageing of poly(3,4-ethylenedioxythiophene) : Kinetics of conductivity decay and lifespan. **Synth. Met**. 101:474

Sakaran, B., and J. R. Reynoldes. 1997. High-contrast electrocromic polymers from alkyl-derivatized poly(3,4-ethylenendioxythiophenes). **Macromolecules**. 30: 2582-2588.

Salzner, U., P. G. Pickup and R. A. Poirier. 1998. Accurate method for obtaining band gaps in conducting polymers using a DFT/hybrid approach. **J. Phys. Chem. A**. 102: 2572-2578.

Schottland, P., O. Fichet, D. Teyssie and C. Chevrot. 1999. Lnagmuir-Blodgett films of an alkoxy derivative of poly(3,4-ethylenedioxythiophene). **Synth. Met**. 101: 7-8.

Suramitr, S., T. Kerdcharern, T.Srikhirin and S. Hannongbua. 2005. Electronic properties of alkoxy derivatives of poly(para-phenylenevinylene), investigated by time dependent density functional theory calculations, computational and theoretical polymer science. **Synth. Met**. 155: 27-34.

Tran-Van, F., M. Carrier and C. Chevrot. 2004. Sulfonated polythiophene and poly(3,4-ethylenedioxythiophene) derivatives with cations exchange properties. **Synth. Met**. 142: 251-258.

Tsou, C-C., H-T. Lu and M. Yokoyama. 2005. Red, green, blue and white organic electroluminescence devices. **J. Growth**. 280: 201-203.

Vardeny, Z. V., A. J. Heeger and A. Dodabalapur. 2005. Fundamental research needs in organic electronic materials. **J. Cryst. Growth**. 148: 1-3.

Wei, H., W. Li, M. Li, W. Su, Q. Xin, J. Zhang and Z. Hu. 2005. White organic electroluminescent device with photovoltaic performances. **Appl. Surf. Sci**. in press.

Wiberg, K. B., R. E. Stratmann and M. J. Frisch. 1998. A time-dependent density functional theory study of the electronically excited states of formaldehyde, acetaldehyde and acetone. **Chem. Phys. Lett**. 297: 60-64.

Wu, W., M. Inbasekaran, M. Hudack, D. Welsh, W. Yu, Y. Cheng, C. Wang, S. Karm, M. Tacey, M. Bernius, R. Fletcher, K. Kiszka, S. Munger and J. O'Brien. 2004. Recent development of polyfluorene-based RGB materials for light emitting diodes. **Microelectronic J**. 35:343-348.

Yang, L., Y. Liao, J. K. Feng and A. M. Ren. 2005. Theoretical studies of the modulation of polymer electronic and optical properties through the introduction of the electron-donating 3,4-ethylenedioxythiophene or electron-accepting pyridine and 1,3,4-oxadiazole moieties. **J. Phys. Chem A.** 109: 7764-7774.

Yohannes, T., F. Zhang, M. Svensson, M. R. Anderson and O. Inganas. 2004. Polyfluorene copolymer based bulk heterojunction solar cells. **Thin Solid Films**. 449: 152-157.

Yu, J. S. K., W. C. Chen and C. H. Yu. 2003. Time-dependent functional study of electroluminescent polymers. **J. Phys. Chem**. 107: 4268-4275.

Zhang, G., J. Ma, and Y. Jiang. 2002. Effect of silole content and doping on the electronic structures and excitation energies of silole/thiophene cooligomers. **Macromolecules.** 36: 1109-1115.

Zhang, X. and S. A. Jenekhe. 2000. Electroluminescence of multicomponent conjugated polymer. 1. Roles of polymer/polymer interfaces in emission enhancement and voltage-tunable multicolor emission in semiconducting polymer/polymer heterojuctions. **Macromolecules**. 33: 2069-2082.

Zotti, G., S. Zecchin and G. Schiavon. 2000. Conductive and magnetic properties of 3,4-dimethoxy and 3,4-ethylenedioxy capped polypyrrole and polythiophene. **Chem. Mater.** 12: 2996-3005.

Zykwinska, A., W. Domagala and M. Lapkowski. 2003. ESR spectroelectrochemistry of poly(3,4-ethylenedioxythiophene) (PEDOT). **Electrochemistry communications**. 5: 603-608.

APPENDIX

APPENDIX A

Theoretical Background

The Theory of Quantum Chemical Calculations

Molecular orbital theory is concerned with predicting the properties of atomic and molecular systems. It is based upon the fundamental laws of quantum mechanics and uses a variety of mathematical transformation and approximation techniques to solve the fundamental equations, in contrast to semi-empirical models.

1. The Schrödinger Equation

The quantum chemical methods are based on finding solutions to the Schrödinger equation on molecular orbital theory. Quantum mechanics explains how entities like electrons have both particle-like and wave-like characteristics. The time independent Schrödinger equation for a molecule (n-electron and N-nuclei system) is:

$$H\psi(\vec{r},\vec{R}) = E\psi(\vec{r},\vec{R}) \qquad (1)$$

and the Hamiltonian is (in atomic units):

$$H = T + V$$

$$H = -\sum_{i=1}^{N}\frac{1}{2}\nabla_i^2 - \sum_{A=1}^{M}\frac{1}{2M_A}\nabla_A^2 - \sum_{i=1}^{N}\sum_{A=1}^{M}\frac{Z_A}{r_{iA}} + \sum_{i=1}^{N}\sum_{j>i}^{N}\frac{1}{r_{ij}} + \sum_{A=1}^{M}\sum_{B>A}^{M}\frac{Z_A Z_B}{R_{AB}} \qquad (2)$$

where T and V are the kinetic and potential energy operators, respectively, which separate out the motion of the nuclei from the motion of the electrons, equation (2) can be rewritten as

$$H = -\sum_{A=1}^{M} \frac{1}{2M_A} \nabla_A^2 + H_{el} \qquad (3)$$

This focuses on the electronic Hamiltonian, H_{el}, and tries to solve the electronic Schrödinger equation in the field of the fixed nuclei. The nuclear-nuclear repulsion term (the final in equation (2)) appears as a constant in H_{el}. Further assume the wave function $\psi(\vec{r}, \vec{R})$ to be a product of an electronic and a nuclear part:

$$\psi(\vec{r}, \vec{R}) = \psi_{elec}(\vec{r}, \vec{R})\psi_{nucl}(\vec{R}) \qquad (4)$$

The justification for this is that the electrons are much lighter than the nuclei. This is called the Born-Oppenheimer approximation. The parametric $\vec{R}$ dependence of ψ_{elec} arises since the electron distribution depends implicitly on the particular nuclear arrangement for the system under study. The nuclear wave function, ψ_{nucl}, describes the vibrational, rotational and translational motion of the nuclei. From (1), (3) and (4), we can obtain;

$$H\psi(\vec{r}, \vec{R}) = H\psi_{elec}(\vec{r}, \vec{R})\psi_{nucl}(\vec{R}) = \left(-\sum_{A=1}^{M} \frac{1}{2M_A} \nabla_A^2 + H_{el} \right) \psi_{elec}(\vec{r}, \vec{R})\psi_{nucl}(\vec{R})$$

$$= \left(-\sum_{A=1}^{M} \frac{1}{2M_A} \nabla_A^2 + E_{el} \right) \psi_{elec}(\vec{r}, \vec{R})\psi_{nucl}(\vec{R}) = E\psi_{elec}(\vec{r}, \vec{R})\psi_{nucl}(\vec{R}) = E\psi \qquad (5)$$

The electronic wavefunction $\psi_{elec}(\vec{r}, \vec{R})$ can be divided out from both sides of equation (5), provided that terms in $\nabla^2 \psi_{elec}(\vec{r}, \vec{R})$ are small, i.e. the electronic wavefunction changes slowly upon small displacements of the nuclear positions. Thus, if we neglect the influence of the nuclear derivative on the electron wave function (ψ_{el}) (i.e. the nuclei move slowly compared with the electrons) we can separate equation (5) into two equations, an electronic part:

$$H_{el}\psi_{el}(\vec{r}, \vec{R}) = E_{el}(\vec{R})\psi_{el}(\vec{r}, \vec{R}) \qquad (6)$$

where

$$H_{el} = -\sum_{i=1}^{N} \frac{1}{2} \nabla_i^2 - \sum_{i=1}^{N} \sum_{A=1}^{M} \frac{Z_A}{r_{iA}} + \sum_{i=1}^{N} \sum_{j>i}^{N} \frac{1}{r_{ij}} + \sum_{A=1}^{M} \sum_{B>A}^{M} \frac{Z_A Z_B}{R_{AB}} \qquad (7)$$

and a nuclear part:

$$H_{nucl} \psi_{nucl}(\vec{R}) = E \psi_{nucl}(\vec{R}) \qquad (8)$$

where

$$H_{nucl} = -\sum_{A=1}^{M} \frac{1}{2M_A} \nabla_A^2 + E_{el}(\vec{R}) \qquad (9)$$

2. Hartree Fock Theory

An exact solution to the Schrödinger equation is not possible for any but the most trivial molecular systems. However, a number of simplifying assumptions and procedures do make an approximate solution possible for a large range of molecules. To simplify the treatment further, the next step is to assume that the electrons are non-interacting. This implies that (apart from the constant nuclear-nuclear repulsion term) we can rewrite the total n-electron Hamiltonian as a sum of n one-electron Hamiltonians,

$$H_{el} = \sum_{i=1}^{N} h(i) \qquad (10)$$

$$h(i) = \left(-\frac{1}{2} \nabla_i^2 - \sum_{A=1}^{M} \frac{Z_A}{r_{iA}} \right) \qquad (11)$$

This is clearly an oversimplification, since we have neglected the electron-electron repulsion term $\frac{1}{r_{ij}}$. Equation (10) defines the independent particle model. The one-electron Hamiltonians (equation (11)) are termed core-Hamiltonians, since the only interactions included are those between the electrons and the bare nuclei. Including an average interaction term in the $\{h(i)\}$, these become effective one-electron Hamiltonians. As a consequence of equation (10), the total wave function can be rewritten as a product of n single-particle wave functions,

$$\psi(\vec{r}) = \phi_1(\vec{r}_1)\phi_2(\vec{r}_2)..\phi_n(\vec{r}_n) \tag{12}$$

or, taking the electron spin into account,

$$\psi = \chi_1(\vec{x}_1)\chi_2(\vec{x}_2)..\chi_n(\vec{x}_n) \tag{13}$$

The spin orbitals $\{\chi_i(\vec{x}_i)\}$ are the products of the spatial orbitals $\phi_i(\vec{r}_i)$ and the spin functions ($\alpha(\omega)$ and $\beta(\omega)$); $\vec{x}_i$ denotes both the space and spin coordinates of electron i. The total independent particle spin-orbital wave function (equation (13)) is called a Hartree-product. This is an eigenfunction of the n-electron model Hamiltonian defined in equation (10), and the corresponding eigenvalue is a sum of the single-particle spin-orbital energies,

$$E_{el} = \sum_{i=1}^{M} \varepsilon_i \tag{14}$$

A further requirement on the state wave function (13) is that it must be anti-symmetric with respect to the interchange of coordinate r (both space and spin) of any two electrons,

$$\left|\psi(\vec{x}_1, \vec{x}_{2,...,} \vec{x}_n)\right|^2 = \left|\psi(\vec{x}_2, \vec{x}_1, ..., \vec{x}_n)\right|^2 \tag{15}$$

$$\psi(\vec{x}_1, \vec{x}_2, ..., \vec{x}_n) = \pm\psi(\vec{x}_2, \vec{x}_1, ..., \vec{x}_n) \tag{16}$$

It is also possible to write equation (16) in terms of a $n \times n$ determinant, a Slater determinant, which has the same antisymmetric properties:

$$\psi = (n!)^{-1/2} \begin{vmatrix} \chi_1(\vec{x}_1) & \chi_2(\vec{x}_1) & \cdots & \chi_n(\vec{x}_1) \\ \chi_1(\vec{x}_2) & \chi_2(\vec{x}_2) & & \\ \cdots & & \cdots & \\ \chi_1(\vec{x}_n) & \chi_2(\vec{x}_n) & \cdots & \chi_n(\vec{x}_n) \end{vmatrix} \tag{17}$$

This is commonly written as:

$$|\psi\rangle = (n!)^{-1/2} |\chi_1(\vec{x}_1), \chi_2(\vec{x}_2), ..., \chi_n(\vec{x}_n)\rangle \tag{18}$$

It can easily be verified that the Slater determinant obeys the Pauli principle, as the determinant then becomes zero. The pre-factor $(n!)^{-1/2}$ is a normalization constant, and the $\{\chi_i\}$ are assumed orthonormal. By antisymmetrizing the Hartree-product (13) in the form of a Slater determinant (17), the probability of finding any two electrons at the same point in space (i.e. $\vec{x}_1 = \vec{x}_2$) is zero.

Through the wave functions, the effective potential is generated. This potential allows to refine wave functions, from which a new potential is obtained. The procedure is repeated until a stable, self-consistent solution is reached. Due to the iterative procedure, the initial guess of the wave function, can of course be chosen ad hoc. However, the better the initial guess is, the easier it is to reach a stable solution to the eigenvalue problems in a relatively short computational time, is provided by the variation principle. This can be stated in the following way: Given any approximate wave function, satisfying the correct boundary conditions, the expectation value of the energy obtained by this wave function never lies below the exact energy of the ground state. Expressed in mathematical terms:

$$E_e = \frac{\langle \psi | H_e | \psi \rangle}{\langle \psi | \psi \rangle} \geq E_{exact} \tag{19}$$

A conceptually appealing model for the (trial) wave function of our molecular system is to regard it as being constructed from molecular orbitals (MO). This description in analogous to the model used for the atomic orbitals (AO). The MO's, the elements of the wave function determinant, are in turn thought of as being constructed by a Linear Combination of Atomic Orbitals (LCAO),

$$\psi_i^{MO} = \sum_{\mu} c_{\mu i} \phi_{\mu}^{AO} \tag{20}$$

The variational principle leads to following equations describing the molecular orbital expansion coefficients, $c_{\nu i}$, derived by Roothaan and by Hall:

$$\sum_{\nu=1}^{N} \left(F_{\mu\nu} - \varepsilon_i S_{\mu\nu} \right) c_{\nu i} = 0 \quad \mu = 1,2,..., N \tag{21}$$

Equation 21 can be rewritten in matrix form:

$$FC = SC\varepsilon \tag{22}$$

with

$$F_{\mu\nu} = H_{\mu\nu}^{core} + \sum_{\lambda\sigma} P_{\lambda\sigma} \left[(\mu\nu|\lambda\sigma) - \frac{1}{2} (\mu\lambda|\nu\sigma) \right] \tag{23}$$

$$F_{\mu\nu} = H_{\mu\nu}^{core} + G_{\mu\nu} \tag{24}$$

where $H_{\mu\nu}^{core}$, core-Hamiltonian matrix, defined as

$$H_{\mu\nu}^{core} = \int dr_1 \phi_{\mu}^{*}(1) h(1) \phi_{\nu}(1) \tag{25}$$

The matrix P is the density matrix or charge- and bond-order matrix,

$$P_{\mu\nu} = 2\sum_{a}^{N/2} C_{\mu a} C_{\nu a}^{*} \tag{26}$$

The matrix S is the overlap matrix, indicating the overlap between orbitals.

$$S_{\mu\nu} = \int dr_1 \phi_{\mu}^{*}(1)\phi_{\nu}(1) \tag{27}$$

The term $(\mu\nu|\lambda\sigma)$ in Equation 23 signified the two-electron repulsion integrals, defined as

$$(\mu\nu|\lambda\sigma) = \int dr_1 dr_2 \phi_{\mu}^{*}(1)\phi_{\nu}(2) r_{12}^{-1} \phi_{\lambda}^{*}(2)\phi_{\sigma}(2) \tag{28}$$

The (initial) wave function is used to generate an effective potential, which applies this potential in order to refine the coefficient matrix. The modified MO's form the new input in the Roothaan or Pople-Nesbet (1986) equations, and a new potential is generated. The iterative procedure is repeated until convergence is reached, i.e. when the changes in energy and/or charge density in two subsequent iterations are below a pre-set threshold value.

Before a more technical description of the SCF-procedure is presented, first need to define a new transformation matrix X, used for orthogonalisation of the basis set. This orthogonalisation can be either symmetric or canonical. A symmetric orthogonalisation implies that X is formed through the relation

$$X = S^{-1/2} = U s^{-1/2} U^{\tau} \tag{29}$$

where S is the overlap matrix, U is an unitary matrix which diagonalizes S, and the diagonal matrix of the eigenvalues of S is given by the relations. In the canonical orthogonalisation procedure, X is instead given by

$$X = Us^{-1/2} \tag{30}$$

Consider a new coefficient matrix C' related to the old coefficient matrix C by

$$C' = X^{-1}C, \qquad C = XC' \tag{31}$$

where it is assumed that X possesses an inverse. Substituting $C = XC'$ into the Roothaan equations gives

$$FXC' = SXC'\varepsilon \tag{32}$$

Multiplying on the left by X^{τ} gives

$$\left(X^{\tau}FX\right)C' = \left(X^{\tau}SX\right)C'\varepsilon \tag{33}$$

if we define a new matrix F^{τ} by

$$F^{\tau} = X^{\tau}FX \tag{34}$$

and use (27),then

$$F'C' = C'\varepsilon \tag{35}$$

The SCF procedure, outlined in Appendix figure A1, is as follows

1. Specify a molecule (a set of nuclear coordinates $\{R_A\}$, atomic numbers $\{Z_A\}$, and number of electron N) and a basis set $\{\phi_\mu\}$.
2. Calculate all required molecular integrals, $S_{\mu\nu}$, $H_{\mu\nu}^{core}$ and $(\mu\nu|\lambda\sigma)$.
3. Diagonalize the overlap matrix S and obtain a transformation matrix X from either equation $X \equiv S^{-1/2} = Us^{-1/2}U^\tau$ or $X = Us^{-1/2}$.
4. Obtain a guess at the density matrix P.
5. Calculate the matrix G of equation $F_{\mu\nu} = H_{\mu\nu}^{core} + G_{\mu\nu}$ from the density matrix P and the two-electron integral $(\mu\nu|\lambda\sigma)$.
6. Add G to the core-Hamiltonian to obtain the Fock matrix $F = H^{core} + G$.
7. Calculate the transformed Fork matrix $F^\tau = X^\tau FX$
8. Diagonalize F^τ to obtain C' and ε.
9. Calculate $C = XC'$.
10. Form a new density matrix P from C using $P_{\mu\nu} = 2\sum_a^{N/2} C_{\mu a} C_{\nu a}^*$.
11. Determine whether the procedure has converged, i.e. determine whether the new density matrix of step (10) is the same as the previous density matrix within a specified criterion. If the procedure has not converged, return to step (5) with the new density matrix.
12. If the procedure has converged, then use the resultant solution, represented by C, P, F, etc., to calculate expectation values and other quantities of interest.

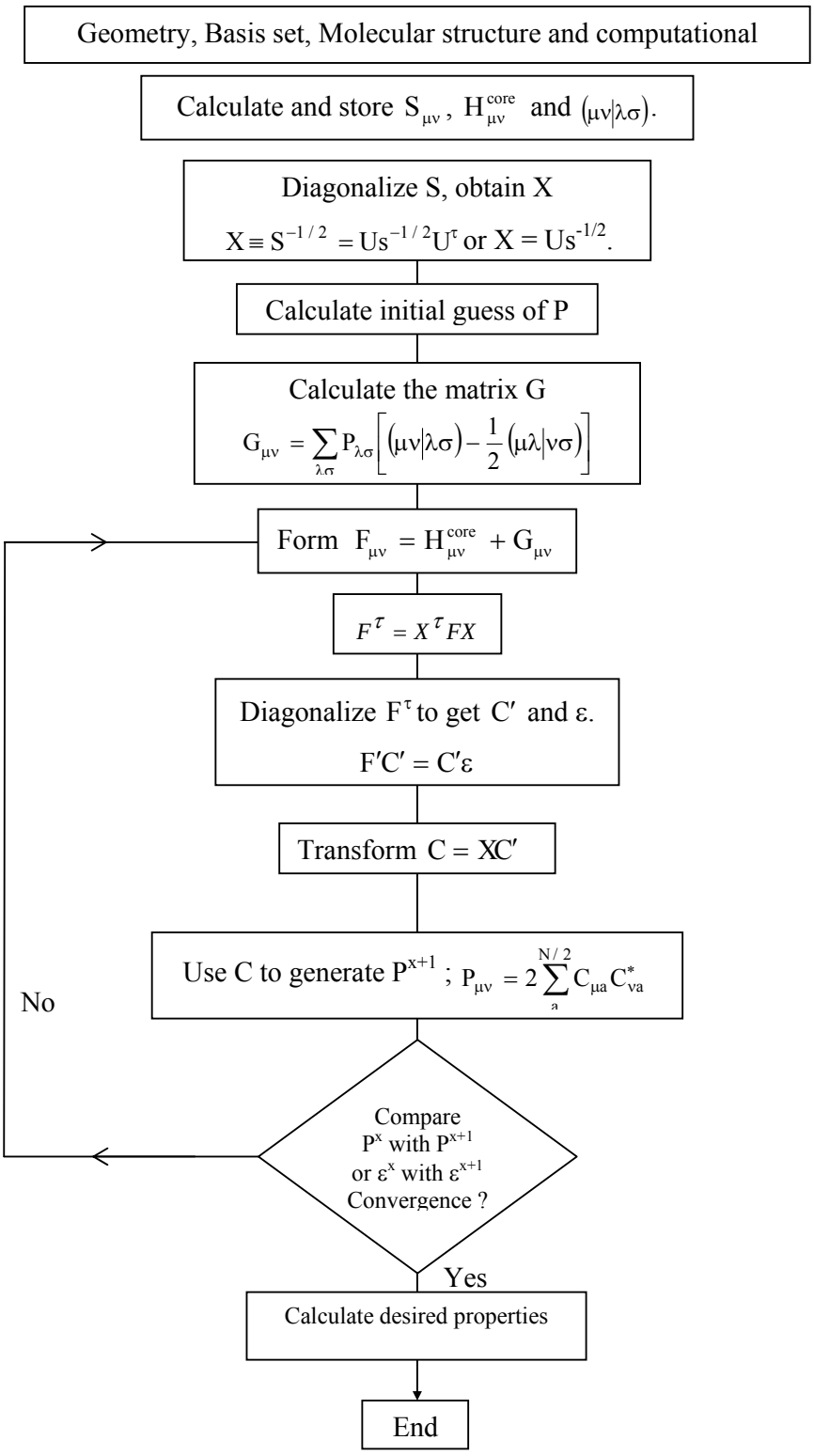

Appendix Figure A1 Schematic view of a Hartree-Fock self consistent field calculation.

3. Basis Set

The basis set most commonly used in quantum mechanical calculations is composed of atomic functions. The next approximation involves expressing the molecular orbitals as linear combinations of a pre-defined set of one-electron functions known as basis function. An individual molecular orbital is defined as:

$$\phi_i = \sum_{\mu=1}^{N} c_{\mu i}\chi_\mu \tag{36}$$

where the coefficients $c_{\mu i}$ are known as molecular orbital expansion coefficients. The basis functions $\chi_1 \ldots \chi_N$ are also chosen to be normalized. Gaussian-type atomic functions were used as basis functions. Gaussian functions have the general form

$$g(\alpha, \vec{r}) = cx^n y^m z^l e^{-\alpha r^2} \tag{37}$$

where $\vec{r}$ is of course composed of x, y, and z. α is a constant determining the size (radical extent) of the function. In Gaussian function, $e^{-\alpha r}$ is multiplied by powers (possibly 0) of x, y, and z and a constant for normalization, so that:

$$\int_{\text{allspace}} g^2 = 1 \tag{38}$$

Thus, c depends on α, l, m, and n.

Here are three representative Gaussian functional (s, p_y and d_{xy} types, respectively):

$$g_s(\alpha, \vec{r}) = \left(\frac{2\alpha}{\pi}\right)^{3/4} e^{-\alpha r^2}$$

$$g_y(\alpha, \vec{r}) = \left(\frac{128\alpha^5}{\pi^3}\right)^{1/4} ye^{-\alpha r^2}$$

$$g_{xy}(\alpha, \vec{r}) = \left(\frac{2048\alpha^7}{\pi^3}\right)^{1/4} xye^{-\alpha r^2} \qquad (39)$$

Linear combinations of primitive gaussians like these are used to form the actual basis functions; the latter are called contracted Gaussians and have the form

$$\chi_\mu = \sum_P d_{\mu p} g_p \qquad (40)$$

where the $d_{\mu p}$'s are fixed constants within a given basis set. Note that contracted functions are also normalized in common practice. A few commonly used basis sets are listed as following.

Minimal Basis Sets: Minimal basis sets contain the minimum number of basis functions needed for each atom, as in these examples:

H: 1s
C: 1s, 2s, $2p_x$, $2p_y$, $2p_z$

Minimal basis sets use fixed-size atomic-type orbitals. The STO-3G basis set is a minimal basis set (although it is not the smallest possible basis set). It used three gaussian primitives per basis function, which accounts for the "3G" in its name. "STO" stands for "Slater-type orbitals," and the STO-3G basis set approximates Slater orbitals with gaussian functions.

Split Valence Basis Sets

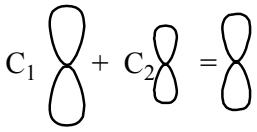

The first way that a basis set can be made larger is to increase the number of basis functions per atom. Split valence basis sets, such as 3-21G and 6-31G, have two (or more) sized of basis function for each valence orbital. For example, hydrogen and carbon are represented as:

H: 1s, 1s'
C: 1s, 2s, 2s', $2p_x$, $2p_y$, $2p_z$, $2p'_x$, $2p'_y$, $2p'_z$

where the primed and unprimed otbitals differ in size.

The double zeta basis sets, such as the Dunning-Huzinaga basis set (D95), form all molecular orbitals from linear combinations of two sized of functions for each atomic orbital. Similarly, triple split valence basis sets, like 6-311G, use three sizes of contracted functions for each orbital-type.

Polarized Basis Sets

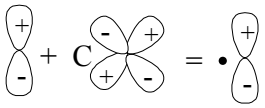

Split valence basis sets allow orbitals to change size, but not to change shape. Polarized basis sets remove this limitation by adding orbitals with angular momentum beyond what is required for the ground state to the description of each atom. For example, polarized basis sets add d functions to carbon atoms and f functions to transition metals, and some of them add p functions to hydrogen atoms.

So far, the only polarized basis set 6-31G(d) is used. Its name indicates that it is the 6-31G basis set with d functions added to heavy atoms. This basis set is becoming very common for calculations involving up to medium-sized systems. This basis set is also known as 6-31G*. Another popular polarized basis set is 6-31G(d,p), also known as 6-31G**, which adds p functions to hydrogen atoms in addition to the d functions on heavy atoms.

Diffuse Functions

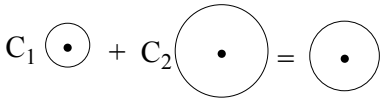

Diffuse functions are large-size versions of s- and p- type functions (as opposed to the standard valence-size functions) which allow orbitals to occupy a larger region of space. Basis sets with diffuse functions are important for systems where electrons are relatively far from the nucleus: molecules with lone pairs, anions and other systems with significant negative charge, systems in their excited states, systems with low ionization potentials, descriptions of absolute acidities. The 6-31+G(d) basis set is the 6-31G(d) basis set with diffuse functions added to heavy atoms. The double plus version, 6-31++G(d), adds diffuse functions to the hydrogen atoms as well. Diffuse functions on hydrogen atoms seldom make a significant difference in accuracy.

High Angular Momentum Basis Sets

Even larger basis sets are now practical for many systems. Such basis sets add multiple polarization functions per atom to triple zeta basis set. For example, the 6-31G(2d) basis set adds two d functions per heavy atom instead of just one, while the 6-311++G(3df,3pd) basis set contains three sets of valence region functions, diffuse functions on both heavy atoms and hydrogens, and multiple polarization funtions:3 d functions and 1 f function on heavy atoms and 3 p functions and 1 d

function on hydrogen atoms. Such basis sets are useful for describing the interactions between electrons in electron correlation methods.

4. Semi-empirical Calculations

Because both time and storage requirements of an *ab initio* Hartree-Fock calculation increase as the fourth power of the number of basis functions, calculations on large molecules even with the smallest basis sets are apt to be prohibitive. In such situations, the NDDO (neglect of diatomic differential overlap) formalism affords practical methods for calculating the electronic structure of large systems. Here, only one- and two-centre, two-electron integrals are considered, and the Hartree-Fock matrix, consists only of elements for which basis functions μ and ν are on the same atom, and basis functions λ and σ are on another atom. The individual terms are defined below (the sum α is over all other atoms).

$$
\begin{aligned}
F_{\mu\mu} &= H_{\mu\mu}^{core} + \sum_{\nu} P_{\nu\nu}\left[\langle\mu\mu|\ \nu\nu\rangle - \langle\mu\nu|\mu\nu\rangle\right] + \sum_{\delta}\sum_{\lambda}\sum_{\sigma} P_{\lambda\sigma}\langle\mu\mu|\nu\nu\rangle \\
F_{\mu\nu} &= H_{\mu\nu}^{core} + P_{\mu\nu}\left[3\langle\mu\nu|\ \mu\nu\rangle - \langle\mu\mu|\nu\nu\rangle\right] + \sum_{\delta}\sum_{\lambda}\sum_{\sigma} P_{\lambda\sigma}\langle\mu\nu|\lambda\sigma\rangle \\
F_{\rho\lambda} &= \beta_{\rho\lambda} - \frac{1}{2}\sum_{\nu}\sum_{\sigma} P_{\lambda\sigma}\langle\mu\nu|\lambda\sigma\rangle
\end{aligned}
\qquad (41)
$$

The elimination of three- and four-centre integrals greatly reduces the time and storage requirements for an NDDO calculation (which now increase as the square of the number of atoms) relative to that for a full Hartree-Fock treatment.

Three levels of NDDO theory are included in *SPARTAN'S SEMI EMPIRICAL* module: MNDO Modified Neglect of Diatomic Overlap

AM1 Austin Method 1

PM3 MNDO Parameterization Method 3

In all of these formalisms, only the valence electrons are considered. The one-electron terms are given by,

$$H_{\mu\nu}^{core} = U_{\mu\nu} - Z_A \sum_{B \neq A} Z_B \langle \mu\nu \,|\, \delta\delta \rangle \qquad (42)$$

Here, μ and ν are located on atom A and the summation is over all other atoms. Uνν is related to the binding energy of an electron in atomic orbital ν, and is determined from spectroscopic data. Uνμ is set to zero for $\nu \neq \mu$. The second term in equation 42 represents the attraction on an electron on atom A from the nuclear framework. The two center integral involves only the s function on atom B. Z_A is the charge of atom A without its valence electrons.

All one-centre, two-electron integrals (νν|μμ) and (νμ|νμ) are fitted to spectroscopic data. The two-centre, two-electron repulsion integrals (νμ|λσ) are approximated by classical multipole-multipole charge interactions between atoms A and B. The multipole charge separations within an atom are treated as adjustable parameters, i.e. optimized to fit the experimentally derived one-centre integrals.

The βμλ terms appearing in the Fock matrix (equation 41) are the one-electron, two-centre core resonance integrals and are approximated as,

$$\beta_{\rho\lambda} = \frac{\beta_\rho + \beta_\lambda}{2} S_{\rho\lambda} \qquad (43)$$

where $S_{\alpha\beta}$ is the overlap integral between Slater orbitals α and β, and $\alpha\beta$ and $\beta\alpha$ are adjustable parameters optimized using experimental thermo chemical data for simple molecules. Because all of the adjustable parameters are rooted in experimental data, these methods are known as semi-empirical. As in *ab initio* Hartree-Fock calculations, an SCF procedure is used to converge on a density matrix, and the electronic energy.

The three methods differ only in the core-repulsion terms (they also differ in the detailed parameterization). Core repulsion includes nuclear repulsion and non-

valence electron-electron repulsion, which are not explicitly considered in the calculation of the electronic energy. In the MNDO model, the core repulsion energy is given by,

$$E^{CR} = \sum_{A \neq B} \sum_{B \neq A} Z_A Z_B \langle \delta(A) | \delta(B) \rangle \left(e^{-\sigma_a E_{AB}} + e^{-\sigma_B E_{AB}} \right) \qquad (44)$$

where Rαβ is the internuclear distance and αA and αB are adjustable parameters fit to give the correct empirical behavior. Details are provided in the original papers. MNDO tends to overestimate core repulsion between two atoms at van der Waals distances. For this reason, the AM1 model was developed.

In AM1 a sum of Gaussians is employed to better represent the core repulsion behaviour at van der Waals distances. PM3 uses a similar core repulsion function, but differs in the parameterisation procedure.

One advantage of methods parameterised using experimental data is their implicit inclusion of electron correlation effects. However, dependence on experimental data means that semi-empirical methods would not be expected to perform well on unusual types of molecules for which no data are available from which to construct parameters.

5. Density Functional Theory

Method s that are rooted in the so-called density functional theory are currently regarded as very promising since are able to include a large amount of correlation effects in a formalism that essentially requires very similar computational resources as the Hartree-Fock procedure. In fact the algorithms of the approach, in which the electron density is described in terms of one-electron basis functions, are very similar to the single-determinant HF algorithm. This property has helped to establish density functional methods as a standard tool for chemistry and physics.

While the concept of expressing part or all of the molecular energy as a functional of the electron density goes back to the early days of quantum theory, Density Functional Theory (DFT) was put on a rigorous theoretical foundation by the Hohenberg-Kohn theorem. It states that there exists unique density ρ that yield the exact ground energy of system. The subsequent work of Kohn and Sham laid the basis for practical computational applications of the DFT to real systems. The basis of their formalism are the so-called Kohn-Sham equations.

$$H\Psi_i = E_i\Psi_i \tag{45}$$

in which the Hamiltonian H is defined as

$$H = \left(-\frac{1}{2}\nabla^2 + V_{KS} \right) \tag{46}$$

where V_{KS} is a local potential defined such that the total density of the non-interacting system

$$\rho = \sum_i |\Psi_i|^2 \tag{47}$$

is the same as the density of the "real" system. V_{KS} has the three components V_{ext}, V_C and V_{XC} containing the nuclear and external, Coulomb potential of the electrons and the exchange-correlation interactions.

$$E_{KS} = V_{ext} + \sum_{\mu\nu} P_{\mu\nu} H_{\mu\nu} + \frac{1}{2} \sum_{\mu\nu\lambda\sigma} P_{\mu\nu} P_{\lambda\sigma} \Im + E_x(P) + E_C(P) \tag{48}$$

In most cases the expressions for E_C and E_X cannot be computed analytically and must be obtained by numerical methods. The key difference between the Hartree-Fock and Kohn-Sham approaches to the SCF methods is the term E_{XC}, which was mostly omitted in above discussion. In HF theory, this E_{XC} is written as

$$E_{XC}^{HF} = \frac{1}{2}\sum_{\mu\nu\lambda\sigma}(P_{\mu\nu}^{\alpha}P_{\lambda\sigma}^{\alpha}P_{\mu\nu}^{\beta}P_{\lambda\sigma}^{\beta})(\mu\nu/\lambda\sigma) \tag{49}$$

while the KS theory introduces a functional

$$E_{XC}^{HF} = \int f(\rho^{\alpha},\rho^{\beta},\gamma_{\alpha\alpha},\gamma_{\alpha\beta},\gamma_{\beta\beta})dr \tag{50}$$

for the description. The density gradient invariants γ ($\gamma_{xy} = \nabla\rho_x\nabla\rho_y$)

Density Functionals

It is often customary to make a partition of the density functional into an exchange and correlation part for the separation of

$$E_{XC}(\rho) = E_X(\rho) + E_C(\rho) \tag{51}$$

Although distinction between exchange and correlation contributions is somewhat artificial in the context of DFT, the above separation considerably simplifies the discussion. It should, however, be explicitly noted that the definition of E_C does not correspond to the *ab initio* EC since correlation has, by definition, meaning only in a mean field approximation and DFT is not using such an approximation. The exchange part, on the other hand, follows closely the HF definition of exchange, but does not necessarily reproduce the exact exchange.

Exchange

The exchange energy of a uniform spin-polarized gas of spin density ρ_σ is

$$E_X^S = -\sum\int \rho^{\sigma}(r)f_X^S(\rho_\sigma(r))dr \tag{52}$$

with $f_X^S(\rho_\sigma(r)) = \alpha_X[\rho_\sigma(r)]^{\frac{1}{3}}$ and $\alpha_X = \frac{3}{2}\left(\frac{3}{4\pi}\right)^{\frac{1}{3}}$. The exchange expression is sometimes labeled *Slater exchange*, thus the superscript *S*. This exchange expression serves as a base for other functionals, which can be conveniently expressed in terms of their enhancement factor F_X over the exchange of the uniform electron gas

$$E_X = -\sum_\sigma \int \rho_\sigma(r) f_X^S(\rho_\sigma(r)) F_X(\rho_\sigma), \gamma_{\sigma\sigma}(r))dr \tag{53}$$

For instance, the exchange functional proposed by Perdew and Wang uses the following factor:

$$F_X^{PW}(s) = \left[1 + 0.0864\frac{s^2}{m} + bs^4 + cs^6\right]^m \tag{54}$$

with $m = 1/15$, $b = 14$, $c = 0.2$ and $s = (24\pi^2)^{-1/3}\sqrt{(\gamma_{\sigma\sigma}/\rho^{4/3})}$ $\gamma_{\sigma\sigma}$ here is again the squared density gradient ∇_ω^2. One of the most used exchange functionals is that of Becke 1988, which is often labeled B88 or simply *B*.

$$F_x^B = 1 - \frac{\beta}{\alpha_x}, \frac{x^2}{1 + 6\beta\sinh^{-1}(x)} \tag{55}$$

which uses the values $x = \sqrt{(\gamma_{\sigma\sigma}/\rho_\sigma^{4/3})}$ and $\beta = 0.0042$ in order to maintain correct boundary conditions. In a different approach, Perdew and Wang proposed an exchange formula that is designed from purely first principles.

$$F_X^{PW91} = \frac{1 + (a_1 s)(a_2 s)\sinh^{-1} + (a_3 + a_4\exp(-100s^2))s^2}{1 + (a_1 s)(a_2 s)\sinh^{-1} + a_5 s^4} \tag{56}$$

where $a_1 = 0.19645$, $a_2 = 7.7956$, $a_3 = 0.2743$, $a_4 = -0.1508$, $a_5 = 0.004$ and s the same as in eq. 32.

In practice, the three above exchange functionals are very similar, and are in fact based on minor corrections to the previous ones. Therefore they can be expected

to produce very similar results. The enhancements over the simple electron gas, however, are significant enough and usually constitute a major improvement.

Correlation

While it is possible to obtain E_C by some numerical methods from E_{XC} and the already known EX (cf. eq. 31) for the uniform electron gas, it is much more common to use separate correlation functionals. Distinction is made between local and gradient corrected functionals, referring to the absence or presence of first order terms of the density ρ_σ. The local functional proposed by Vosko, Wilk and Nusair (VWN) was obtained using Pad'e approximated interpolations of Ceperley and Alder results of their accurate quantum Monte Carlo calculations for the homogeneous electron gas. The functional is,

$$E_C^{VWN} = \frac{A}{2}\left[\ln\frac{x^2}{X(x)} + \frac{2b}{Q}\tan^{-1}\frac{Q}{2x+b} - \frac{bx_0}{X(x_0)}\left(\ln\frac{(x-x_0)^2}{X(x)} + \frac{2(b+2x_0)}{Q}\tan^{-1}\frac{Q}{(2x+b)} \right) \right] \quad (57)$$

where the functions are $x = r_b^{1/2}$, $X(x) = x^2 + bx + c$ and $Q = (4c - b^2)^{1/2}$ and the constants are $A = 0.0621814$, $x_0 = -0.409286$, $b = 13.0720$ and $c = 42.7189$. r_b represents are the Wigner-radius and is defined by $1/\rho = \frac{4\pi}{3}(r_b)^3$. Together with the exchange expression from eq. 40 this constitutes what is often called the local density approximation (LDA) or local spin density approximation (LSDA) when spin is considered (Gies and Gerhardts, 1987).

Due to the experiences with the LDA and as a consequence of some of its shortcomings, recent developments have resulted in a number of gradient corrections to local functionals like the aforementioned VWN or a completely new class of gradient corrected functionals.

Another frequently used functional has been published by Lee, Yang and Parr. It replaces both the local and the gradient part of the LDA correlation functional.

$$E_C^{LYP} = -a\frac{1}{1+d\rho^{-1/3}}\left\{\rho + b\rho^{-2/3}\left[C_F\rho^{-5/3} - 2t_w + \frac{1}{9}\left(t_w + \frac{1}{2}\nabla^2\rho\right)\right]e^{-2c\rho^{-1/3}}\right\} \qquad (58)$$

where $t_w = \frac{1}{8}\left(\frac{|\nabla\rho|^2}{\rho} - \nabla^2\rho\right)$ and $C_F = \frac{3}{10}(3\pi^2)^{2/3}$, $a = 0.04918$, $b = 0.132$, $c = 0.2533$ and $d = 0.349$

Hybrid Functionals

More recently, following an approach proposed by Becke, the combination of DFT functionals with *ab initio* formulations led to a class of expressions which are essentially a mixture of both DFT and HF contributions with fitted coefficients for each contribution. The aim of this approach is to provide expressions that include the full exchange contribution and avoid side-effects arising from a complete replacement of the DFT exchange expression by the HF one. As an example, the B3LYP functional looks like this:

$$E_{XC}^{B3LYP} = a_{X0}E_X^S + (1-a_{X0})E_X^{HF} + a_{X1}\Delta E_X^B + E_C^{VWN} + a_C\Delta E_C^{LYP} \qquad (59)$$

with $a_{X0} = 0.80$, $a_{X1} = 0.72$ and $a_C = 0.81$, which are values fitted for a selected set of molecules to reproduce the heat of formation. The term E_X^{HF} is calculated using the Kohn-Sham orbitals in the manner of the HF procedure by computing the exchange integrals $(\mu\nu/\nu\mu)$. The B3LYP functional often uses $\Delta E_C^{3LYP} = E_C^{LYP} - E_C^{VWN}$.

6. Time Dependent density Functional Theory

Ground-state DFT is based on the papers by Hohenberg and Kohn, and by Kohn and Sham. The main result is that the density of the system is identical to the

density of an associated noninteracting particle system moving in a local potential v_s (r) defined by the Khon-Sham equations (atomic units are used throughout):

$$\left[-\frac{1}{2}\nabla^2 + v_s[\rho(r)]\right]\varphi_i(r) = \varepsilon_i\varphi_i(r) \tag{60}$$

Here the local potential $v_s[\rho](r)$ is the so-call Kohn-Sham potential, consisting of the external potential v_{ext} (the Coulomb field of the nuclei and external field if present), the Hatree potential v_H , which is trivially calculated from the density, and the *xc* potential v_{xc} which is the only unknown part:

$$v_s(r) = v_{ext}(r) + v_H(r) + v_{xc}(r) \tag{61}$$

The Kohn-Sham orbitals ϕ_i move in the effective field v_s which depends upon the electron density $\rho(r)$. This density is exactly obtained by summing the squares of the Kohn-Sham orbitals and multiplying by their occupation numbers n_i.

$$\rho(r) = \sum_i^{occ} n_i \left|\varphi_i(r)\right|^2 \tag{62}$$

As the KS potential $v_s(r)$ and the density $\rho(r)$ are inter-dependent, the equation has to be solved in a Self-Consistent Field (SCF) procedure, which means that one iteratively adapts the effective potential v_s and the density ρ until the difference in the energy between two subsequent cycles is sufficiently small. In the most straightforward fashion, this can be performed by mixing the density of the previous cycle with a small part of the density in the present cycle. This “simple damping” approach usually converges very slowly, and in practice the Direct Inversion in the Iterative Subspace (DIIS) procedure by Pulay and co-workers, is much to be preferred. In the DIIS approach, not only the result of a previous cycle, but the results of all, or many, previous cycles are taken into account, in order to obtain the optimal guess for the next cycle. If one is close to self-consistency, this procedure converges with the SCF equation above.

In order to solve the KS equations an approximation for the exchange-correlation (*xc*) potential $v_{xc}(r)$ is required and the simplest one is the LDA which is based upon the local density of the system. The GGAs go beyond this and take the local gradient of the density into account as well, allowing for a much improved accuracy in the results for energies and geometries. Many other approximations, for examples those based directly on the KS orbitals, are also available.

The usual ground state DFT scheme enables one to determine the density, and consequently the dipole moment, of a molecule with or without external electric fields (Gisbergen *et. al*., 1989, 1999). This affords the determination of the static polarizability and hyperpolarizability tensors α,β and γ, by performing calculations in small electric fields of varying magnitudes and directions. In this so-call finite field (FF) approach, the tensor are then determined from finite difference techniques. The main advantage of this approach is that no programming work is needed. Any standard DFT code will allow the determination of static properties in this manner. However, for the determination of higher order tensors, such as γ, one needs very well converged solution to the KS equations in order to make reliable predictions, which may be technically hard to achieve and which will certainly lead to a considerable increase in CPU time consumption.

The most fundamental disadvantage of the FF approach, however, is that one has access to static properties only. The frequency-dependent polarizability and hyperpolarizability tensors are not accessible. Excitation energies and oscillator strengths can also not be obtained from the FF calculations. This is and important drawback of the FF approach, as it makes a direct comparison with experimental results impossible. Especially for hyperpolarizabilities, it is known that there are substantial differences between the frequency-dependent and zero frequency results.

If one is interested in the time dependent properties mentioned above (Bartolotti, 1981, 1982), a time dependent theory is required. In the DFT framework, this means that one has to start from the time dependent KS (TDKS) equations as derived by Runge and Gross;

$$i\frac{\partial}{\partial t}\varphi_i(r,t)=\left[-\frac{\nabla^2}{2}+v_s(r,t)\right]\varphi_i(r,t)\equiv F_s\varphi_i(r,t) \tag{63}$$

The time dependent KS potential $v_s(r,t)$ is subdivided in the same manner as its static counterpart:

$$v_s(r,t)=v_{ext}(r,t)+v_H(r,t)+v_{xc}(r,t) \tag{64}$$

the Hatree potential being explicitly given by:

$$v_H(r,t)=\int dr'\frac{\rho(r',r)}{|r-r'|} \tag{65}$$

and the time dependent *xc* potential $v_{xc}[\rho](r,t)$ being an unknown functional of the time dependent density $\rho(r,t)$ now given by:

$$\rho(r,t)=\sum_i^{occ} n_i\left|\varphi_i(r,t)\right|^2 \tag{66}$$

If a certain approximation for the time dependent *xc* potential v_{xc} (r,t) has been chosen, the TDKS equations can be solved iteratively to yield the time dependent density of system, which may be exposed to an external time dependent electric field. If one is interested in the effects due to extremely large laser fields, the perturbative expansion of the dipole moment become meaningless, and the TDKS equations have to be solved non-perturbatively. This has until now been performed for atoms, by Ullrich and gross (Hirata *et.al.*, 1999), and more recently also by others, and gives access to such effects as higher harmonic generation (HHG), which are not accessible in a perturbative approach. The drawback of this is that the calculations are very time consuming, forbidding the treatment of medium-sized molecules. If one restricts oneself to properties which are accessible through perturbative methods, as we will do here, a much more efficient approach is possible,

allowing the treatment of large molecules (>100 atoms). This approach will be the subject of the next section. For more information on time dependent DFT in general, the reader is referred to the excellent reviews by Gross and co-workers.

The structural geometrical parameters of PEDOT dimer to pentamer

Appendix Table A1 The structural geometrical parameters of PEDOT dimer to pentamer calculated at B3LYP/6-31G* level.

Geometrical parameters	PEDOT			
	dimer	trimer	tetramer	pentamer
S1-C2	1.739	1.739	1.739	1.739
C2-C3	1.364	1.365	1.365	1.365
C3-O4	1.370	1.370	1.371	1.371
O4-C5	1.432	1.431	1.431	1.431
C5-C6	1.522	1.522	1.522	1.523
C6-O7	1.433	1.432	1.432	1.432
O7-C8	1.371	1.371	1.371	1.371
C8-C9	1.379	1.381	1.381	1.381
C9-C10	1.443	1.440	1.439	1.439
C10-C11	1.379	1.380	1.381	1.381
C11-O12	1.370	1.371	1.371	1.371
O12-C13	1.433	1.432	1.432	1.432
C13-C14	1.522	1.522	1.522	1.522
C14-O15	1.432	1.432	1.432	1.432
O15-C16	1.370	1.371	1.371	1.371
C16-C17	1.365	1.380	1.382	1.382
C17-S18	1.739	1.765	1.767	1.768
S18-C10	1.765	1.765	1.765	1.766
C9-S1	1.765	1.766	1.766	1.768
C17-C19	-	1.440	1.436	1.435
C19-C20	-	1.381	1.382	1.382
C20-O21	-	1.371	1.371	1.371
O21-C22	-	1.432	1.432	1.431
C22-C23	-	1.522	1.522	1.522
C23-O24	-	1.431	1.432	1.431
O24-C25	-	1.370	1.371	1.371
C25-C26	-	1.365	1.381	1.382
C26-S27	-	1.739	1.765	1.767
S27-C19	-	1.766	1.770	1.767
C26-C28	-	-	1.439	1.436
C28-C29	-	-	1.381	1.382
C29-O30	-	-	1.371	1.371
O30-C31	-	-	1.432	1.432
C31-C332	-	-	1.522	1.522
C32-O33	-	-	1.431	1.432
O33-C34	-	-	1.371	1.371
CC34-C35	-	-	1.365	1.381
C35-S36	-	-	1.739	1.766

Appendix Table A1 (cont'd)

Geometrical parameters	PEDOT			
	dimer	trimer	tetramer	pentamer
S36-S28	-	-	1.766	1.768
C35-C37	-	-	-	1.439
C37-C38	-	-	-	1.381
C38-O39	-	-	-	1.371
O39-C40	-	-	-	1.432
C40-C41	-	-	-	1.523
C41-O42	-	-	-	1.431
O42-C43	-	-	-	1.371
C43-C44	-	-	-	1.365
C44-S45	-	-	-	1.739
S45-C37	-	-	-	1.768

APPENDIX B

Oral Presentation and Poster Contributions to Conferences

Oral Presentation

Rotpradit K., P. Poolmee, S. Hannongbua. **Theoretical Investigation on Electronic Structures and Energy gaps of poly(3,4-ethylenedioxythiophene) (PEDOT) : Quantum Chemical Calculations.** The 9th Annual National Symposium, on Computational Science and Engineering (ANSCSE 2005), University of Technology , Nakhon Ratchasima, Thailand, 23-25 March 2005.

Theoretical Investigation on Electronic Structures and Energy Gaps of Poly(3,4-ethylenedioxythiophene) (PEDOT) : Quantum Chemical Calculations

Kanjana Rotpradit, Supa Hannongbua, Potjaman Poolmee

Department of Chemistry, Kasetsart University, Bangkok 10900, Thailand.
E-mail address: piyasornc@hotmail.com, fscisph@ku.ac.th

Abstracts

Rotatable potential energy and excitation energy of poly(3,4-ethylenedi-oxythiophene) (PEDOT) have been computed using a variety of methods. Rotatable potential energy were investigated on the torsion angle between the two monomer by using quantum chemical calculations. Conformational analysis was performed, based on semi-empirical (AM1), *ab initio* (at HF/6-31G* ,HF/6-31G** and HF/6-31+G* levels) and density functional theory (at B3LYP/6-31G* , B3LYP/6-31G** and B3LYP/6-31+G* levels). The obtained results indicate that PEDOT shows anti conformation with the dihedral angle (S1-C2-C7-C15) equals to 180 degrees. However, it was found that the PEDOT geometry, calculated by semi-empirical (AM1) method was distorted and the dihedral angle was located around 106.9 degrees.

Geometries of oligomers up to pentamers have been optimized, while excitation energies have been computed using ZINDO and time-dependent density functional theory (TDDFT) methods. Energy gaps have been extrapolated from excitation energies. The obtained results indicated that geometries from semi-empirical (AM1) method are non-planar structure but from *ab intio* and DFT are planar structures. However the geometry calculations obtained from 6-31G*, 6-31G** and 6-31+G* levels show similar structures. The energy gap calculated by ZINDO and TDDFT (B3LYP/6-31G** level) methods at the optimized ground state geometry at B3LYP method provide 1.48 and 1.52 eV respectively. These results are agree with the experiment data (1.60 eV).

Poster Presentation

Rotpradit K., P. Poolmee, S. Hannongbua. **Rotatable Potential Energy of Poly(3,4-ethylenedioxythiophene) (PEDOT): Quantum Chemical Calculations.** The abstract of 30th Congress on Science and Technology of Thailand (STT 2004), IMPACT Exhibition and Convention Center (Hall 1-8), Bangkok, Thailand, 19-23 October 2004.

Rotatable Potential Energy of Poly(3,4-ethylenedioxythiophene) (PEDOT), Based on Quantum Chemical Calculations

Kanjana Rotpradit, Potjaman Poolmee and Supa Hannongbua,
Department of Chemistry, Faculty of Science, Kasetsart University, Bangkok 10900, Thailand.
E-mail : g4664189@ku.ac.th

INTRODUCTION

In the last 20 years, conducting polymers are rising to a great amount of researches. Among the promising family of polythiophenes, the poly(3,4-ethylenendioxythiophene) (PEDOT) showed a remarkable high stability, high electrical conductivity and a low optical energy gap of approximately 1.6 eV, making this material to be a candidate for many industrial applications in the conducting polymer families. As antistatic material, PEDOT is already being used industrially in a large scale.

Quantum-chemical calculations have been recently employed to investigate different aspects related to the structure and properties of PEDOT. However, the number of such studies is still very scarce and, in some cases, the structural and energetic properties obtained are unclear. Therefore, in this work we have performed rotatable potential energy calculations of this PEDOT dimer in order to further study on its energetic property prediction.

Model and Method

The ground state geometries were partial optimized by using the semi-empirical (AM1), ab initio (at HF/6-31G, HF/6-31G** and HF/6-31+G* levels), and density functional theory (at B3LYP/6-31G*, B3LYP/6-31G** and B3LYP/6-31+G* levels). Conformational analysis was done by changing the torsion angles θ by 30 degrees steps between θ = 0 degrees and θ = 360 degrees. In order to obtain the full geometrical structures at each local minima, calculations were performed without constraint on the dihedral angle. All calculations were performed by Gaussian03 packages and running on a Linux PC 2.4 GHz.*

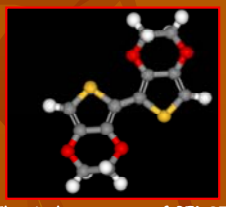

Fig.1 Chemical structure of PEDOT.

Results and discussion

Conformational Analysis

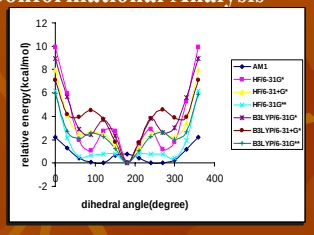

Fig. 2 Conformational analysis of EDOT dimer.

According to Fig. 2, the conformational potential energy curves of PEDOT calculated by AM1 method are quite different from that of HF and B3LYP. The obtained results show that the conformational curves, calculated by HF and B3LYP give similar flat conformation (α=180 degrees). In contrast, the conformational curve of PEDOT calculated by AM1 method exhibits local minima between α = 90 - 120 degrees and another local between 240 - 270 degrees. The full optimized geometry of PEDOT by AM1 method shows the distort structure as showed in the Fig. 4(a) which provided a similar result obtained by Sung Y. Hong2. Comparision the geometrical structure of PEDOT dimer calculated by semi-empirical (AM1) and quantum calculations (HF and B3LYP) are shown in the Fig.3.

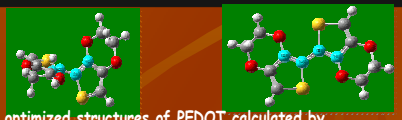

Fig.3 Full optimized structures of PEDOT calculated by a) AM1 method b) B3LYP/6-31+G* methods.

Table 1 inter ring and dihedral angle of PEDOT dimer.

method	inter ring(Å)	dihedral angle (degree)
AM1	1.42	107.8
HF/6-31G*	1.46	179.4
HF/6-31G**	1.46	179.2
HF/6-31+G*	1.46	179.4
B3LYP/6-31G*	1.44	179.9
B3LYP/6-31G**	1.44	179.8
B3LYP/6-31+G*	1.44	179.9

Conclusions

The conformational analysis on PEDOT showed that the geometries of PEDOT calculated by ab initio (HF/6-31G*, HF/6-31G** and HF/6-31+G*) and density functional theory (B3LYP/6-31G*, B3LYP/6-31G** and B3LYP/6-31+G*) are anti conformation which α equal to 180 degrees. On the other hand, the geometry of PEDOT calculated by semi-empirical (AM1) method are distort conformation which located around α equal to 107.9 degrees.

References

1. Carlos Aleman and Jordy Casanovas. *Theoretical Investigation of the 3,4-ethylenedioxythiophene Dimer and Unsubstituted Heterocyclic Derivatives* J. Physics. Chem. 108 (2004) 1440.
2. Sung Y. Hong. *Comparison of Conformations and Electronic Structures of Poly3,4-ethylenedioxythiophene, in the Neutral and Doped State* J. Synthetics Metal 135-136 (2003) 439.

ACKNOWLEDGEMENTS:
& Postgraduate Education and Research Programs in Petroleum and Petrochemical Technology (ADB-MUA)
& Muang Langsuan School , LCAC and Computing Center of Kasetsart University

CURRICULUM VITAE

NAME : Miss. Kanjana Rotpradit

BIRTH DATE : Dec 3, 1973

BIRTH PLACE : Nakhonsritammarat, THAILAND

NATIONALITY : Thai

EDUCATION : **YEAR INSTITUTION DEGREE/DIPLOMA**

: 1996 Prince of Songkla Univ. B. Sc. (Chemistry)

: 2006 Kasetsart Univ. M. Sc. (Physical Chemistry)

SCHOLARSHIP : Postgraduate Education and Research Program in Petroleum and Petrochemical Technology (MUA-ADB) 2003-2006

PRESENTATION :

Rotpradit K., P. Poolmee, S. Hannongbua. **Rotatable Potential Energy of Poly(3,4-ethylenedioxythiophene) (PEDOT) :Quantum Chemical Calculations.** The abstract of 30th Congress on Science and Technology of Thailand (STT 2004), IMPACT Exhibition and Convention Center (Hall 1-8), Bangkok, Thailand, 19-23 October 2004.

Rotpradit K., P. Poolmee, S. Hannongbua. **Theoretical Investigation on Electronic Structures and Energy gaps of poly(3,4-ethylenedioxythiophene) (PEDOT) : Quantum Chemical Calculations.** The 9th Annual National Symposium, on Computational Science and Engineering (ANSCSE 2005), University of Technology , Nakhon Ratchasima, Thailand, 23-25 March 2005.